University of Arkansas, Fayetteville

ScholarWorks@UARK

Graduate Theses and Dissertations

7-2021

Resilience-Driven Post-Disruption Restoration of Interdependent Critical Infrastructure Systems Under Uncertainty: Modeling, Risk-Averse Optimization, and Solution Approaches

Basem A. Alkhaleel
University of Arkansas, Fayetteville

Follow this and additional works at: https://scholarworks.uark.edu/etd

 Part of the Industrial Engineering Commons, Industrial Technology Commons, Operational Research Commons, and the Risk Analysis Commons

Citation

Alkhaleel, B. A. (2021). Resilience-Driven Post-Disruption Restoration of Interdependent Critical Infrastructure Systems Under Uncertainty: Modeling, Risk-Averse Optimization, and Solution Approaches. *Graduate Theses and Dissertations* Retrieved from https://scholarworks.uark.edu/etd/4146

This Dissertation is brought to you for free and open access by ScholarWorks@UARK. It has been accepted for inclusion in Graduate Theses and Dissertations by an authorized administrator of ScholarWorks@UARK. For more information, please contact scholar@uark.edu.

Resilience-Driven Post-Disruption Restoration of Interdependent Critical Infrastructure Systems Under Uncertainty: Modeling, Risk-Averse Optimization, and Solution Approaches

A dissertation submitted in partial fulfillment
of the requirements for the degree of
Doctor of Philosophy in Engineering with a concentration in Industrial Engineering

by

Basem A. Alkhaleel
King Saud University
Bachelor of Science in Industrial Engineering, 2012
Texas A&M University
Master of Science in Industrial Engineering, 2015

July 2021
University of Arkansas

This dissertation is approved for recommendation to the Graduate Council.

Haitao Liao, Ph.D. Dissertation Co-Director	Kelly M. Sullivan, Ph.D. Dissertation Co-Director
Xiao Liu, Ph.D. Committee Member	Jingxian Wu, Ph.D. Committee Member

ABSTRACT

Critical infrastructure networks (CINs) are the backbone of modern societies, which depend on their continuous and proper functioning. Such infrastructure networks are subjected to different types of inevitable disruptive events which could affect their performance unpredictably and have direct socioeconomic consequences. Therefore, planning for disruptions to CINs has recently shifted from emphasizing pre-disruption phases of prevention and protection to post-disruption studies investigating the ability of critical infrastructures (CIs) to withstand disruptions and recover timely from them. However, post-disruption restoration planning often faces uncertainties associated with the required repair tasks and the accessibility of the underlying transportation network. Such challenges are often overlooked in the CIs resilience literature. Furthermore, CIs are not isolated from each other, but instead, most of them rely on one another for their proper functioning. Hence, the occurrence of a disruption in one CIN could affect other dependent CINs, leading to a more significant adverse impact on communities. Therefore, interdependencies among CINs increase the complexity associated with recovery planning after a disruptive event, making it a more challenging task for decision makers.

Recognizing the inevitability of large-scale disruptions to CIs and their impacts on societies, the research objective of this work is to study the recovery of CINs following a disruptive event. Accordingly, the main contributions of the following two research components are to develop: (i) resilience-based post-disruption stochastic restoration optimization models that respect the spatial nature of CIs, (ii) a general framework for scenario-based stochastic models covering scenario generation, selection, and reduction

for resilience applications, (iii) stochastic risk-related cost-based restoration modeling approaches to minimize restoration costs of a system of interdependent critical infrastructure networks (ICINs), (iv) flexible restoration strategies of ICINs under uncertainty, and (v) effective solution approaches to the proposed optimization models.

The first research component considers developing two-stage risk-related stochastic programming models to schedule repair activities for a disrupted CIN to maximize the system resilience. The stochastic models are developed using a scenario-based optimization technique accounting for the uncertainties of the repair time and travel time spent on the underlying transportation network. To assess the risks associated with post-disruption scheduling plans, a conditional value-at-risk metric is incorporated into the optimization models through the scenario reduction algorithm. The proposed restoration framework is illustrated using the French RTE electric power network.

The second research component studies the restoration problem for a system of ICINs following a disruptive event under uncertainty. A two-stage mean-risk stochastic restoration model is proposed to minimize the total cost associated with ICINs unsatisfied demands, repair tasks, and flow. The model assigns and schedules repair tasks to network-specific work crews with consideration of limited time and resources availability. Additionally, the model features flexible restoration strategies including a multicrew assignment for a single component and a multimodal repair setting along with the consideration of full and partial functioning and dependencies between the multi-network components. The proposed model is illustrated using the power and water networks in Shelby County, Tennessee, United States, under two hypothetical earthquakes.

Finally, some other topics are discussed for possible future work.

©2021 Basem A. Alkhaleel
All Rights Reserved

ACKNOWLEDGMENTS

All praises and glory are for Almighty Allah, the Powerful and Exalted in Might, who gave me the courage, knowledge and patience to carry out the work in this dissertation. Peace and blessings of Allah be upon his prophet Mohammad and all his family and companions (May Allah be pleased with them all).

My deepest gratitude and appreciation to all my beloved family members for their love, support, and encouragement. Extraordinary gratitude to my wife, Suhad, and my lovely two sons, Dahome and Yasser, for their unmatched support and patience throughout this journey.

I would like to thank my advisor, Dr. Haitao Liao, for his invaluable help and support. I acknowledge his encouragement, insightful feedback, concern, valuable time, patience, kindness, and guidance throughout the duration of my study.

I would like to express my special thanks to my co-advisor, Dr. Kelly M. Sullivan, whose expertise was invaluable in formulating the research methodology. His insightful feedback pushed me to sharpen my thinking and brought my work to a higher level.

I extend my gratitude to my committee members, Dr. Xiao Liu, and Dr. Jingxian Wu for their interest, cooperation, and valuable feedback.

DEDICATION

To

my parents

my wife Suhad

my sons Dahome and Yasser

my brothers

TABLE OF CONTENTS

LIST OF FIGURES

LIST OF TABLES

LIST OF PUBLISHED PAPERS

- **Alkhaleel, B. A.**, Liao, H., and Sullivan, K. M. (2021). Risk and resilience-based optimal post-disruption restoration for critical infrastructures under uncertainty. *European Journal of Operational Research*. doi:10.1016/j.ejor.2021.04.025. [**In Press**] [**Chapter 3**]

- **Alkhaleel, B. A.**, Liao, H., and Sullivan, K. M. (2021). Model and solution method for mean-risk cost-based post-disruption restoration of interdependent critical infrastructure networks. *Computers and Operations Research.* [**Submitted**] [**Chapter 4**]

Chapter 1

Introduction

1.1 Overview

Critical infrastructures (CIs) are defined as networks of independent, mostly privately-owned, man-made systems and processes that function collaboratively and synergistically to produce and distribute a continuous flow of essential goods and services (Ellis *et al.*, 1997). Hence, critical infrastructure networks such as electric power, water distribution, natural gas, transportation, and telecommunications, among others, are the backbone of modern societies, which depend on their continuous and proper functioning (Almoghathawi *et al.*, 2019; Zio, 2016). Such critical infrastructure networks provide the fundamental services that support the economic productivity, security, and quality of life of citizens.

Moreover, infrastructure networks are subjected to different types of disruptive events, including random failures, technical accidents, malevolent attacks, and natural hazards, which could affect their performance unpredictably and have direct consequences on communities and people's daily lives. Such disruptions become inevitable in today's increasingly complex and risky operating environment (Helbing, 2013). Hence, for several years, the United States (U.S.), as well as many countries around the globe, have shown an increasing interest in effectively preparing for and responding promptly to such disruptive events (Karagiannis *et al.*, 2017; O'Donnell, 2013; White House, 2013). Therefore, it is increasingly important to not only protect current infrastructure networks against disruption,

but to be able to restore them once they have been disrupted.

In addition, interdependencies among infrastructure networks have become more frequent and complex due to the increasing trend of globalization and technological developments (Karakoc *et al.*, 2019; Rinaldi *et al.*, 2001; Saidi *et al.*, 2018). However, although interdependencies can improve the efficiency of networks functionality, this type of complex coordination often causes them to become more vulnerable to disruptions (e.g., random failures, terrorist attacks, or natural disasters). As a result, a disruption in some components of one of the infrastructure networks could cause a malfunction in the undisrupted components of other dependent networks, resulting in a series of cascading failures affecting the whole infrastructure network system (Buldyrev *et al.*, 2010; Danziger *et al.*, 2016; Eusgeld *et al.*, 2011; Karakoc *et al.*, 2019; Little, 2002; Ouyang, 2014; Wallace *et al.*, 2003). Therefore, this high vulnerability of infrastructure networks against disruptions is a critical concern for decision-makers, especially where accounting for interdependencies through recovery planning is essential to obtain a realistic analysis of their performance (Holden *et al.*, 2013). Moreover, scheduling the restoration processes separately for interdependent infrastructure networks without considering their interdependencies could cause misutilization of resources, waste of time and funds, and even might trigger additional inoperability of distribution systems (Baidya & Sun, 2017).

Risk management strategies generally emphasized disruptive events mitigation options in the form of prevention and protection: designing systems to avoid or absorb undesired events from occurring (Hosseini *et al.*, 2016). While such strategies are critical to prevent undesired events or consequences, recent events suggested that not all undesired events can be prevented. Natural events such as Hurricane Harvey are among the recent

examples of unpreventable disruptions; in fact, this particular event impacted multiple networked systems including the transportation network and power network, which has not been restored fully even after a few months of the incident (Manuel, 2013). In a recent report by the European Commission's science and knowledge service, the Joint Research Centre (JRC) has addressed challenges in power grid recovery after natural hazards (Karagiannis *et al.*, 2017). The study covered different natural events and their impact on power grid networks by collecting worldwide data about at least 50 events from different sources, including technical reports, field survey reports, and research papers (Karagiannis *et al.*, 2017). The report used two thresholds to assess power grid recoverability: (1) The restoration of power supply to customers, (2) The complete repair of the network; moreover, two of the significant challenges that face recovery actions were found to be the repair times uncertainty and poor access to damaged facilities due to landslides or traffic congestions. In addition, the report was concluded with multiple recommendations to improve power grid recovery, ranging from integrating risk-related strategies to stockpiling spare parts for urgent maintenance actions (Luo *et al.*, 2020).

All such recovery planning actions after disruptions are part of the rising concept of resilience, which can be defined generally as the ability of a system or an organization to react and recover from unanticipated disturbances and events (Hollnagel *et al.*, 2006). Resilience, and in particular CI resilience, has emerged in recent years due to the awareness of governments about the possible risks associated with CIs and the catastrophic impacts of various disruptive events affecting CIs (White House, 2013). This has encouraged practitioners and researchers to develop various resilience improvement techniques ranging from system design to recovery optimization (Hosseini *et al.*, 2016). In addition, resilience

can be effectively improved by developing optimum plans for timely restoring the disrupted service after the occurrence of disruptive events. In planning CIs restoration, prioritizing components is a key in improving the recovery process; hence, optimization approaches are typically used to facilitate the identification and scheduling of effective restoration strategies for the rapid reestablishment of system functionality.

Post-disruption restoration of CIs problems studied in this context are related to general classical maintenance repair problems (MRPs) (Cassady *et al.*, 2001; Fang & Sansavini, 2019; Pandey *et al.*, 2013). However, the main differences between these two categories of problems can be summarized as follows (Fang & Sansavini, 2019):

- Post-disruption restoration of CIs problems focus only on the restoration stage after a single large-scale disruption on a critical infrastructure network (or a system of interdependent networks), i.e., it is assumed that damages to the system components have occurred. In contrast, MRPs usually cover the whole failure and repair process considering component failures as the main source of uncertainty.

- Post-disruption restoration of CIs problems focus on the identification and scheduling of optimal restoration strategies for the rapid reestablishment of system functionality under limited amount of repair resources. Conversely, MRPs usually focus on the long term strategies for system maintenance and repair, e.g., different choices of the maintenance periods for the system components and of the number of repair teams to keep on site (Fang & Sansavini, 2019; Marseguerra & Zio, 2000).

- Post-disruption restoration of CIs problems are considered as planning (scheduling) problems and thus often studied in a mathematical programming and optimization

framework in the literature. On the other hand, MRPs typically discuss the failure and repair processes from a statistical point of view, represent the processes through stochastic models (e.g., using failure and recovery rates), and often adopt simulation methods to find the best maintenance policies (Marseguerra & Zio, 2000).

There are many studies that have been proposed in the literature in the context of post-disruption CI restoration under a mathematical programming framework (Almoghathawi *et al.*, 2019; Fang & Sansavini, 2017; Nurre & Sharkey, 2014; Vugrin *et al.*, 2014; Zhang *et al.*, 2018). In this context, the main goal is to schedule recovering tasks of failed components in order to accelerate the restoration process (Vugrin *et al.*, 2014). However, almost all studies focus on deterministic approaches and unrealistic assumptions such as complete information on the restoration resources and full knowledge of the activities durations. However, the restoration of infrastructure systems is complicated by the many decisions to be made in a highly uncertain environment exacerbated by the disaster itself, people's reaction, and limited capability of information gathering (Fang & Sansavini, 2019). Several factors introduce uncertainty into the parameters of a disaster situation, e.g., availability of restoration resources, number of repair crews, the time duration for repairing failed components, and the accessibility to such failed components through the related transportation network. Clearly, optimal task planning under uncertainty appears to be the closest to a real-life situation. In addition, existing optimization approaches usually do not account for risk measures related to the execution of the optimal plan. For example, if the time duration of some repair activities were longer than expected, the doubt would be if the suggested plan will still perform well. Clearly, when optimizing CI

restoration, risks associated with the restoration plan must be considered to identify the possible worst-case scenarios and alter the plan accordingly. Additionally, the travel time between failed components, an often overlooked aspect of the restoration plan, may also affect the proposed plan along with the accessibility of components under the transportation network condition.

1.2 Problem statement and objective

There are multiple challenges facing the recovery planning of CIs after disruptions. According to JRC, two of the significant challenges that face recovery actions were the repair times uncertainty and poor access to damaged facilities due to landslides or traffic congestion (Karagiannis *et al.*, 2017). However, the vast majority of CIs restoration models do not consider traffic travel times to access damaged facilities nor uncertainty in restoration tasks. Besides, knowing that the restoration process is a one-shot operation, the restoration plan needs to be assessed from a risk analysis point of view. Therefore, linking restoration optimization models with risk measures is significant in order to find restoration plans that are robust even in the worst-case scenarios involving longer than expected repairing tasks or travel times. Furthermore, another challenge facing the restoration process is the interdependencies across critical infrastructure networks. Such interdependencies often increase the complexity associated with recovery planning, making it a more challenging task to simultaneously coordinate multiple networks' restoration plans.

Hence, the main research objective of the work presented in this dissertation is to study the recovery of systems of critical infrastructure networks following a disruptive event under uncertainty. This includes developing stochastic resilience-driven restoration models

with uncertainty-related coherent risk measures and consideration of CIs interdependencies. Moreover, developed models need to respect the spatial nature of such CIs by relaxing a general assumption in the literature that restoration tasks can be performed sequentially, where the long mile-measured distances between failed components translated into lost time are ignored. Additionally, given the complex nature of stochastic models compared to deterministic ones, effective solution methodologies need to be developed to solve the proposed models. Accordingly, we try to develop: (i) risk-related stochastic restoration models that enhance CIs resilience, and (ii) interdependent CIs mean-risk cost-based stochastic restoration modeling approaches, considering the physical interdependency among the infrastructure networks. The two research components presented in this dissertation are summarized below.

First, we develop two-stage risk-averse and risk-neutral stochastic programming models to schedule repair activities for a disrupted CI network to maximize the system resilience. Both models are developed based on a scenario-based optimization technique that accounts for the repair time uncertainties and the travel time spent on the underlying transportation network. Given the large number of uncertainty realizations associated with post-disruption restoration tasks, an improved fast forward algorithm based on a wait-and-see optimal solution is provided to scale down the number of chosen scenarios, which results in desired probabilistic performance metrics. To assess the risks associated with post-disruption scheduling plans, a conditional value-at-risk (CVaR) metric is incorporated into the optimization models through the scenario reduction algorithm. The proposed restoration framework is applied to the French RTE electric power network with a DC power flow procedure. The results demonstrate the added value of using the stochastic

programming models incorporating the travel times related to repair activities. It is essential that risk-averse decision-making under uncertainty largely impacts the optimum schedule and the expected resilience, especially in the worst-case scenarios.

Second, we study the interdependent critical infrastructure networks restoration problem, which seeks to minimize the total cost associated with unmet demand (resilience loss), repair tasks, and network flow by improving the restoration strategy of a system of interdependent infrastructure networks following a disruption event under uncertainty. A two-stage mean-risk stochastic restoration model is proposed, based on the developed one in our first study, using mixed-integer linear programming (MILP). The model assigns and schedules repair tasks to network-specific work crews with consideration of limited time and resources availability. In particular, the proposed model determines (i) the set of failed components to be restored, (ii) the repair mode for each failed component, (iii) the set of failed components for each crew to restore individually or concurrently, (iv) the baseline restoration sequence across scenarios for each crew in order to minimize the total cost associated with the restoration process (i.e., resilience loss, repair, and flow costs). Additionally, the model features flexible restoration strategies including multicrew assignment for a single component and a multimodal repair setting along with the consideration of full and partial functioning and dependencies between the multi-network components. The proposed model is illustrated using the power and water networks in Shelby County, Tennessee, United States, under two hypothetical earthquakes.

1.3 Dissertation outline

This dissertation consists of five chapters where the content of each chapter is briefly described in this section.

In Chapter 1, we give an overview of the studies on post-disruption restoration of critical infrastructure networks. In addition, we address the problem statement as well as the objectives of this dissertation.

In Chapter 2, we present some background information about the resilience of critical infrastructure concept. Additionally, we provide a literature survey on available definitions of resilience, assessment techniques, and modeling approaches in engineering fields.

In Chapter 3, we present risk-related restoration models for an infrastructure network using MILP with respect to the underlying transportation network. Additionally, we present and discuss the results of a case study based on the French RTE electric power network. This chapter is based on a published paper in the European Journal of Operational Research.

In Chapter 4, we present a two-stage mean-risk stochastic restoration model for a system of interdependent critical infrastructure networks using MILP, based on the work in Chapter 3. Additionally, we discuss the the results of a case study based on the power and water networks in Shelby County, Tennessee, United States. This chapter is based on a submitted manuscript to the Journal of Computers and Operations Research.

In Chapter 5, we discuss possible extensions to the current work and different research topics for future work.

References

Almoghathawi, Y., Barker, K., & Albert, L. A. (2019). Resilience-driven restoration model

for interdependent infrastructure networks. *Reliability Engineering and System Safety*, *185*, 12–23. doi: 10.1016/j.ress.2018.12.006

Baidya, P. M., & Sun, W. (2017). Effective restoration strategies of interdependent power system and communication network. *The Journal of Engineering*, *2017*(13), 1760–1764. doi: 10.1049/joe.2017.0634

Buldyrev, S. V., Parshani, R., Paul, G., Stanley, H. E., & Havlin, S. (2010). Catastrophic cascade of failures in interdependent networks. *Nature*, *464*(7291), 1025–1028. doi: 10.1038/nature08932

Cassady, C. R., Murdock, W. P., & Pohl, E. A. (2001). Selective maintenance for support equipment involving multiple maintenance actions. *European Journal of Operational Research*, *129*(2), 252–258. doi: 10.1016/s0377-2217(00)00222-8

Danziger, M. M., Shekhtman, L. M., Bashan, A., Berezin, Y., & Havlin, S. (2016). Vulnerability of interdependent networks and networks of networks. In *Understanding complex systems* (pp. 79–99). Switzerland: Springer International Publishing. doi: 10.1007/978-3-319-23947-7_5

Ellis, J., Fisher, D., Longstaff, T., Pesante, L., & Pethia, R. (1997). *Report to the president's commission on critical infrastructure protection.* (Tech. Rep.). Pittsburgh, PA: Carnegie Mellon University Software Engineering Institute. (Available at: https://apps.dtic.mil/docs/citations/ADA324232) doi: 10.21236/ada324232

Eusgeld, I., Nan, C., & Dietz, S. (2011). "system-of-system" approach for interdependent critical infrastructures. *Reliability Engineering and System Safety*, *96*(6), 679–686. doi: 10.1016/j.ress.2010.12.010

Fang, Y., & Sansavini, G. (2017). Emergence of antifragility by optimum postdisruption restoration planning of infrastructure networks. *Journal of Infrastructure Systems*, *23*(4), 04017024. doi: 10.1061/(ASCE)IS.1943-555X.0000380

Fang, Y., & Sansavini, G. (2019). Optimum post-disruption restoration under uncertainty for enhancing critical infrastructure resilience. *Reliability Engineering and System Safety*, *185*(January 2019), 1–11. doi: 10.1016/j.ress.2018.12.002

Helbing, D. (2013). Globally networked risks and how to respond. *Nature*, *497*(7447), 51–59. doi: 10.1038/nature12047

Holden, R., Val, D. V., Burkhard, R., & Nodwell, S. (2013). A network flow model for interdependent infrastructures at the local scale. *Safety Science*, *53*, 51–60. doi: 10.1016/j.ssci.2012.08.013

Hollnagel, E., Woods, D. D., & Leveson, N. (2006). *Resilience engineering: Concepts and*

precepts. Aldershot, UK: Ashgate Publishing, Ltd.

Hosseini, S., Barker, K., & Ramirez-Marquez, J. E. (2016). A review of definitions and measures of system resilience. *Reliability Engineering and System Safety*, *145*, 47–61. doi: 10.1016/j.ress.2015.08.006

Karagiannis, G. M., Chondrogiannis, S., Krausmann, E., & Turksezer, Z. I. (2017). *Power grid recovery after natural hazard impact* (Tech. Rep. No. EUR 28844 EN). Luxembourg: Publications Office of the European Union. doi: 10.2760/87402

Karakoc, D. B., Almoghathawi, Y., Barker, K., González, A. D., & Mohebbi, S. (2019). Community resilience-driven restoration model for interdependent infrastructure networks. *International Journal of Disaster Risk Reduction*, *38*, 101228. doi: 10.1016/j.ijdrr.2019.101228

Little, R. G. (2002). Controlling cascading failure: Understanding the vulnerabilities of interconnected infrastructures. *Journal of Urban Technology*, *9*(1), 109–123. doi: 10.1080/106307302317379855

Luo, H., Alkhaleel, B. A., Liao, H., & Pascual, R. (2020). Resilience improvement of a critical infrastructure via optimal replacement and reordering of critical components. *Sustainable and Resilient Infrastructure*, 1–21. doi: 10.1080/23789689.2019.1710072

Manuel, J. (2013). *The long road to recovery: Environmental health impacts of hurricane sandy* (Vol. 121) (No. 5). Environmental Health Perspectives. doi: 10.1289/ehp.121-a152

Marseguerra, M., & Zio, E. (2000). Optimizing maintenance and repair policies via a combination of genetic algorithms and monte carlo simulation. *Reliability Engineering and System Safety*, *68*(1), 69–83. doi: 10.1016/s0951-8320(00)00007-7

Nurre, S. G., & Sharkey, T. C. (2014). Integrated network design and scheduling problems with parallel identical machines: Complexity results and dispatching rules. *Networks*, *63*(4), 306–326. doi: 10.1002/net.21547

O'Donnell, K. (2013). Critical infrastructure resilience: Resilience thinking in australia's federal critical infrastructure protection policy. *Salus Journal*, *1*(3), 13.

Ouyang, M. (2014). Review on modeling and simulation of interdependent critical infrastructure systems. *Reliability Engineering and System Safety*, *121*, 43–60. doi: 10.1016/j.ress.2013.06.040

Pandey, M., Zuo, M. J., Moghaddass, R., & Tiwari, M. (2013). Selective maintenance for binary systems under imperfect repair. *Reliability Engineering and System Safety*, *113*, 42–51. doi: 10.1016/j.ress.2012.12.009

Rinaldi, S. M., Peerenboom, J. P., & Kelly, T. K. (2001). Identifying, understanding, and analyzing critical infrastructure interdependencies. *IEEE Control Systems*, *21*(6), 11–25. doi: 10.1109/37.969131

Saidi, S., Kattan, L., Jayasinghe, P., Hettiaratchi, P., & Taron, J. (2018). Integrated infrastructure systems—a review. *Sustainable Cities and Society*, *36*, 1–11. doi: 10.1016/j.scs.2017.09.022

Vugrin, E. D., Turnquist, M. A., & Brown, N. J. (2014). Optimal recovery sequencing for enhanced resilience and service restoration in transportation networks. *International Journal of Critical Infrastructures*, *10*(3/4), 218–246. doi: 10.1504/IJCIS.2014.066356

Wallace, W., Mendonca, D., Lee, E., Mitchell, J., Wallace, J., & Monday, J. (2003). Managing disruptions to critical interdependent infrastructures in the context of the 2001 world trade center attack. in beyond september 11th: An account of. *Post-Disaster Research, special publication*, *39*, 165–198.

White House. (2013). *Presidential Policy Directive/PPD-21 : Critical Infrastructure Security and Resilience. Office of the Press Secretary: Washington, DC.* [Administration of Barack Obama]. Washington, DC..

Zhang, C., Kong, J.-j., & Simonovic, S. P. (2018). Restoration resource allocation model for enhancing resilience of interdependent infrastructure systems. *Safety Science*, *102*, 169–177. doi: 10.1016/j.ssci.2017.10.014

Zio, E. (2016). Challenges in the vulnerability and risk analysis of critical infrastructures. *Reliability Engineering and System Safety*, *152*, 137–150. doi: 10.1016/j.ress.2016.02.009

Chapter 2

Resilience of Critical Infrastructure

2.1 Introduction

Resilient infrastructure systems such as electric power, water, and telecommunication are essential for minimizing the impact of extreme events. In fact, building a resilient infrastructure is an important goal for every nation's Critical Infrastructure Protection (CIP) program (Lindström & Olsson, 2009). However, the first step toward this goal is to develop an evaluation methodology that enables decision makers to quantify an infrastructure's resilience. The developed methodology is then used to evaluate the possible measures for improving infrastructure resilience.

In this chapter, we review effective cross-infrastructure resilience assessment frameworks. Such frameworks incorporate three main steps: (i) defining resilience attributes, (ii) modeling critical infrastructure, and (iii) measuring resilience. The reviewed assessment frameworks can be used to evaluate and optimize preparedness, response, and mitigation plans against natural and man-made disasters. The rest of this chapter is organized as follows. Section 2.2 of this chapter presents a literature review on existing resilience definitions in the engineering field literature. Section 2.3 lists the different measures used to assess, quantify, and optimize resilience of networked systems. Finally, in Section 2.4, we conclude the review and discuss our findings.

2.2 Resilience definition

The word *resilience* has been originally originated from the Latin word "resiliere," which means to "bounce back." The common use of the resilience word implies the ability of an entity or system to return to its normal condition after the occurrence of an event that disrupts its state. Moreover, the term *resilience* has increasingly been seen in the research literature (Hosseini *et al.*, 2016; Park *et al.*, 2012) due to its role in reducing the risks associated with the inevitable disruption of systems. In fact, the concept of resilience exists in various fields such as ecology, economics, and engineering (Hosseini *et al.*, 2016).

Several definitions of resilience have been offered in the literature of different disciplines. Many of these definitions are similar, although many overlap with a number of already existing concepts such as robustness, fault-tolerance, flexibility, survivability, and others (Fang, 2015; Hosseini *et al.*, 2016). However, in this literature review, we primarily focus on the quantitative perspective of modeling resilience in engineering applications along with popular definitions in this field of study.

Among the general definitions of resilience existing in multidiscipline literature is the one proposed by Allenby and Fink (2000) who defined resilience as the "capability of a system to maintain its functions and structure in the face of internal and external change and to degrade gracefully when it must." This definition seems to be applicable even in the engineering field; nonetheless, the context of this definition is in ecological and social sciences. Another multidisciplinary definition is the one provided by Pregenzer (2011) stating that resilience is the "measure of a system's ability to absorb continuous and unpredictable change and still maintain its vital functions." Haimes (2009) defined resilience as the "ability

of system to withstand a major disruption within acceptable degradation parameters and to recover with a suitable time and reasonable costs and risks." Such definitions focus on the ability of a *system* to *resist* a *change* and/or *adapt* with it, which shows that all definitions of resilience (general and field-specific) are related to the concept of resisting an internal or external undesired change, adapting and functioning under effect, and recovering rapidly after effect.

Disaster resilience constitutes an important part of the literature on resilience, which is characterized by The Infrastructure Security Partnership (TISP, 2006) as the capability to prevent or protect against significant multi-hazard threats and incidents, including terrorist attacks, and to recover and reconstitute critical services with minimum devastation to public safety and health. Vugrin *et al.* (2010) defined system resilience as: "Given the occurrence of a particular disruptive event (or set of events), the resilience of a system to that event (or events) is that system's ability to reduce efficiently both the magnitude and duration of deviation from targeted system performance levels." Two elements of this definition are noted by Hosseini *et al.* (2016): system impact, which is the negative impact that a disruption imposes to a system and measured by the difference between targeted and disrupted performance level of the system, and total recovery effort, which is the amount of resources expended to recover the disrupted system. Both elements of the previous definition are the base of resilience mathematical measures. Furthermore, infrastructure systems such as water distribution systems, nuclear plants, transportation systems, and others have a critical connection with the resilience concept. Hence, the National Infrastructure Advisory Council (NIAC) defined the resilience of infrastructure systems as their ability to predict, absorb, adapt, and/or quickly recover from a disruptive event such as natural disasters

(NIAC, 2009). Due to the crucial role of infrastructures on society and economy, research efforts have recently focused on infrastructure resilience (DiPietro *et al.*, 2014; Morshedlou *et al.*, 2018; Shafieezadeh & Burden, 2014; Vugrin & Camphouse, 2011). Ouyang and Wang (2015) assessed the resilience of interdependent electric power and natural gas infrastructure systems under multiple hazards, noting how interdependent network performance could be measured in physical engineering terms or in terms of societal impact.

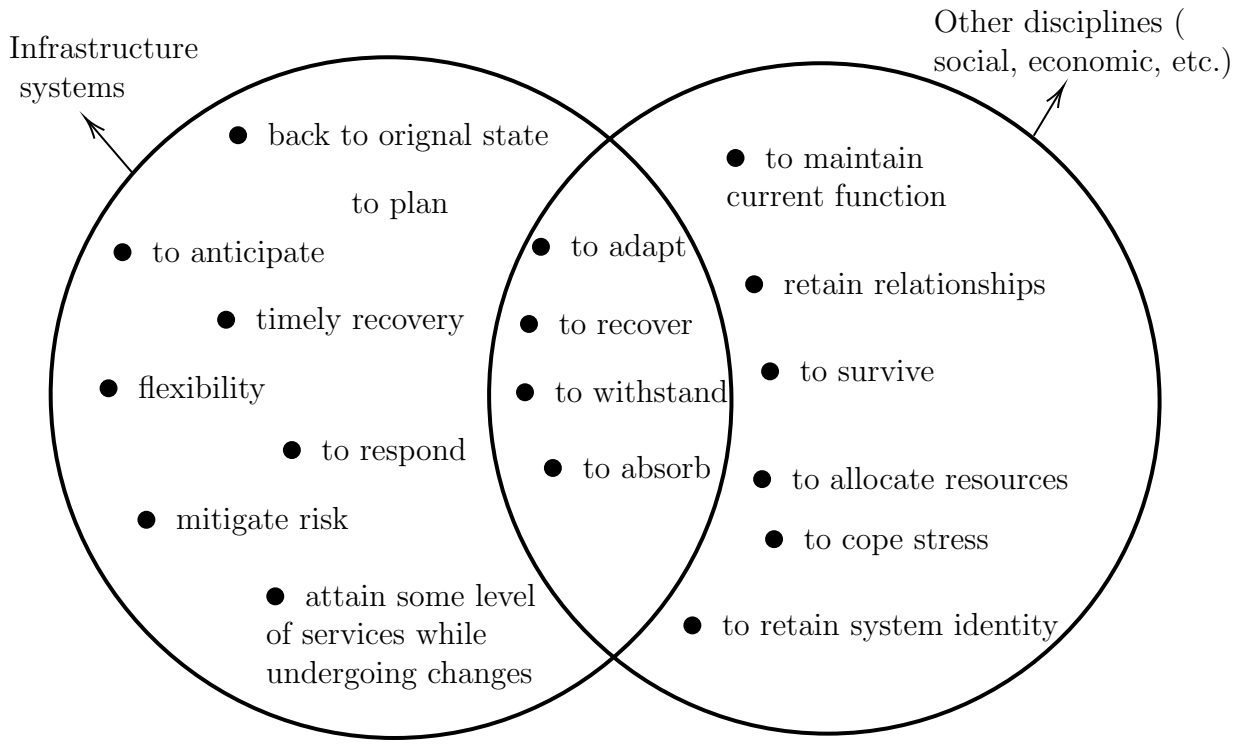

Figure 2.1. Key characteristics of resilience definitions from different disciplines

In the engineering domain, resilience is usually associated with reliability and robustness terms, both of which are important concepts in such field. Youn *et al.* (2011) defined engineering resilience as the sum of the passive survival rate (reliability) and proactive survival rate (restoration) of a system. Another definition of engineering resilience is offered by Hollnagel *et al.* (2006) as the intrinsic ability of a system to adjust its functionality in the

presence of a disturbance and unpredicted changes. In addition, Hollnagel (2011) pointed out that, for resilience engineering, understanding the normal functioning of a technical system is important as well as understanding how it fails. The American Society of Mechanical Engineers (ASME) defined resilience as the ability of a system to sustain external and internal disruptions without discontinuity of performing the system's function or, if the function is disconnected, to fully recover the function rapidly (ASME, 2009). Dinh *et al.* (2012) identified six factors that enhance the resilience engineering of industrial processes, including minimization of failure, limitation of effects, administrative controls/procedures, flexibility, controllability, and early detection.

Overall, it can be seen that there are several commonalities and differences among the proposed resilience definitions. Figure 2.1 shows some of the key resilience characteristics as identified by CIP community and other disciplines. The main highlights of resilience definitions reviewed above can be summarized as follows (Hosseini *et al.*, 2016):

- Some definitions do not specify mechanisms to achieve resilience; however, they focus on the capability of systems to *absorb* and *adapt* to disruptive events. In addition, the term *recovery* is considered the critical part of resilience under this group of definitions.

- Some definitions, such as ASME (2009), emphasize that returning to steady state performance level is needed for resilience, while other definitions do not impose that the system has to return to its pre-disaster state.

- The definition offered by Haimes (2009) suggests multidimensionality to the quantification of resilience, that is, particular states of a system are inherently more resilient than others. Furthermore, Haimes stresses that the resilience of a system is

threat-dependent.

- Some definitions such as Allenby and Fink (2000) and Pregenzer (2011) defined resilience in terms of preparedness (pre-disaster) activities, while the role of recovery (post-disaster) activities is discarded. Definitions presented by organizations such as NIAC (2009) emphasized the role of both preparedness and recovery activities to achieve resilience.

2.3 Resilience measures

There are different approaches to measure the resilience of systems in the literature. However, such measures can be broadly classified into (Hosseini *et al.*, 2016):

- *Deterministic vs. Stochastic:* where a deterministic approach does not incorporate uncertainty into the metric, while a stochastic or probabilistic performance-based approach quantifies uncertainty in terms of probabilities and statistical distributions.

- *Dynamic vs. Static:* where a dynamic performance-based approach accounts for time-dependent behavior, while a static performance-based approach does not consider any time factor.

In this section, we start our review of resilience measures with deterministic ones in Section 2.3.1, and then we discuss the stochastic measures in Section 2.3.2.

2.3.1 Deterministic measures

There are four dimensions of resilience, defined by Bruneau *et al.* (2003), in the well-known resilience triangle model in civil infrastructure: (i) robustness, the strength of

a system, or its ability to prevent damage propagation through the system in the presence of a disruptive event, (ii) rapidity, the speed or rate at which a system could return to its original state or at least an acceptable level of functionality after the occurrence of disruption, (iii) resourcefulness, the level of capability in applying material (i.e., information, technological, physical) and human resources (i.e., labor) to respond to a disruptive event, and (iv) redundancy, the extent to which carries by a system to minimize the likelihood and impact of disruption. Based on that, Bruneau *et al.* (2003) proposed a deterministic static metric for measuring the resilience loss of a community to an earthquake. The metric is expressed as in Equation (2.1), where the time at which the disruption occurs is t_0, and the time at which the community returns to its normal pre-disruption state is t_1. The quality of the community infrastructure at time t, which could represent several kinds of performance measures, is denoted with $Q(t)$. Thus, the quality of degraded infrastructure is compared to the as-planned infrastructure quality of 100 during the recovery period. Hence, resilience loss (RL) can be represented mathematically as shown in Equation (2.1) and can be be illustrated graphically as the shaded area in Figure 2.2.

$$RL = \int_{t_0}^{t_1} [100 - Q(t)]dt \tag{2.1}$$

Zobel (2011) proposed a metric specified by "calculating the percentage of the total possible loss over some suitably long time interval T^*" as shown in Equation (2.2):

$$R(X,T) = \frac{T^* - XT/2}{T^*} = 1 - \frac{XT}{2T^*} \tag{2.2}$$

Parameters include $X \in [0,1]$ as the percentage of functionality lost after a disruption, $T \in [0, T^*]$ as the time required for full recovery, and T^* as a suitably long time interval over which lost functionality is determined. Zobel also provided a visualization of the tradeoffs

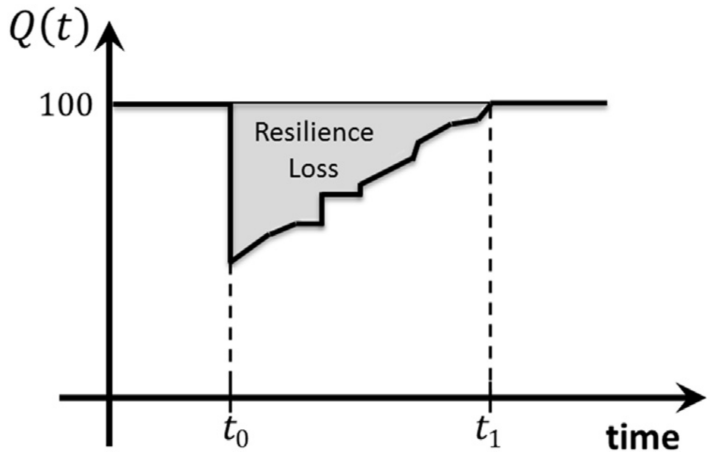

Figure 2.2. Resilience loss measurement (adapted from Bruneau *et al.* (2003))

between lost functionality and recovery time for the same level of resilience as shown in Figure 2.3:

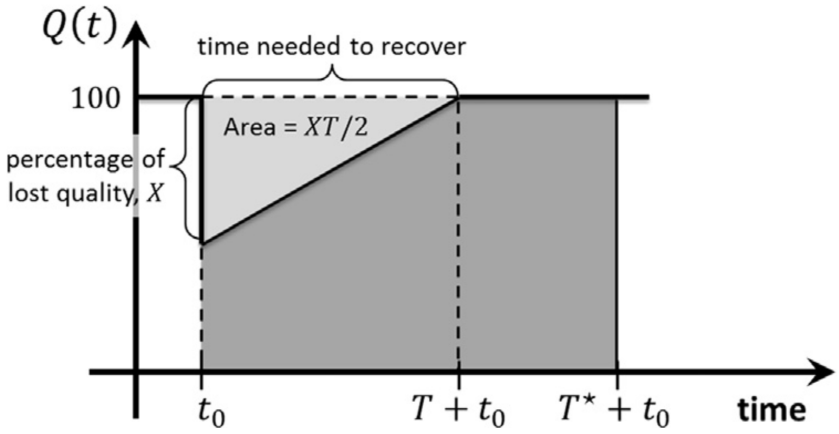

Figure 2.3. Zobel's resilience visualization (adapted from Zobel (2011))

Rose (2007) defined economic resilience as "the ability of an entity or system to maintain system functionally when a disruption occurs." This metric measures the ratio of the avoided drop in system output and the maximum possible drop in system output as shown in Figure 2.4.

The proposed metric, provided in Equation (2.3), is classified as a deterministic static

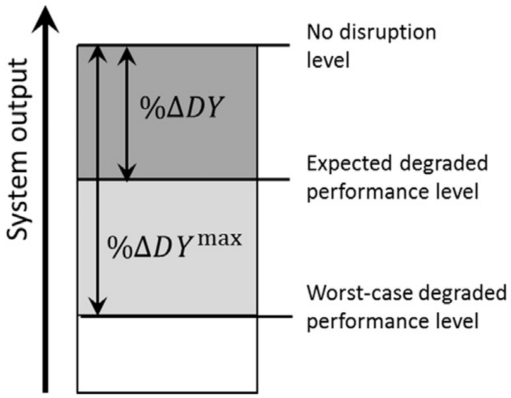

Figure 2.4. Illustration of the economic resilience measure (adapted from Rose (2007))

model, where $\%\Delta DY$ is the difference between non-disrupted and expected disrupted system performance and $\%\Delta DY^{\max}$ is the difference between non-disrupted and worst-case disrupted system performance:

$$R = \frac{\%\Delta DY^{\max} - \%\Delta DY}{\%\Delta DY^{\max}} \tag{2.3}$$

Rose (2007) also considered the time-dependent aspects of recovery in his definition of dynamic resilience (DR):

$$DR = \sum_{i=1}^{N} SO_{HR}(t_i) - SO_{WR}(t_i) \tag{2.4}$$

The DR measure is a function of SO_{HR}, the output of the system under hastened recovery, and SO_{WR}, the system's output without hastened recovery, where t_i is the ith time step during recovery and N is the number of time steps considered. DR is presented graphically in Figure 2.5. Note that the dynamic economic resilience is not bounded between 0 and 1, which does not provide a convenient understanding of the score.

Henry and Ramirez-Marquez (2012) developed a time-dependent resilience metric that quantifies resilience as ratio of recovery to loss. Given that the performance of the system at a point in time is measured with performance function $\varphi(t)$, three system states

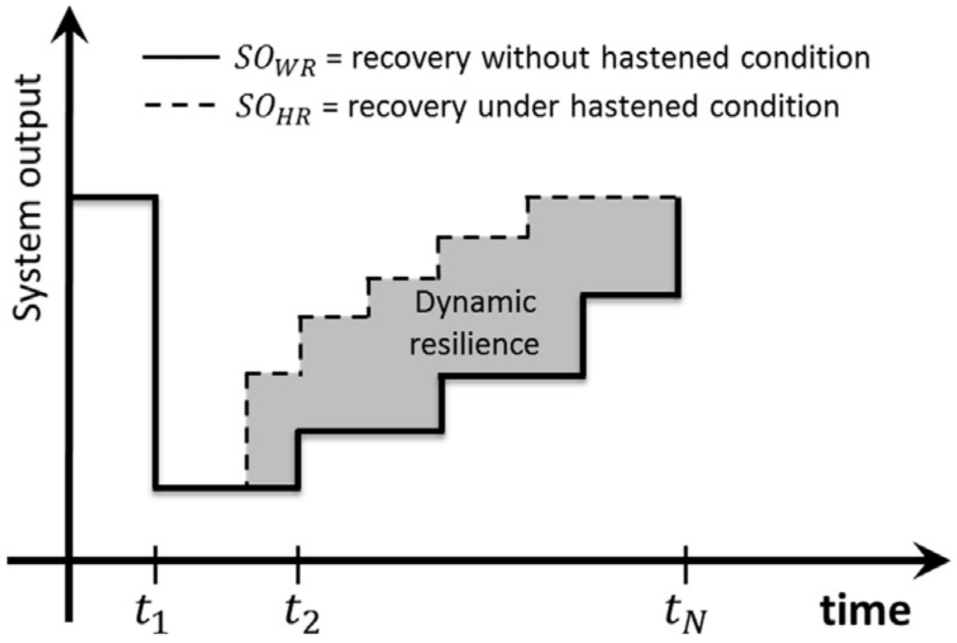

Figure 2.5. The dynamic economic resilience (adapted from Rose (2007))

that are important in quantifying resilience are represented in Figure 2.6: (i) the stable original state which represents normal functionally of a system before disruption occurs, starts from time t_0 and ends by time t_e, (ii) the disrupted state, which is brought about by a disruptive event (e^j) at time t_e whose effects set in until time t_d, describes the performance of the system from time t_d to t_s, (iii) the stable recovered state which refers to the new steady state performance level once the recovery action initiated at time t_s is over. The time-dependent measure of resilience is defined mathematically as follows:

$$Я_{\varphi}\left(t \mid e^j\right) = \frac{\varphi\left(t \mid e^j\right) - \varphi\left(t_d \mid e^j\right)}{\varphi\left(t_0\right) - \varphi\left(t_d \mid e^j\right)} \tag{2.5}$$

Notation Я was adopted as R is commonly reserved for reliability. The mathematical formulation indicates that the numerator of this metric implies recovery up to time t, while the denominator refers to the total loss due to disruption e_j.

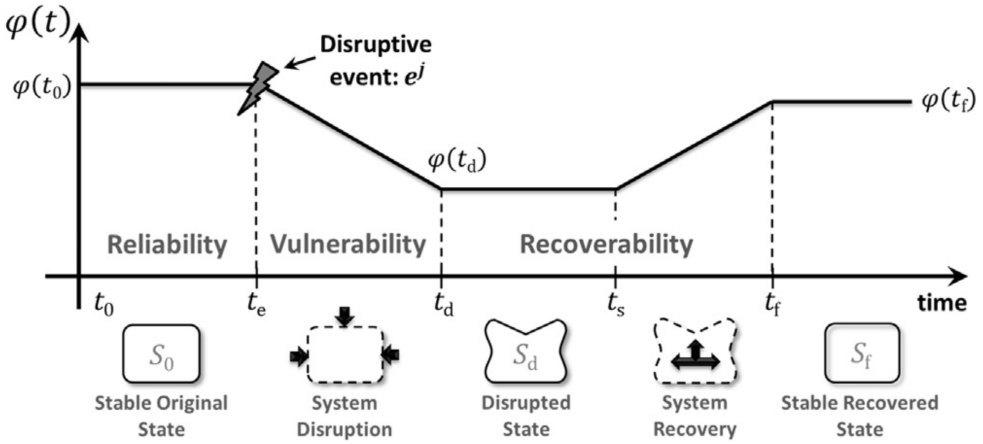

Figure 2.6. System state transition to describe resilience (adapted from Henry and Ramirez-Marquez (2012))

Chen and Miller-Hooks (2012) introduced an indicator for measuring resilience in transportation networks. The resilience indicator, represented in Equation (2.6), quantifies the post-disruption expected fraction of demand that, for a given network, can be satisfied within pre-determined recovery budgets. Parameter d_w quantifies the maximum demand that can be satisfied for origin–destination (O–D) pair w following a disruption, and D_w is demand that can be satisfied for O–D pair w prior to the disruption. A limitation of this formulation includes its lack of specifying the contribution of pre-disaster and post-disaster recovery activities, especially in accounting for recovery time.

$$\text{Resilience } = E\left(\sum_{w\in W} d_w / \sum_{w\in W} D_w\right) = \frac{1}{\sum_{w\in W} D_w} E\left(\sum_{w\in W} d_w\right) \tag{2.6}$$

Orwin and Wardle (2004) introduced a measurement metric by linking resilience with instantaneous and maximum disturbance as follows:

$$\text{Resilience} = \left(\frac{2\times|E_{\max}|}{|E_{\max}|+|E_j|}\right) - 1 \tag{2.7}$$

where E_{max} refers to the maximum intensity of absorbable force without perturbing

the system's function, and E_j refers to the magnitude of the disturbance's effect on safety at time T_j. The resilience measure is ranged between 0 and 1 (when $E_j = 0$).

Enjalbert *et al.* (2011) introduced local and global resilience assessment metrics for public transportation systems, as shown in Equations (2.8) and (2.9), respectively. Function $S(t)$ is a safety indicator of the system, measured as the "sum of effect of factors which can affect the system safety" (Enjalbert *et al.*, 2011). Local resilience measures instantaneous resilience based on the safety indicator, and global resilience is obtained by integrating local resilience over time, between when the disturbance effect commences (represented by t_b) and the end time of disturbance effect (represented by t_e).

$$\text{Local resilience } = \frac{dS(t)}{dt} \tag{2.8}$$

$$\text{Global resilience} = \int_{t_b}^{t_e} \text{local resilience} = \int_{t_b}^{t_e} \frac{dS(t)}{dt} \tag{2.9}$$

Francis and Bekera (2014) proposed a dynamic resilience metric ρ_i for event i as shown in Equations (2.10)–(2.11). In their mathematical representation, S_p refers to the speed of recovery, F_o is the performance level of the system at its original state, F_r is the performance level at a new stable level after recovery efforts, and F_d is the performance level immediately following the disruption.

$$\rho_i = S_p \frac{F_r}{F_o} \frac{F_d}{F_o} \tag{2.10}$$

$$S_p = \begin{cases} (t_\delta / t_r^*) \exp\left[-a\left(t_r - t_r^*\right)\right] & \text{for } t_r \geq t_r^* \\ (t_\delta / t_r^*) & \text{otherwise} \end{cases} \tag{2.11}$$

Speed of recovery in Equation (2.11) assumes exponential growth, with t_δ representing the slack time or the maximum amount of time post-disaster that is acceptable before recovery ensues, t_r representing the time to final recovery or time to reach a new equilibrium state, t_r^* representing the time to complete the initial recovery actions, and a representing the parameter controlling the "decay" in resilience until the new equilibrium is met. This measure describes the absorptive capacity in terms of the proportion of original steady-state functionality maintained after the new steady-state functionality, F_r/F_0.

Cimellaro *et al.* (2010) expressed resilience in terms of quality of service, as shown in Equation (2.12), where α is a weighting factor representing the importance of per-disruption and post-disruption service qualities, $Q_1(t)$ and $Q_2(t)$ are the quality service of the system before and after the disruption, respectively, and T_{LC} is the control time of the system. This metric is intended to be applied to measure healthcare resilience using patients waiting time as an indicator of service quality.

$$R = \alpha \int_{T_{LC}} \frac{Q_1(t)}{T_{LC}} dt + (1-\alpha) \int_{T_{LC}} \frac{Q_2(t)}{T_{LC}} dt \tag{2.12}$$

Fang (2015) suggested a resilience measure suitable to represent different systems and performance measures (such as amount of flow in networks and number of customers served in service sectors). The measure is shown in Equation (2.13) as the ratio between the cumulative system performance that has been restored from disruption to time t and the cumulative target system performance without disruption; $F(t)$ in this metric represents the system performance function and $TF(t)$ is the target system performance function. The provided metric is bounded between 0 and 1, undefined when $F(t_d) = TF(t)$, which means that there is no loss in performance, and undefined when $t < t_d$ since restoration actions

take place after disruption.

$$R(t) = \frac{\int_{t_d}^{t} [F(\tau) - F(t_d)]\, d\tau}{\int_{t_d}^{t} [TF(\tau) - F(t_d)]\, d\tau}, t \geq t_d \tag{2.13}$$

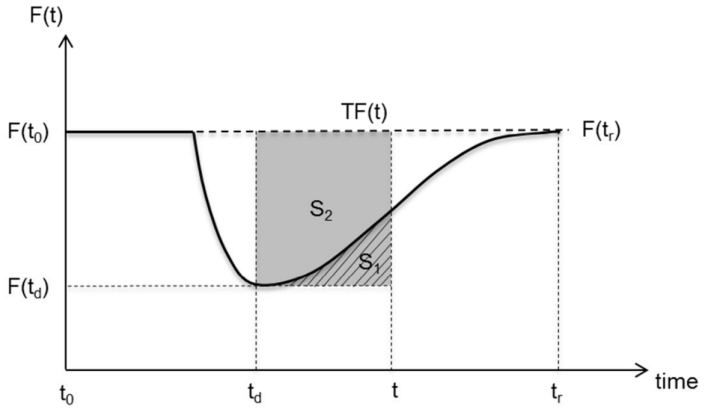

Figure 2.7. Conceptual illustration of Fang's resilience metric (adapted from Fang (2015)

A list of deterministic measures along with their parameters and variables are summarized below in Table 2.1.

Table 2.1. Resilience deterministic measures by reference

Reference	Measure	Parameters and variables
Bruneau *et al.* (2003)	$RL = \int_{t_0}^{t_1} [100 - Q(t)]dt$	• t_0: the time at which the disruption occurs • t_1: the time at which the community returns to its normal pre-disruption state • $Q(t)$: the quality of the community infrastructure at time t

Table 2.1 (Cont.)

Zobel (2011)	$R(X,T) = \frac{T^* - XT/2}{T^*} = 1 - \frac{XT}{2T^*}$	• $X \in [0,1]$: the percentage of functionality lost after a disruption • $T \in [0,T^*]$: the time required for full recovery • T^*: a suitably long time interval over which lost functionality is determined
Rose (2007)	$R = \frac{\%\Delta DY^{\max} - \%\Delta DY}{\%\Delta DY^{\max}}$	• $\%\Delta DY$: the difference in non-disrupted and expected disrupted system performance and • $\%\Delta DY^{\max}$: the difference in non-disrupted and worst-case disrupted system performance
	$DR = \sum_{i=1}^{N} SO_{HR}(t_i) - SO_{WR}(t_i)$	• SO_{HR},: the output of the system under hastened recovery • SO_{WR}: the system's output without hastened recovery • t_i : the ith time step during recovery and • N: the number of time steps considered

Table 2.1 (Cont.)

Henry and Ramirez-Marquez (2012)	$\text{Я}_{\varphi}\left(t \mid e^{j}\right) = \dfrac{\varphi\left(t \mid e^{j}\right) - \varphi\left(t_d \mid e^{j}\right)}{\varphi\left(t_0\right) - \varphi\left(t_d \mid e^{j}\right)}$	• $\varphi(t)$: performance function at time t • e^{j}: disruptive event at time t_e with effect until time t_d • t_s: recovery action initiated at time
Chen and Miller-Hooks (2012)	$\text{Resilience} = E\left(\sum_{w \in W} d_w / \sum_{w \in W} D_w\right) = \dfrac{1}{\sum_{w \in W} D_w} E\left(\sum_{w \in W} d_w\right)$	• d_w: quantifies the maximum demand that can be satisfied for origin–destination (O–D) pair w following a disruption • D_w: demand that can be satisfied for O–D pair w prior to the disruption
Orwin and Wardle (2004)	$\text{Resilience} = \left(\dfrac{2 \times \lvert E_{\max}\rvert}{\lvert E_{\max}\rvert + \lvert E_j\rvert}\right) - 1$	• E_{max}: the maximum intensity of absorbable force without perturbing the system's function, • E_j: the magnitude of the disturbance's effect on safety at time T_j

Table 2.1 (Cont.)

Enjalbert *et al.* (2011)	$$\text{Local resilience } = \frac{dS(t)}{dt}$$ $$\text{Global resilience} = \int_{t_b}^{t_e} \text{local resilience} = \int_{t_b}^{t_e} \frac{dS(t)}{dt}$$	• $S(t)$: sum of effect of factors that can impact the system safety • t_b: time when the disturbance effect commences • t_e: end time of disturbance effect
Francis and Bekera (2014)	$$\rho_i = S_p \frac{F_r}{F_o} \frac{F_d}{F_o}$$ $$S_p = \begin{cases} (t_\delta / t_r^*) \exp\left[-a\left(t_r - t_r^*\right)\right] & \text{for } t_r \geq t_r^* \\ (t_\delta / t_r^*) & \text{otherwise} \end{cases}$$	• S_p: refers to the speed of recovery • F_o: the performance of level of the system at its original state • F_r: the performance level at a new stable level after recovery efforts • F_d: the performance level immediately following the disruption • t_δ: maximum amount of time post-disaster that is acceptable before recovery ensues • t_r: time to final recovery or time to reach a new equilibrium state • t_r^*: time to complete the initial recovery actions • a: parameter controlling the "decay" in resilience until the new equilibrium is met

Table 2.1 (Cont.)

Cimellaro *et al.* (2010)	$R = \alpha \int_{T_{LC}} \frac{Q_1(t)}{T_{LC}} dt + (1-\alpha) \int_{T_{LC}} \frac{Q_2(t)}{T_{LC}} dt$	• $Q_1(t)$: quality service of the system before disruption • $Q_2(t)$: quality service of the system after disruption • α: weighting factor representing the importance $Q_1(t)$ and $Q_2(t)$ • T_{LC}: the control time of the system
Fang (2015)	$R(t) = \frac{\int_{t_d}^{t} [F(\tau) - F(t_d)] \, d\tau}{\int_{t_d}^{t} [TF(\tau) - F(t_d)] \, d\tau}, t \geq t_d$	• $F(t)$: system performance function • $TF(t)$: target system performance function • t_d: disruption time

2.3.2 Stochastic measures

Chang and Shinozuka (2004) introduced a probabilistic approach for assessing resilience, measured with two elements: (i) loss of performance and (ii) length of recovery. According to Chang and Shinozuka (2004), resilience is defined as the probability of the initial system performance loss after a disruption being less than the maximum acceptable performance loss with the time to full recovery being less than the maximum acceptable

disruption time. In mathematical form, the measure is shown in Equation (2.14):

$$R = P(A|i) = P\left(r_0 < r^* \text{ and } t_1 < t^*\right) \tag{2.14}$$

where A represents the set of performance standards for maximum acceptable loss of system performance, r^*, and maximum acceptable recovery time, t^*, for a disruption of magnitude i.

Ouyang *et al.* (2012) developed a stochastic time-dependent metric for measuring "annual resilience" under multi-hazard events, shown in Equation (2.15). Their primary metric measures the mean ratio of the area between the actual performance curve, $P(t)$, and the time axis to the area between the target performance curve, $TP(t)$, and the time axis over a length of time T. In their mathematical formulation, $P(t)$ is modeled as a stochastic process and multiple hazards can be included with the $\sum_{n=1}^{N(T)} AIA_n\left(t_n\right)$ term, where n refers to the nth event, $N(T)$ is the total number of events that occur during T, t_n is a random variable describing the time at which the nth event occurs, and $AIA_n\left(t_n\right)$ is the area between $P(t)$ and $TP(t)$ for the nth event.

$$AR = E\left[\frac{\int_0^T P(t)dt}{\int_0^T TP(t)dt}\right] = E\left[\frac{\int_0^T TP(t)dt - \sum_{n=1}^{N(T)} AIA_n\left(t_n\right)}{\int_0^T TP(t)dt}\right] \tag{2.15}$$

Youn *et al.* (2011) considered both mitigation and contingency strategies to define their resilience metric. The metric, provided in Equations (2.16) and (2.17), is defined as the sum of the passive survival rate (reliability) and proactive survival rate (restoration) following a disruption.

$$\Psi(\text{ resilience }) = R(\text{ reliability}) \ + \rho \text{ (restoration)} \tag{2.16}$$

$$\rho = P\left(E_{mr}|E_{cp}E_{cd}E_{sf}\right) \times P\left(E_{cp}|E_{cd}E_{sf}\right) \times P\left(E_{cd}|E_{sf}\right) \times P\left(E_{sf}\right) \tag{2.17}$$

In this metric, restoration is defined to be the degree of reliability recovery and is calculated as the joint probability of a system failure event, E_{sf}, a correct diagnosis event, E_{cd}, a correct prognosis event, E_{cp}, and a successful recovery action event, E_{mr}. Hence, the measure proposed by Youn *et al.* (2011) accounts for system reliability in assessing resilience, which is a unique feature not found in other resilience measures. In fact, such feature makes it suitable to assess resilience of engineered systems that require a certain degree of reliability in order to balance resilience and reliability. Moreover, the metric is bounded on $[0, 1]$, which makes it suitable for comparison of systems on a normalized scale.

Ayyub (2013) defined a stochastic resilience metric that considers the effects of aging on the system. The system's performance is defined as the difference between the system's strength and load. The metric is shown in Equation (2.18), where T_i is the time to incident, T_f is the time to failure, T_r is the time to recovery, $\Delta T_f = T_f - T_i$ is the duration of failure, and $\Delta T_r = T_r - T_f$ is the duration of recovery.

$$R_e = \frac{T_i + F\Delta T_f + R\Delta T_r}{T_i + \Delta T_f + \Delta T_r} \tag{2.18}$$

The failure profile, F, in Equation (2.18) is a measure of robustness and redundancy, calculated using Equation (2.19). Similarly, the recovery profile, R, measures recoverability with Equation (2.20) while Q represents the system performance.

$$F = \frac{\int_{t_i}^{t_f} f dt}{\int_{t_i}^{t_f} Q dt} \tag{2.19}$$

$$R = \frac{\int_{t_f}^{t_r} r dt}{\int_{t_f}^{t_r} Q dt} \tag{2.20}$$

This metric proposed by Ayyub (2013) is among the most comprehensive resilience measures, prescribing both mitigation (reliability) and contingency (recovery duration) strategies.

Hashimoto *et al.* (1982) defined the resilience of a system as conditional probability of a satisfactory (i.e., non-failure) state in time period $t+1$ given an unsatisfactory state in time period t, shown in Equation (2.21). $S(t)$ represents the state of the system at time t and NF and F represent non-failure and failure states, respectively.

$$R = P\{S(t+1) \in NF | S(t) \in F\} \tag{2.21}$$

Franchin and Cavalieri (2014) introduced a probabilistic metric for assessing infrastructure resilience in the presence of an earthquake. Their definition of resilience is based on the efficiency of the spatial distribution of an infrastructure network. The efficiency of two nodes in an infrastructure network is defined as being inversely proportional to their shortest distance.

$$R = \frac{1}{P_D E_0} \int_0^{P_D} E\left(P_r\right) dP_r \tag{2.22}$$

The metric is provided in Equation (2.22), where P_D is the fraction of displaced population, E_0 is the efficiency of the city network before the earthquake, P_r is the measure of progress of recovery, and $E(P_r)$ is the recovery curve of the fraction of the displaced population. In their study, the efficiency of a city road network is measured in terms of population density. P_D in this metric is stochastic which makes the suggested measure stochastic; also, the measure is restricted between 0 and 1.

Table 2.2. Resilience Stochastic measures by reference

Reference	Measure	Parameters & Variables
Chang and Shinozuka (2004)	$R = P(A\|i) = P\left(r_0 < r^* \text{ and } t_1 < t^*\right)$	• r^*: maximum acceptable loss of system performance • t^*: maximum acceptable recovery time • A: set of performance standards for r^* and t^* • i: magnitude of disruption
Ouyang *et al.* (2012)	$RAR = E\left[\frac{\int_0^T P(t)dt}{\int_0^T TP(t)dt}\right] = E\left[\frac{\int_0^T TP(t)dt - \sum_{n=1}^{N(T)} AIA_n\left(t_n\right)}{\int_0^T TP(t)dt}\right]$	• $P(t)$: the actual performance curve • $TP(t)$: the target performance curve • $AIA_n\left(t_n\right)$: the area between $P(t)$ and $TP(t)$ for the nth event • $N(T)$: the total number of events that occur during T
Youn *et al.* (2011)	$\Psi(\text{ resilience }) = R(\text{ reliability}) + \rho\ (\text{restoration})$ $\rho = P\left(E_{mr}\|E_{cp}E_{cd}E_{sf}\right) \times P\left(E_{cp}\|E_{cd}E_{sf}\right) \times P\left(E_{cd}\|E_{sf}\right) \times P\left(E_{sf}\right)$	• E_{sf}: system failure event • E_{cd}: a correct diagnosis event • E_{cp}: a correct prognosis event • E_{mr}: a successful recovery action event

Table 2.2 (Cont.)

Ayyub (2013)	$R_e = \frac{T_i + F\Delta T_f + R\Delta T_r}{T_i + \Delta T_f + \Delta T_r}$ $F = \frac{\int_{t_i}^{t_f} f dt}{\int_{t_i}^{t_f} Q dt}$ $R = \frac{\int_{t_f}^{t_r} r dt}{\int_{t_f}^{t_r} Q dt}$	• T_i: time to incident • T_f: time to failure • T_r: time to recovery • $\Delta T_f = T_f - T_i$: the duration of failure • $\Delta T_r = T_r - T_f$: the duration of recovery • F: the failure profile • R: recoverability measure • Q: system performance
Hashimoto *et al.* (1982)	$R = P\{S(t+1) \in NF \mid S(t) \in F\}$	• $S(t)$: state of the system at time t • F: represent failure state • NF: represents non-failure state
Franchin and Cavalieri (2014)	$R = \frac{1}{P_D E_0} \int_0^{P_D} E(P_r)\, dP_r$	• P_D: the fraction of displaced population • E_0: efficiency of the city network before the earthquake • P_r: the measure of progress of recovery • $E(P_r)$: the recovery curve of the fraction of the displaced population

2.4 Discussion and conclusion

Over the past few years, the significance of the concept of resilience has been well recognized among researchers and practitioners. Many efforts have been devoted to quantify resilience in engineering systems and differentiate this concept with other close-related ones such as reliability, robustness, and flexibility. These efforts started by defining resilience theoretically in different fields of study in order to develop suitable mathematical representations for this concept in different applications, especially in networked systems such as critical infrastructures.

Resilience measures could be classified broadly into deterministic and stochastic measures as seen in our review. This classification could also be further extended into static, where the measure does not depend on time, and dynamic, where functions included in the metric are time-dependent. Such measures have helped researchers develop optimization models to improve resilience by considering these metrics as the objective function to be maximized in such models.

To sum up, the term "resilience" is increasingly used in research journals, government documents, and media. Different measures and optimization models have been developed to quantify it in engineering and networked systems. Nonetheless, there is more work needed to make resilience assessment usable in more applications. For instance, some of the resilience quantification research gaps are evaluating resilience of communities (Barkerring *et al.*, 2018; Karakoc *et al.*, 2019; Kelly *et al.*, 2015), developing resilience standards and guidelines in order for stakeholders to apply (NIST, 2016), and integrating tri-level measures of resilience planning, mitigation, and restoration. Such research directions need to be explored by the

resilience-interested research community.

References

Allenby, B., & Fink, J. (2000). Social and ecological resilience: Toward inherently secure and resilient societies. *Science*, *24*(3), 347–364.

ASME, American Society of Mechanical Engineers . (2009). *Innovative Technological Institute (ITI).* Washington, DC.

Ayyub, B. M. (2013). Systems resilience for multihazard environments: Definition, metrics, and valuation for decision making. *Risk Analysis*, *34*(2), 340–355. doi: 10.1111/risa.12093

Barkerring, K., Karakoc, D., & Almoghathawi, Y. (2018). Interdependent infrastructure network restoration from a community resilience perspective. In *Safety and reliability – safe societies in a changing world* (pp. 1261–1267). CRC Press. doi: 10.1201/9781351174664-159

Bruneau, M., Eguchi, R. T., Lee, G. C., O'Rourke, T. D., Reinhorn, A. M., Shinozuka, M., ... Chang, S. E. (2003). A framework to quantitatively assess and enhance the seismic resilience of communities. *Earthquake Spectra*, *19*(4), 733–752. doi: 10.1193/1.1623497

Chang, S. E., & Shinozuka, M. (2004). Measuring improvements in the disaster resilience of communities. *Earthquake Spectra*, *20*(3), 739–755. doi: 10.1193/1.1775796

Chen, L., & Miller-Hooks, E. (2012). Resilience: An indicator of recovery capability in intermodal freight transport. *Transportation Science*, *46*(1), 109–123. doi: 10.1287/trsc.1110.0376

Cimellaro, G. P., Reinhorn, A. M., & Bruneau, M. (2010). Seismic resilience of a hospital system. *Structure and Infrastructure Engineering*, *6*(1-2), 127–144. doi: 10.1080/15732470802663847

Dinh, L. T., Pasman, H., Gao, X., & Mannan, M. S. (2012). Resilience engineering of industrial processes: Principles and contributing factors. *Journal of Loss Prevention in the Process Industries*, *25*(2), 233–241. doi: 10.1016/j.jlp.2011.09.003

DiPietro, G. S., Matthews, H. S., & Hendrickson, C. T. (2014). Estimating economic and resilience consequences of potential navigation infrastructure failures: A case study of the monongahela river. *Transportation Research Part A: Policy and Practice*, *69*, 142–164. doi: 10.1016/j.tra.2014.08.009

Enjalbert, S., Vanderhaegen, F., Pichon, M., Ouedraogo, K. A., & Millot, P. (2011).

Assessment of transportation system resilience. In C. Cacciabue, M. Hjälmdahl, A. Luedtke, & R. Chuman (Eds.), *Human modelling in assisted transportation* (pp. 335–341). Springer Milan. doi: 10.1007/978-88-470-1821-1_36

Fang, Y. (2015). *Critical infrastructure protection by advanced modelling, simulation and optimization for cascading failure mitigation and resilience* (Theses, Ecole Centrale Paris). Retrieved from https://tel.archives-ouvertes.fr/tel-01150318

Franchin, P., & Cavalieri, F. (2014). Probabilistic assessment of civil infrastructure resilience to earthquakes. *Computer-Aided Civil and Infrastructure Engineering*, *30*(7), 583–600. doi: 10.1111/mice.12092

Francis, R., & Bekera, B. (2014). A metric and frameworks for resilience analysis of engineered and infrastructure systems. *Reliability Engineering & System Safety*, *121*, 90–103. doi: 10.1016/j.ress.2013.07.004

Haimes, Y. Y. (2009). On the definition of resilience in systems. *Risk Analysis*, *29*(4), 498–501. doi: 10.1111/j.1539-6924.2009.01216.x

Hashimoto, T., Stedinger, J. R., & Loucks, D. P. (1982). Reliability, resiliency, and vulnerability criteria for water resource system performance evaluation. *Water Resources Research*, *18*(1), 14–20. doi: 10.1029/wr018i001p00014

Henry, D., & Ramirez-Marquez, J. E. (2012). Generic metrics and quantitative approaches for system resilience as a function of time. *Reliability Engineering and System Safety*, *99*, 114–122. doi: 10.1016/j.ress.2011.09.002

Hollnagel, E. (2011). Prologue: the scope of resilience engineering. In E. Hollnagel, J. Paries, D. D. Woods, & J. Wreathall (Eds.), *Resilience engineering in practice: A guidebook* (pp. xxix–xxxix). Boca Raton, FL: CRC Press.

Hollnagel, E., Woods, D. D., & Leveson, N. (2006). *Resilience engineering: Concepts and precepts*. Aldershot, UK: Ashgate Publishing, Ltd.

Hosseini, S., Barker, K., & Ramirez-Marquez, J. E. (2016). A review of definitions and measures of system resilience. *Reliability Engineering and System Safety*, *145*, 47–61. Retrieved from https://www.sciencedirect.com/science/article/pii/S0951832015002483 doi: 10.1016/j.ress.2015.08.006

Karakoc, D. B., Almoghathawi, Y., Barker, K., González, A. D., & Mohebbi, S. (2019). Community resilience-driven restoration model for interdependent infrastructure networks. *International Journal of Disaster Risk Reduction*, *38*, 101228. doi: 10.1016/j.ijdrr.2019.101228

Kelly, C., Ferrara, A., Wilson, G. A., Ripullone, F., Nolè, A., Harmer, N., & Salvati,

L. (2015). Community resilience and land degradation in forest and shrubland socio-ecological systems: Evidence from gorgoglione, basilicata, italy. *Land Use Policy*, *46*, 11–20. doi: 10.1016/j.landusepol.2015.01.026

Lindström, M., & Olsson, S. (2009). The european programme for critical infrastructure protection. In *Crisis management in the european union* (pp. 37–59). Springer Berlin Heidelberg. doi: 10.1007/978-3-642-00697-5_3

Morshedlou, N., Barker, K., Nicholson, C. D., & Sansavini, G. (2018). Adaptive capacity planning formulation for infrastructure networks. *Journal of Infrastructure Systems*, *24*(4), 04018022. doi: 10.1061/(asce)is.1943-555x.0000432

NIAC, National Infrastructure Advisory Council (US). (2009). *Critical infrastructure resilience: Final report and recommendations.* National Infrastructure Advisory Council.

NIST, National Institute of Standards and Technology. (2016). *Community resilience planning guide for buildings and infrastructure systems : volume II* (Tech. Rep.). Gaithersburg, MD: National Institute of Standards and Technology. Available at: https://www.nist.gov/topics/community-resilience/planning-guide. doi: 10.6028/nist.sp.1190v2

Orwin, K., & Wardle, D. (2004). New indices for quantifying the resistance and resilience of soil biota to exogenous disturbances. *Soil Biology and Biochemistry*, *36*(11), 1907–1912. doi: 10.1016/j.soilbio.2004.04.036

Ouyang, M., Dueñas-Osorio, L., & Min, X. (2012). A three-stage resilience analysis framework for urban infrastructure systems. *Structural Safety*, *36-37*, 23–31. doi: 10.1016/j.strusafe.2011.12.004

Ouyang, M., & Wang, Z. (2015). Resilience assessment of interdependent infrastructure systems: With a focus on joint restoration modeling and analysis. *Reliability Engineering & System Safety*, *141*, 74–82. doi: 10.1016/j.ress.2015.03.011

Park, J., Seager, T. P., Rao, P. S. C., Convertino, M., & Linkov, I. (2012). Integrating risk and resilience approaches to catastrophe management in engineering systems. *Risk Analysis*, *33*(3), 356–367. doi: 10.1111/j.1539-6924.2012.01885.x

Pregenzer, A. L. (2011). *Systems resilience : a new analytical framework for nuclear nonproliferation.* (Vol. 8; Tech. Rep.). Albuquerque, NM. Retrieved from http://prod.sandia.gov/techlib/access-control.cgi/2011/119463.pdf doi: 10.2172/1034890

Rose, A. (2007). Economic resilience to natural and man-made disasters: Multidisciplinary origins and contextual dimensions. *Environmental Hazards*, *7*(4), 383–398. doi: 10.1016/j.envhaz.2007.10.001

Shafieezadeh, A., & Burden, L. I. (2014). Scenario-based resilience assessment framework for critical infrastructure systems: Case study for seismic resilience of seaports. *Reliability Engineering & System Safety*, *132*, 207–219. doi: 10.1016/j.ress.2014.07.021

TISP, The Infrastructure Security Partnership. (2006). Regional disaster resilience: a guide for developing on action plan. Reston, VA: American Society of Civil Engineers.

Vugrin, E. D., & Camphouse, R. C. (2011). Infrastructure resilience assessment through control design. *International Journal of Critical Infrastructures*, *7*(3), 243. doi: 10.1504/ijcis.2011.042994

Vugrin, E. D., Warren, D. E., Ehlen, M. A., & Camphouse, R. C. (2010). A framework for assessing the resilience of infrastructure and economic systems. In K. Gopalakrishnan & P. Ssustainable (Eds.), *Sustainable and resilient critical infrastructure systems* (pp. 77–116). Berlin. doi: 10.1007/978-3-642-11405-2_3

Youn, B. D., Hu, C., & Wang, P. (2011). Resilience-driven system design of complex engineered systems. In *Proceedings of the asme 2011 international design engineering technical conferences and computers and information in engineering conference. volume 5: 37th design automation conference, parts a and b.* Washington, DC: ASMEDC. doi: 10.1115/detc2011-48314

Zobel, C. W. (2011). Representing perceived tradeoffs in defining disaster resilience. *Decision Support Systems*, *50*(2), 394–403. doi: 10.1016/j.dss.2010.10.001

Chapter 3

Risk and Resilience-Based Optimal Post-Disruption Restoration for Critical Infrastructures under Uncertainty

Basem A. Alkhaleel, Haitao Liao, Kelly M. Sullivan

Abstract

Post-disruption restoration of critical infrastructures (CIs) often faces uncertainties associated with the required repair tasks and the related transportation network. However, such challenges are often overlooked in most studies on the improvement of CI resilience. In this chapter, two-stage risk-averse and risk-neutral stochastic optimization models are proposed to schedule repair activities for a disrupted CI network with the objective of maximizing system resilience. Both models are developed based on a scenario-based optimization technique that accounts for the uncertainties of the repair time and the travel time spent on the underlying transportation network. Given the large number of uncertainty realizations associated with post-disruption restoration tasks, an improved fast forward algorithm based on a wait-and-see solution methodology is provided to reduce the number of chosen scenarios, which results in the desired probabilistic performance metrics. To assess the risks associated with post-disruption scheduling plans, a conditional value-at-risk (CVaR) metric is incorporated into the optimization models through a scenario reduction algorithm. The proposed restoration framework is applied to the French RTE electric power network with a DC power flow procedure, and the results demonstrate the added value of using the stochastic optimization models incorporating the travel times related to repair activities. It

is essential that risk-averse decision-making under uncertainty largely impacts the optimum schedule and the expected resilience, especially in the worst-case scenarios.

3.1 Introduction

3.1.1 Background

Critical infrastructures (CIs) are defined as networks of independent, mostly privately-owned, man-made systems and processes that function collaboratively and synergistically to produce and distribute a continuous flow of essential goods and services (Ellis *et al.*, 1997). Specially, those CI networks for electric power, water distribution, natural gas, transportation, and telecommunications are the backbone of modern societies (Almoghathawi *et al.*, 2019; Zio, 2016). Their continuous and proper functioning provides the fundamental services that support the economic productivity, security, and quality of life of citizens.

Unfortunately, CI networks are often subject to different types of disruptive events, including random failures, technical accidents, malevolent attacks, and natural hazards, which could affect their performance unpredictably and have direct consequences on the communities and people's daily lives. Such disruptions become inevitable in today's increasingly complex and risky operating environment (Helbing, 2013). Hence, for several years, the United States (U.S.), as well as many countries around the globe, have shown an increasing interest in effectively preparing for and responding promptly to such disruptive events (Karagiannis *et al.*, 2017; O'Donnell, 2013; White House, 2013). Indeed, it is increasingly important to not only protect the current CI networks against disruption, but also to be able to restore them once they are disrupted.

In 2011, the U.S. president released a report setting a four-pillared strategy for modernizing the electric grid (Executive Office of the President, 2011). The presidential

initiative directed billions of dollars toward the investments in 21st century smart grid technologies aiming at increasing the grid's efficiency, reliability, and resilience, and at making the grid less vulnerable to outages and reducing the time it takes to restore power after an outage. A subsequent report in 2013 has addressed explicitly the importance of increasing electric grid resilience, especially against weather-related outages, and the economic benefits of resilience improvement (Executive Office of the President, 2013). According to the report, severe weather is the leading cause of power outages in the U.S. In fact, between 2003 and 2012, an estimated 679 widespread power outages occurred due to severe weather. Such weather-outages are expected to rise as climate change increases the frequency and intensity of hurricanes, blizzards, floods, and other extreme weather events (Zamuda *et al.*, 2013). In addition, weather-related outages are estimated to have cost the U.S. economy an inflation-adjusted annual average of $18 billion to $33 billion (Executive Office of the President, 2013). The annual estimation could reach $70 billion according to another congressional study (Campbell & Lowry, 2012).

It is worth pointing out that the annual losses fluctuate significantly and reach the greatest in the years of major storms. For example, Hurricane Sandy, which struck the entire East Coast of the U.S. in October 2012, caused significant damages to the infrastructure systems, resulting in an estimated cost of $33 billion for repairs and cleanup in the aftermath and an approximate total of $65 billion in damages and economic loss (Force, 2013). Moreover, about 8.5 million customers were left without power, and the commuting time increased significantly due to the disabled roads and public transit. When Hurricane Harvey struck the southern coast, it caused about $200 billion in damages and $20 to $30 billion in lost economic output (CNBC, 2017). According to the U.S. Federal

Emergency Management Agency (FEMA), nearly 40,000 people were in the shelters in Texas and Louisiana, considering the most were without essential lifeline services, over 160 drinking water systems were damaged with 50 of them being totally shut down, and 800 water waste facilities were partially damaged (FEMA, 2017). Furthermore, nearly 80,000 homes had at least 18 inches of floodwater, 23,000 of which had more than 5 feet, 24 hospitals were evacuated, 61 communities lost drinking water capability, 23 ports were closed, 781 roads were impassable, about 780,000 people evacuated their homes, and first responders rescued 122,331 people (FEMA, 2017). Altogether, the experience from these events underlines the needs for timely, efficient, and effective network restoration and recovery activities in the aftermath of large-scale disruptive events, so that both short-term and long-term reliance on the infrastructure networks can be assured.

Risk management strategies generally emphasize disruptive events mitigation options in the form of prevention and protection by designing the systems to avoid or absorb undesired events from occurring (Hosseini *et al.*, 2016). While such strategies are crucial to preventing undesired events or consequences, recent events suggest that not all undesired events can be prevented. Natural events such as Hurricane Harvey are among the recent examples of unpreventable disruptions. In fact, this particular event impacted multiple networked systems including the transportation network and power network, which has not been restored fully even after few months of the incident (Manuel, 2013). In a recent report by the European Commission's science and knowledge service, the Joint Research Centre (JRC) has addressed challenges in power grid recovery after natural hazards (Karagiannis *et al.*, 2017). The study covered different natural events and their impact on power grid networks by collecting worldwide data about at least 50 events from different sources including technical

reports, field survey reports, and research papers (Karagiannis *et al.*, 2017). The report used two thresholds to assess power grid recoverability: (1) The restoration of power supply to customers, and (2) The complete repair of the network. Moreover, two of the significant challenges that face recovery actions were found to be the repair times uncertainty and poor access to damaged facilities due to landslides or traffic congestions. In addition, the report was concluded with multiple recommendations to improve power grid recovery ranging from integrating risk-related strategies to stockpiling spare parts for urgent maintenance actions (Luo *et al.*, 2020).

All such recovery planning actions after disruptions are part of the rising concept of resilience, which can be defined generally as the ability of a system or an organization to react and recover from unanticipated disturbances and events (Hollnagel *et al.*, 2006). Resilience, and in particular CI resilience, has emerged in recent years due to the awareness of governments about the possible risks associated with CIs and the catastrophic impacts of various disruptive events affecting CIs (White House, 2013). This has encouraged practitioners and researchers to develop various resilience improvement techniques ranging from system design to recovery optimization (Hosseini *et al.*, 2016). In addition, resilience can be effectively improved by developing optimum plans for timely restoring the disrupted service after the occurrence of a disruptive event. In planning CIs restoration, prioritizing components is key in improving the recovery process. To this end, optimization approaches are typically used to facilitate the identification and scheduling of effective restoration strategies for the rapid reestablishment of system functionality. Many studies have been reported in the literature in the context of post-disruption CI restoration under a mathematical programming framework (Fang & Sansavini, 2017; Nurre & Sharkey, 2014;

Vugrin *et al.*, 2014; Zhang *et al.*, 2018). The main goal is to schedule recovering tasks of failed components in order to accelerate the restoration process (Vugrin *et al.*, 2014).

3.1.2 Related literature

The concept of resilience has been investigated by different disciplinary perspectives and across various application domains. Specially, several definitions of resilience have been offered from an engineering point of view (Hosseini *et al.*, 2016). Many are similar and overlap with a number of existing concepts such as robustness, fault tolerance, flexibility, survivability, and agility, among others. However, most definitions are based around pre- and post-disruption related concepts, such as protection, risk mitigation, adaption and restoration (Barker *et al.*, 2017). In addition, developing mathematical and statistical modeling approaches to improve, analyze and optimize resilience needs resilience quantification to compare proposed models. As a result, in the literature, resilience has been quantified by different approaches and mathematical interpretations (Gasser *et al.*, 2019; Hosseini *et al.*, 2016). Many of these resilience measures try to scale the performance measure as a ratio between the actual level of performance and the desired (undisrupted) level over time (for a full review see Gasser *et al.* (2019) and Hosseini *et al.* (2016)). Some examples are the ratio of the probability of failure and recovery (Li & Lence, 2007), the ratio of the expected degradation and the maximum possible degradation of a system due to a disruption (Rose, 2007), and the measure of system performance (Henry & Ramirez-Marquez, 2012). In this work, the focus will be on post-event resilience-based actions (i.e., restoration and/or recovery).

There are multiple studies addressing post-disruption CI restoration with different

goals and mathematical approaches. Anaya-Arenas *et al.* (2014) and Özdamar and Ertem (2015) reviewed post-disruption restoration plans in humanitarian logistics, such as relief delivery, casualty transportation, and mass evacuation. In addition, considerable research in this area has been focused on specific types of critical infrastructures such as transportation networks and electrical power grids (Morshedlou, 2018). In contrast, other studies developed general restoration models that can be applied to almost any CI network without changes or with slight modifications (e.g., adding power flow constraints in power grids). Although the literature review will not be restricted to one type of CIs models, restrictions associated with a single CI model will be mentioned.

Many of the mathematical models found in the literature are formulated as mixed integer programs (MIPs) and mixed integer linear programs (MILPs). Bryson *et al.* (2002) applied an MIP approach for selecting a set of recovery subplans leading to the greatest benefit to business operation. Matisziw *et al.* (2010) proposed an MIP model to restore networks where the connectivity between pairs of nodes is considered as the performance measure associated with the network. Nurre *et al.* (2012) studied an integrated network design and scheduling problem for the restoration of CI systems. They formulated the problem as an integer programming problem, and a dispatch rule-based heuristic approach was proposed for its efficient solution. To account for power flow law in electrical networks, they adopted the method by Bienstock and Mattia (2007). Furthermore, Nurre and Sharkey (2014) provided a comparative study focusing mainly on model complexity and heuristic dispatch rules for their integer optimization problem.

Regarding cascading failures in power networks, Bienstock and Mattia (2007) proposed an MIP model to protect power grid networks at minimum costs to increase

the networks survivability against cascading failures. Their DC power flow model can be implemented in general MIPs and MILPs by just adding a small set of constraints to control the power flow. To control power transmission networks, Chang and Wu (2011) explored a quantitative method to measure the stability and reliability of electric power networks under the triggered cascading failures. In addition, Bienstock and Grebla (2015) introduced a stochastic algorithm to minimize the lost power load at the termination of the cascade considering noise and errors in the model. Fang *et al.* (2017) introduced a pattern for searching for the optimal limited resource allocation to increase the capacity of some links in electric power networks to be able to maximize the networks resistance to cascading failures.

Multiple infrastructures restoration models can also be found in the literature. Casari and Wilkie (2005) discussed multiple infrastructures restoration when CIs are operated by different firms. Lee II *et al.* (2007) proposed an MIP model to minimize the operating costs for temporary emergency restoration, where network restoration involves selecting the locations of temporary arcs needed to completely reestablish network services over a set of interdependent networks. Ouyang and Wang (2015) studied and compared the effectiveness of five strategies for joint restoration of interdependent infrastructures, and a Genetic Algorithm (GA) was applied to generate recovery sequences. Sharkey *et al.* (2015) studied the restoration of multiple interdependent CI networks under a centralized decision-making framework and suggested an MIP model to solve the problem. Furthermore, González *et al.* (2016) proposed an MIP model for optimizing infrastructure system restoration considering joint restoration due to the geographical interdependence between multiple CI systems. Recently, Garay-Sianca and Pinkley (2021) studied the restoration of interdependent CIs considering the movement of work crews through a damaged transportation network being

restored and proposed an MIP to solve the problem under a deterministic problem setting.

When only transportation networks are concerned, Aksu and Ozdamar (2014) considered a multi-vehicle problem to maximize network accessibility during transportation network recovery by identifying critical blocked links and restoring them with limited resources. Çelik *et al.* (2015) also considered debris removal problems and developed a stochastic debris removal approach over discrete time periods to determine the optimal schedule of blocked links under uncertainty. It was assumed that the information corresponding to clearance time changes as the amount of debris changes, and thus as the information is updated, the restorative vehicles assignment schedule changes. Furthermore, Kasaei and Salman (2016) studied arc routing problems to regain network connectivity by clearing blocked roads, developing heuristic algorithms to attain the maximum benefit gained by network connectivity while minimizing the time horizon. Recently, Iloglu and Albert (2020) proposed a restoration model of transportation networks to deliver critical services after disasters by heuristically optimizing the relocation process of emergency responders to maximize the coverage of emergency services demand over time.

One can see that the vast majority of these studies are based on deterministic assumptions such as complete information on the restoration resources and full knowledge of the activities durations. However, the restoration of infrastructure systems is complicated by the many decisions to be made in a highly uncertain environment exacerbated by the disaster itself, people's reaction, and limited capability of information gathering (Fang & Sansavini, 2019). Several factors introduce uncertainty into the parameters of a disaster situation, e.g., availability of restoration resources, number of repair crews, the time duration for repairing failed components and the accessibility to such failed components through the

related transportation network. Clearly, optimal task planning under uncertainty appears to be the closest to a real-life situation. In addition, existing optimization approaches usually do not account for risk measures related to the execution of the optimal plan. For example, if the time durations of some repair activities were longer than expected, the doubt would be if the suggested plan will still perform well. Obviously, when optimizing CI restoration, risks associated with the restoration plan must be considered to identify the possible worst-case scenarios and alter the plan accordingly. Furthermore, the travel time between failed components may also affect the proposed plan along with the accessibility of components under the transportation network condition.

In the literature, few studies have tackled uncertainty in post-disruption CI restoration. Xu *et al.* (2007) optimized a power network restoration by scheduling inspection, assessment, and repair operations, which were assumed to have random durations with known probability distributions. Instead of solving the stochastic model, the authors used a GA to produce a priority list of repair tasks, which might be suboptimal. Recently, Fang and Sansavini (2019) proposed a stochastic optimization approach for infrastructure restoration under uncertainty and showed the added value of the stochastic model compared to the deterministic counterpart. However, risk measures, the effects of travel time and the impact of different network failure modes were not considered in their model.

3.1.3 Overview and research contributions

The aim of this paper is to schedule restoration actions on failed CI components using multiple maintenance crews by solving a two-stage stochastic optimization model. The first stage schedules repair tasks, and the second stage resolves the CI performance

for each time period. The scheduled tasks have uncertain duration, and the travel times between different tasks are also uncertain. Considering these sources of uncertainty, two variants of the proposed stochastic optimization model are: (1) a risk-neutral model to optimize restoration activities accounting for uncertainty and (2) a conditional value-at-risk (CVaR)-based risk-averse model that enables the decision maker to choose plans that perform well even in worst-case scenarios.

The main contributions of this paper are three-fold. (1) To the best of our knowledge, this is the first paper that incorporates risk measures into resilience-based optimization in the context of post-disruption restoration; (2) it provides a general framework for the generation, selection and reduction of scenarios based on an improved fast forward selection algorithm for resilience optimization; and (3) it provides the first stochastic optimization models that account for the travel time between failed components for post-disruption restoration.

The remainder of this paper is organized as follows. Section 3.2 presents the background and methodology pertinent to our models and summarizes the proposed mathematical formulations. Section 3.3 shows the solution approach used in this paper. Section 3.4 presents a case study on the RTE electric power network to illustrate the use and advantage of the suggested models. Finally, concluding remarks and future research directions are provided in Section 3.5.

3.2 Methodology and model development

3.2.1 Resilience of critical infrastructure

The resilience of a CI is commonly characterized with respect to a measure of performance (e.g., flow, connectivity, amount of demand satisfied) $\varphi(t)$ that evolves over

time (Henry & Ramirez-Marquez, 2012; Hosseini *et al.*, 2016). As depicted in Figure 3.1, let $t_e \leq t_d \leq t_s \leq t_f$ denote instants in time such that (i) a disruptive event occurs at time t_e causing $\varphi(t)$ to begin decreasing; (ii) the effects of the disruption are fully realized at time t_d, causing $\varphi(t)$ to stop decreasing; (iii) recovery of the CI begins at time t_s, causing $\varphi(t)$ to begin increasing; and (iv) recovery of the CI is complete at time t_f, causing $\varphi(t)$ to stop increasing.

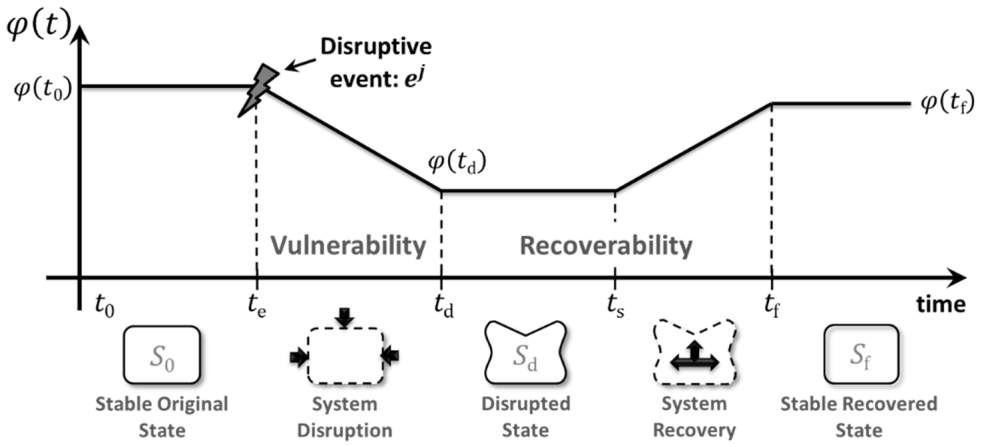

Figure 3.1. Illustration of decreasing network performance $\varphi(t)$ (adapted from Henry and Ramirez-Marquez (2012))

In this study, the focus is on the recovery period after t_d, for which a model that optimizes a restoration plan over a finite planning horizon is proposed. Without loss of generality, let $t \in \{1 \dots T\}$ denote the time periods over which the CI network is restored and $t = t_d = 0$ denote the instant of planning. The system performance $\varphi(t)$, $t \in \{1 \dots T\}$ is defined using a maximum weighted flow performance metric defined over an undirected network $G(V, E)$ that represents the CI. The nodes V are partitioned into supply nodes V^+, transshipment nodes V^*, and demand nodes such that $V^+ \cup V^* \cup V^- = V$. Each supply node $i \in V^+$ has a supply $P_i^+ \in \mathbb{R}_0^+$ that specifies the maximum amount of flow that may

originate at the node within a single time period. Associated with each demand node $j \in V^-$ is a demand $P_j^- \in \mathbb{R}_0^+$ that specifies the maximum amount of flow that may be consumed by the node in one time period. Each edge $\{i, j\} \in E$ has an associated capacity $P_{ij} \in \mathbb{R}_0^+$ that specifies the maximum amount of flow that can be carried on the edge within a single time period.

Given the mechanics expressed above, system performance is defined as the maximum amount of weighted flow consumed by the demand nodes. Let weights $w_j \in \mathbb{Z}^+$ be assigned to each demand node $j \in V^-$. These weights are incorporated in order to enable prioritizing the importance certain types of demand nodes (e.g., it is more important to deliver power to a hospital than to a residential household). Formally, system performance is defined as:

$$\varphi(t) = \sum_{j \in V^-} w_j f_j(t) \tag{3.1}$$

where $f_j(t)$ is the total flow reaching demand node j in time period $t \in \{1 \dots T\}$.

The proposed restoration planning model aims to reestablish connectivity between supply and demand nodes of a disrupted network by repairing damaged components over a fixed planning horizon. Disruptions are modeled by the removal of a subset of edges, without loss of generality, at time $t = 0$. Hereafter, these edges are referred to as *failed edges*. As edges are repaired in subsequent time periods, the system performance $\varphi(t)$ improves. Following Fang *et al.* (2016), the resilience $R(T)$ is defined as the cumulative performance restored during the restoration horizon normalized by dividing by the cumulative performance that would be restored over the same horizon if the system could be restored to pre-disruption performance instantaneously. That is, the system resilience is given by:

$$R(T) = \frac{\sum_{t=1}^{t=T} [\sum_{j \in V^-} w_j f_j(t) - \varphi(0)]}{T(\sum_{j \in V^-} w_j P_j^- - \varphi(0))}, \quad T \geq 1 \tag{3.2}$$

where $\sum_{j \in V^-} w_j P_j^- = \varphi(t_0)$ denotes the system performance if not affected by the disruption.

3.2.2 Risk measure approach

Generally, two-stage stochastic optimization approaches in the literature are risk-neutral. In other words, these approaches incorporate randomness by comparing different solutions on the basis of expectation. Though solutions to risk-neutral models perform well on average, they may be prone to poor performance for certain realizations in practice. Given the non-repetitive nature of CI restoration and its significant impact on society, it is of interest to consider risk-averse models for planning restoration (Noyan, 2012). That is, a desirable restoration plan may seek to limit the chance of realizations that result in poor performance.

Toward stating a risk-averse restoration optimization model in Section 3.2.3, we now summarize the Conditional Value at Risk (CVaR) risk measure (Krokhmal *et al.*, 2002; Rockafellar & Uryasev, 2000) and recap results pertinent to the optimization model. Let Z denote a *loss* random variable with cumulative distribution function (CDF) $F(\cdot)$. The term "loss" is used here to indicate that large values of Z are undesirable. Although this convention seemingly conflicts with the "maximize resilience" objective, it has been employed here because it is standard in the CVaR literature. Section 3.2.3 details the procedure for applying these results to our model.) For a given risk level $\alpha \in [0, 1]$, the Value at Risk (VaR) of Z is defined as:

$$\text{VaR}_\alpha(Z) = \min\{t | F(t) \geq \alpha\} = \min\{t | P(Z \leq t) \geq \alpha\} \tag{3.3}$$

Thus, for a continuous random variable Z, $\text{VaR}_\alpha[Z]$ is the quantile of Z that exceeds the

loss with probability α.

The CVaR for Z with risk level $\alpha \in [0, 1]$ is the expected loss given that the loss is at least $\text{VaR}_\alpha(Z)$, i.e.:

$$\text{CVaR}_\alpha(Z) = \mathbb{E}\left(Z | Z \geq \text{VaR}_\alpha(Z)\right) \tag{3.4}$$

It is known that CVaR can also be expressed as the optimal solution to the optimization problem:

$$\text{CVaR}_\alpha[Z] = \min_{\eta \in \mathbb{R}} \left\{ \eta + \frac{1}{1-\alpha} \mathbb{E}\left[(Z - \eta)_+\right] \right\} \tag{3.5}$$

where $(a)_+ := \max(a, 0)$ (Rockafellar & Uryasev, 2000).

Equation (3.5) enables conveniently formulating risk-averse stochastic optimization models with respect to a CVaR risk measure. Formally, let x be a vector of decision variables, ξ be a random vector of data, and $G(x, \xi)$ be a cost function depending on x and ξ. Then, the CVaR minimization problem:

$$\min_{x \in X} \quad \text{CVaR}_\alpha[G(x, \xi)] \tag{3.6}$$

can be formulated as:

$$\min_{x \in X, \eta \in \mathbb{R}} \quad \left\{ \eta + \frac{1}{1-\alpha} \mathbb{E}\left[(G(x, \xi) - \eta)_+\right] \right\} \tag{3.7}$$

allowing us to linearize the model by expressing the expected value term as a probability-weighted summation of ξ discrete realizations.

3.2.3 Two-stage stochastic optimization model formulation

This section formulates a two-stage stochastic optimization model in which the first stage schedules the repair of failed edges using multiple repair crews, and the second stage

determines the resilience that results under a given realization of the random variables. Rather than optimize explicitly over all random variables, it is common to sample scenarios from their joint distribution. Let Ω denote the set of scenarios. For a given scenario $\omega \in \Omega$, let $ttr_{ij\omega}$ denote the time to repair edge $\{i', j'\} \in E'$ and let $tt_{iji'j'}$ denote the travel time incurred if edge $\{i, j\} \in E'$ and edge $\{i', j'\} \in E'$ are repaired in sequence. It will also be convenient to define $\xi(\omega)$ as a vector specifying the realized values of all random variables in scenario ω.

The maximum weighted flow for each time period $t \in \{1 \dots T\}$ depends on $\xi(\omega)$, and therefore the resilience depends on $\xi(\omega)$ as well. Let $f_{j\omega}(t)$ denote the flow into demand node $j \in V^-$ at time $t \in \{1 \dots T\}$ in scenario $\omega \in \Omega$, and define the resilience $R(T, \xi(\omega))$ in scenario $\omega \in \Omega$ as:

$$R(T, \xi(\omega)) = \frac{\sum_{t=1}^{t=T} [\sum_{j \in V^-} w_j f_{j\omega}(t) - \varphi(0)]}{T(\sum_{j \in V^-} w_j P_j^- - \varphi(0))}, \quad T \geq 1 \tag{3.8}$$

In what follows, $R(T, \xi(\omega))$ is optimized with respect to both expectation and a CVaR risk measure. For simplicity of exposition, the model for the case of maximizing expected resilience is stated first.

Notation

A summary of notation follows. In addition to the notation already defined, the summary defines binary variables z_{ijk} and $x_{iji'j'k}$ in order to encode a restoration plan, auxiliary binary variables $s_{ij\omega}(t)$ and $y_{ijk\omega}(t)$ in order to resolve the status of each disrupted edge for each time period and realized scenario, and flow variables $f_{ij\omega}(t)$ in order to facilitate determining the maximum weighted flow for each time period and realized scenario. The

feasible region of the optimization problem is denoted by X and the sets of decision variables are represented as $\{f,\ s,\ y,\ st,\ z,\ x\}$.

Parameters & Sets

$G(V, E)$	Undirected graph consisting of nodes V and edges E
$\{V^+, V^*, V^-\}$	Set of {supply, transshipment, demand} nodes
T	The number of time periods in restoration planning
E'	Set of failed edges before restoration ($E' \subset E$)
K	Set of repair crews
P_i^+	Supply of node $i \in V^+$ per time period
P_j^-	Demand of node $j \in V^-$ per time period
P_{ij}	Flow capacity of edge $\{i, j\} \in E$ per time period
$tt_{iji'j'\omega}$	Travel time between edge $\{i, j\} \in E'$ and $\{i', j'\} \in E'$ in scenario ω
$ttr_{ij\omega}$	Time to repair edge $\{i, j\} \in E'$ for each scenario ω

Decision Variables

$f_{ij\omega}(t)$	Flow on edge $\{i, j\} \in E$ in time $t \in \{1 \dots T\}$ for each scenario ω
$f_{j\omega}(t)$	Total flow reaching demand node $j \in V^-$ in each scenario ω
$s_{ij\omega}(t)$	Binary variable indicating whether ($s_{ij\omega} = 1$) or not ($s_{ij\omega} = 0$) edge $\{i, j\} \in E$ is functioning at time $t \in \{0 \dots T\}$

$y_{ijk\omega}(t)$	Binary variable that equals 1 if edge $\{i,j\} \in E'$ is assigned to crew $k \in K$ and it is functioning at time $t \in \{0 \dots T\}$; 0 otherwise
$st_{ijk\omega}$	Time at which crew $k \in K$ begins repairing edge $\{i,j\} \in E'$
z_{ijk}	Binary variable that equals 1 if edge $\{i,j\} \in E'$ is assigned to crew $k \in K$; 0 otherwise
$x_{iji'j'k}$	Binary variable that equals 1 if crew $k \in K$ repairs edge $\{i,j\} \in E'$ before edge $\{i',j'\} \in E' \setminus \{i,j\}$

The two-stage stochastic optimization model for maximizing the expected resilience follows:

$$\max_{\{f,s,y,st,z,x\} \in X} \mathbb{E}(R(T, \xi(\omega))) \tag{3.9}$$

s.t.

$$\sum_{ij \in E} f_{ij\omega}(t) - \sum_{ji \in E} f_{ji\omega}(t) \ \leq P_i^+, \ \forall i \in V^+, \ \forall t \in \{1 \dots T\}, \ \forall \omega \in \Omega \tag{3.10}$$

$$\sum_{ij \in E} f_{ij\omega}(t) - \sum_{ji \in E} f_{ji\omega}(t) = 0, \ \forall i \in V^*, \ \forall t \in \{1 \dots T\}, \ \forall \omega \in \Omega \tag{3.11}$$

$$\sum_{ij \in E} f_{ij\omega}(t) - \sum_{ji \in E} f_{ji\omega}(t) \ \leq f_{j\omega}(t) \ , \ \forall j \in V^-, \ \forall t \in \{1 \dots T\}, \ \forall \omega \in \Omega \tag{3.12}$$

$$0 \leq f_{j\omega}(t) \ \leq P_j^-, \ \forall j \in V^-, \ \forall t \in \{1 \dots T\}, \ \forall \omega \in \Omega \tag{3.13}$$

$$-s_{ij\omega}(t) P_{ij} \leq f_{ij\omega}(t) \ \leq s_{ij\omega}(t) P_{ij}, \ \forall ij \in E, \ \forall t \in \{1 \dots T\}, \ \forall \omega \in \Omega \tag{3.14}$$

$$s_{ij\omega}(0) = 0, \forall ij \in E', \ \forall \omega \in \Omega \tag{3.15}$$

$$s_{ij\omega}(0) = 1, \forall ij \in E \backslash E', \ \forall \omega \in \Omega \tag{3.16}$$

$$s_{ij\omega}(t) \ \leq s_{ij\omega}(t+1)\ ,\ \forall ij \in E,\ \forall t \in \{0 \dots T-1\},\ \forall \omega \in \Omega \tag{3.17}$$

$$y_{ijk\omega}(t) \ \leq y_{ijk\omega}(t+1)\ ,\ \forall ij \in E',\ \forall t \in \{0 \dots T-1\},\ \forall k \in K,\ \forall \omega \in \Omega \tag{3.18}$$

$$st_{ijk\omega} + ttr_{ij\omega} + tt_{iji'j'\omega} \leq st_{i'j'k\omega} + Mx_{iji'j'k},\ \forall ij, i'j' \ \in E' \ :\ \{i,j\} \neq \{i',j'\},$$

$$\forall k \in K,\ \forall \omega \in \Omega \tag{3.19}$$

$$st_{ijk\omega} + ttr_{ij\omega} + tt_{iji'j'\omega} \leq st_{i'j'k\omega} + M(1 - x_{iji'j'k}), \forall ij, i'j' \ \in E' \ :\ \{i,j\} \neq \{i',j'\},$$

$$\forall k \in K, \forall \omega \in \Omega \tag{3.20}$$

$$t \geq st_{ijk\omega} + ttr_{ij\omega} - M[1 - y_{ijk\omega}(t)]\ , \forall ij \in E',\ \forall t \in \{1 \dots T\},\ \forall k \in K\ , \forall \omega \in \Omega \tag{3.21}$$

$$\sum_{k \in K} y_{ijk\omega}(t) \ = s_{ij\omega}(t)\ , \forall ij \in E',\ \forall t \in \{0 \dots T\},\ \forall \omega \in \Omega \tag{3.22}$$

$$\sum_{\omega \in \Omega} y_{ijk\omega}(t) \ \geq \sum_{\omega \in \Omega} s_{ij\omega}(T) - |\Omega|(1 - z_{ijk})\ , \forall ij \in E',\ \forall k \in K \tag{3.23}$$

$$\sum_{\omega \in \Omega} y_{ijk\omega}(t) \ \leq |\Omega| z_{ijk}\ , \forall ij \in E',\ \forall k \in K \tag{3.24}$$

$$\sum_{k \in K} z_{ijk} \ = 1\ , \forall ij \in E' \tag{3.25}$$

$$x_{iji'j'k} \in \{0,1\},\ \forall ij \in E',\ \forall i'j' \in E' \setminus \{i,j\},\ \forall k \in K \tag{3.26}$$

$$z_{ijk} \in \{0,1\},\ \forall ij \in E',\ \forall k \in K \tag{3.27}$$

$$y_{ijk\omega}(t) \in \{0,1\},\ \forall ij \in E',\ \forall t \in \{1 \dots T\}, \forall k \in K, \forall \omega \in \Omega \tag{3.28}$$

$$s_{ij\omega}(t) \in \{0,1\},\ \forall ij \in E,\ \forall t \in \{1 \dots T\}, \forall \omega \in \Omega \tag{3.29}$$

$$st_{ijk\omega} \geq 0,\ \forall ij \in E',\ \forall k \in K,\ \forall \omega \in \Omega \tag{3.30}$$

The goal of model (3.9)–(3.30) is to determine a sequence of edges for each crew to restore in order to maximize the expected resilience. Constraints (3.10)–(3.12) are flow

balance constraints. Constraint (3.13) ensures that each demand node $j \in V^-$ consumes no more than its demand P_j^- in every time period, and constraint (3.14) ensures that the flow on each edge $\{i,j\} \in E$ in each time period does not exceed its capacity P_{ij} if the edge is functioning or 0 if the edge is failed. Constraints (3.15) and (3.16) set the initial state of edges to be 0 for failed edges and 1 for other edges. Constraint (3.17) ensures that edges $\{i,j\} \in E'$ remain functioning after being restored, and edges $\{i,j\}$ are functioning for the entire restoration period. Constraint (3.18) impose a similar restriction on the $y_{ijk\omega}(t)$-variables; that is, if an edge $\{i,j\} \in E'$ was repaired by crew $k \in K$ by time period $t \in \{1 \dots T-1\}$, where $y_{ijk\omega}(0) = s_{ij\omega}(0)$ at $t = 0$, then the edge was also repaired by crew k by time period $t+1$. Constraints (3.19)–(3.20) ensure each crew $k \in K$ can work on repairing at most one edge at a time, according to the schedule specified by the $x_{iji'j'k}$-variables. Note that one limitation of the proposed model is that the $x_{iji'j'k}$ decision variables controlling the schedule of failed components are first-stage decision variables (i.e., not indexed by scenario ω) which prevents sequential changes over time. Relative to Constraints (3.19)–(3.20), the $x_{iji'j'k}$-variables, and the $st_{ijk\omega}$-variables, an important detail of the model is that *all* edges are sequenced for repair by *all* crews; however, constraints (3.14) and (3.21)–(3.22) impose that no benefit is gained by (i) completing an edge's restoration after the end of the restoration period or (ii) completing an edge's restoration using a different crew from when it was first restored. Therefore, the effect is equivalent to imposing strictly that each edge is restored at most once and that edges cannot be restored unless they can be completed during the restoration horizon. Defining $ttr_{ij\omega}^{\max}$ and $tt_{iji'j'\omega}^{\max}$ as the maximum repair time parameter of any failed edge in all scenarios and the maximum travel time parameter between

any two failed edges in all scenarios, $M = |E'|(ttr^{\max}_{ij\omega} + tt^{\max}_{iji'j'\omega})$ is sufficiently large in Constraints (3.19)–(3.20). Constraint (3.21) ensures that an edge $\{i, j\} \in E'$ cannot have been restored by crew $k \in K$ by time t unless the restoration start time added to the repair time is no more than t. In Constraint (3.21), it is sufficient to use the same value for M as in constraints (3.19)–(3.20). Constraint (3.22) imposes that an edge $\{i, j\} \in E'$ repaired by crew $k \in K$ by time $t \in \{1 \dots T\}$ is an edge that must be functioning at time t, and it prevents duplicate restoration of an edge by multiple crews. Constraints (3.26)–(3.29) require the $x_{iji'j'k}$-, z_{ijk}-, $y_{ijk\omega}(t)$-, and $s_{ij\omega}(t)$ variables to to be binary, and Constraint (3.30) imposes that no repair tasks begin prior to time $t = 0$.

The risk-neutral model (3.9)–(3.30) can be reformulated using a CVaR objective by first introducing the following resilience loss function:

$$\Delta R(T, \xi(\omega)) = 1 - R(T, \xi(\omega)) \tag{3.31}$$

The value of $\Delta R(T\xi(\omega))$ ranges between $[0, 1]$ because $R(T)$ is bounded by the same values. Given that X denotes the feasible region determined by constraints (3.10)–(3.30) and $\{f,\ s,\ y,\ st,\ z,\ x\}$ represents the set of decision variables, then, by using Equation (3.7) the CVaR problem can be formulated as:

$$\min_{\{f,\ s,\ y,\ st,\ z,\ x\} \in X,\ \eta \in \mathbb{R}} \quad \left\{ \eta + \frac{1}{1-\alpha} \mathbb{E}\left[(\Delta R(T, \xi(\omega)) - \eta)_+ \right] \right\} \tag{3.32}$$

To motivate the following section, consider an optimal solution to model (3.32). Observe that the CVaR for this solution corresponds to the average resilience loss of the $\lceil (1-\alpha)|\Omega| \rceil$ worst scenarios (having values greater than η); thus, the remaining $\lfloor \alpha|\Omega| \rfloor$ scenarios contribute to the CVaR only indirectly because their resilience loss must be no

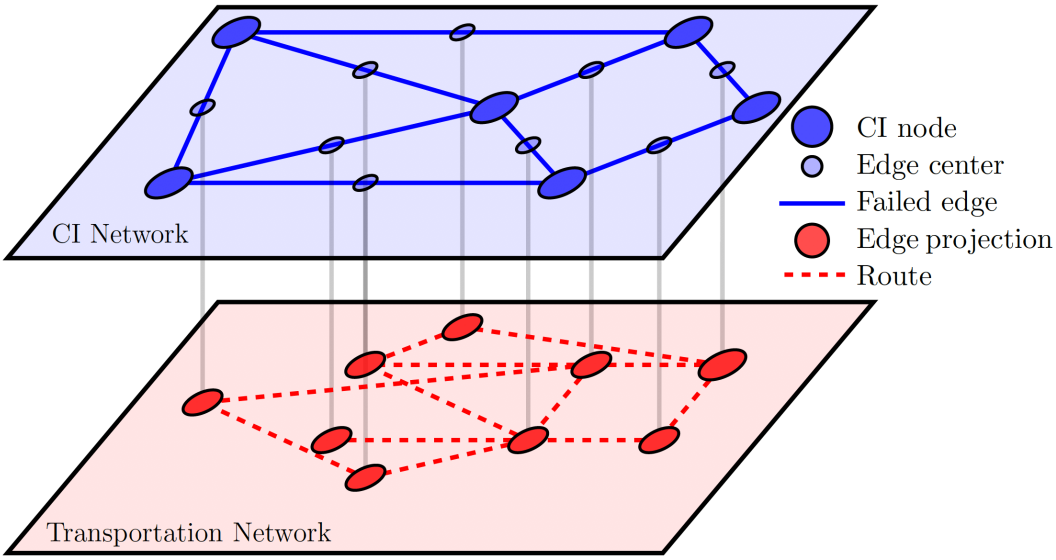

Figure 3.2. Projection of CI network edges on transportation network

more than η. Following Arpón *et al.* (2018) and García-Bertrand and Mínguez (2012), this motivates a computationally efficient strategy for deriving solutions to model (3.32) by reducing the set of scenarios to focus on those that involve high risk.

3.3 Solution approach

3.3.1 Scenario generation and reduction

To ensure a representative set of scenarios, a maxi-min Latin hypercube sampling (LHS) technique (Wyss & Jorgensen, 1998) is used to generate a large set of scenarios Ω. Using LHS ensures some amount of coverage of each random variable's range, and it has been shown to have advantages when incorporated within a sample average approximation approach (Chen *et al.*, 2014; Kleywegt *et al.*, 2002).

When the number of generated scenarios is large, the associated stochastic program tends to become intractable (Morales *et al.*, 2009). To improve tractability, one method is to reduce the number of scenarios such that the resulting problem's optimal solution is

close to the solution of the original optimization problem (Fang & Sansavini, 2019). In these methods, which have received significant attention in the literature (Heitsch & Römisch, 2003; Horejšová *et al.*, 2020), it is common to select scenarios based upon a *probability distance* between the original and reduced set of scenarios. The most common probability distance used in stochastic optimization is the Kantorovich distance, $D_K(\cdot)$, defined between two probability distributions Q and Q' on Ω by the following problem (Dupačová *et al.*, 2003; Rachev, 1991):

$$D_K\left(Q, Q'\right) = \inf_{\theta} \Big\{ \int_{\Omega\times\Omega} c\left(\omega, \omega'\right) \theta\left(d\omega, d\omega'\right) : \int_{\Omega} \theta\left(\cdot, d\omega'\right) = Q \quad \int_{\Omega} \theta(d\omega, \cdot) = Q' \Big\} \tag{3.33}$$

Problem (3.33) is known as the Monge–Kantorovich mass transportation problem (Rachev, 1991), where $c\left(\omega, \omega'\right)$ is a nonnegative, continuous and symmetric function, often referred to as cost function. The infimum is taken over all joint probability distributions defined on $\Omega\times\Omega$ represented by $\theta\left(\omega, \omega'\right)$ in (3.33). Note that $D_K(\cdot)$ can only be properly called Kantorovich distance if function $c(\cdot)$ is given by a norm. When Q and Q' are finite distributions corresponding to the initial set of scenarios Ω and the reduced set of scenarios $\Omega_s \subseteq \Omega$, the Kantorovich distance can be determined (see Dupačová *et al.* (2003) for details) by:

$$D_K\left(Q, Q'\right) = \sum_{\omega\in\Omega\setminus\Omega_s} \pi_\omega \min_{\omega'\in\Omega_s} c\left(\omega, \omega'\right) \tag{3.34}$$

where π_ω represents the probability of scenario ω in Ω (Dupačová *et al.*, 2003). Expression (3.34) can be used to derive several heuristics for generating reduced scenario sets that are close to an original set (Dupačová *et al.*, 2003; Morales *et al.*, 2009). Practically, the fast forward selection algorithm (Heitsch & Römisch, 2003) has been known to perform

well in different stochastic optimization applications. This algorithm is an iterative greedy process that starts with an empty set. In the first step of the algorithm, the scenario that has the minimum probability distance (e.g., Kantorovich distance) with all other scenarios is included. After that, in each step of the algorithm, a scenario that minimizes the Kantorovich distance between the reduced and original sets is selected from the set of non-selected scenarios ($\Omega \backslash \Omega_s$), where Ω_s represents the set of selected scenarios. Then, this scenario is included in the reduced set Ω_s. The stopping criteria of the algorithm is either by finding the pre-specified number of scenarios or by reaching a pre-defined Kantorovich distance threshold (Morales *et al.*, 2009).

In the fast forward selection algorithm, as described in (Heitsch & Römisch, 2003), the distance between two scenarios ω and ω' is expressed by the function $c(\omega, \omega')$ and is computed according to the difference between pairs of random vectors. Choices of the function (distance) $c(\omega, \omega')$ varies between probability metrics (Dupačová *et al.*, 2003), fixed first-stage decision variables objective function (Morales *et al.*, 2009) and the objective value for each scenario, which is shown to practically outperform the other two methods (Bruninx, 2014). Here, we use the objective function value z_ω^{WS} of the *wait-and-see solution* (WS) for each scenario $\omega \in \Omega$ (i.e., the objective function resulting from solving model (3.9)–(3.30) when it is populated with ω as its only scenario) to define $c(\cdot, \cdot)$ as follows:

$$c(\omega, \omega') = \left| z_\omega^{WS} - z_{\omega'}^{WS} \right| \tag{3.35}$$

The resulting fast forward selection algorithm is summarized in Algorithm 1, specifically using the "Algorithm A" subroutine in Step 0. We apply this algorithm, hereafter referred to as "Algorithm 1-A, to the risk-neutral model (3.9). We also compare Algorithm 1-A to

Algorithm 1-B, which is the standard algorithm proposed by Dupačová *et al.* (2003) based on the difference between the realized vectors $\boldsymbol{\lambda}_{\omega}$ and $\boldsymbol{\lambda}_{\omega'}$ consisting of the travel times and repair times for a pair of scenarios $\omega, \omega' \in \Omega$:

$$c\left(\omega, \omega'\right) = \|\boldsymbol{\lambda}_{\omega} - \boldsymbol{\lambda}_{\omega'}\| \tag{3.36}$$

and report our findings in Section 3.4.4.

Following Arpón *et al.* (2018), Fairbrother *et al.* (2019) and Pineda and Conejo (2010), Algorithm 1 is adapted to the CVaR model given in Equation (3.32). Toward this end, we first define an active scenario subset $\Omega_{\alpha} \subseteq \Omega$ of scenarios consisting of the scenarios $\omega \in \Omega$ having the worst WS objective value z_{ω}^{WS} (García-Bertrand & Mínguez, 2012). Formally, let $\eta_{\alpha}^{*} = \text{VaR}_{\alpha}[G(x_{\omega}^{*}, \cdot)]$ and define $\Omega_{\alpha} = \{\omega \in \Omega : G(x_{\omega}^{*}, \xi(\omega)) \geq \eta_{\alpha}^{*}\}$. Algorithm 1-C (i.e., Algorithm 1 with the "Algorithm C" subroutine chosen in Step 0) summarizes the resulting procedure. After performing this initial reduction, Algorithm 1-C proceeds exactly as Algorithm 1-A.

The current risk-averse scenario reduction approach combines the active scenarios concept from García-Bertrand and Mínguez (2012) and the WS reduction metric from Bruninx (2014). One advantage of this hybrid procedure is that the auxiliary variable η in Equation (3.32) is already known ($\eta = \eta_{\alpha}^{*} = \text{VaR}_{\alpha}[G(x_{\omega}^{*}, \cdot)]$) given that individual scenario problems are already solved and that only scenarios whose resilience losses are greater than or equal to η_{α}^{*} are chosen. This allows us to rewrite Equation (3.32) with optimal $\text{VaR}_{\alpha}[G(x_{\omega}^{*}, \cdot)]$ as:

$$\min_{\{f,\, s,\, y,\, st,\, z,\, x\} \in X} \quad \left\{ \eta_{\alpha}^{*} + \frac{1}{1-\alpha} \mathbb{E}\left[(\Delta R(T, \xi(\omega)) - \eta_{\alpha}^{*}) \right] \right\} \tag{3.37}$$

In addition, since the subset of $1 - \alpha$ scenarios in Ω_{α} is treated as a whole set of α- CVaR

included scenarios—with each scenario ω included in Ω_α having the property of $G(x^*_\omega, \xi(\omega)) \geq \eta^*_\alpha$—we can drop the constant η^*_α and express Equation (3.37) as:

$$\min_{\{f,\, s,\, y,\, st,\, z,\, x\} \in X} \quad \left\{ \frac{1}{1-\alpha} \mathbb{E}\left[(\Delta R(T, \xi(\omega)) | \omega \in \Omega_\alpha \right] \right\} \tag{3.38}$$

Thus, the problem has become similar to the risk-neutral one by choosing the risk region Ω_α and the reduction Algorithm 1-C acts similar to Algorithm 1-A as mentioned above. Nonetheless, the disadvantage of the approach suggested by Pineda and Conejo (2010) and its risk-averse extension proposed in this paper is that the algorithm computational time will be higher than other approaches. To overcome the problem, we provide the deterministic solution (DS) as the initial feasible solution to solve the problem associated with each scenario reducing the computational time significantly to a level on par with Morales *et al.* (2009).

3.3.2 Benders decomposition

There are different types of decomposition algorithms for solving continuous and mixed integer large-scale two-stage and multi-stage optimization problems (see Escudero *et al.* (2017) for a recent review). One of those types of algorithms is the time-honored Benders decomposition (Benders, 1962) and its variants (see Rahmaniani *et al.* (2017) for a good review). Benders decomposition is commonly used in the stochastic optimization literature to solve the resulting mixed-integer linear programs (Rahmaniani *et al.*, 2017). In this context, the risk-neutral and risk-averse models separate into one linear program per scenario ω—forming what is known as the subproblem (SP)—in the reduced scenario set Ω_s ($\Omega_{\alpha,s}$ for the CVaR model) after fixing the binary $x_{iji'j'k}$-, z_{ijk}-, $y_{ijk\omega}(t)$-, and $s_{ij\omega}(t)$-variables.

Formally, for each scenario $\omega \in \Omega_s$, let $\overline{\boldsymbol{z}}_\omega$ denote a fixed assignment of values to

Algorithm 1: Fast forward scenario reduction algorithm (Dupačová *et al.*, 2003)

Step 0: Compute the distances of scenario pairs:

Algorithm A: $c(\omega,\omega') = \left|z_{\omega}^{WS} - z_{\omega'}^{WS}\right|;\ \forall\omega,\omega' \in \Omega$ ▷ Risk-neutral WS

Algorithm B: $c(\omega,\omega') = \left\|\boldsymbol{\lambda}_{\omega} - \boldsymbol{\lambda}_{\omega'}\right\|;\ \forall\omega,\omega' \in \Omega$ ▷ $\boldsymbol{\lambda}$ is a vector of random variables

Algorithm C: (a) $\Omega_{\alpha} = \{\omega \in \Omega \mid G(x_{\omega}^{*},\omega) \geq \eta_{\alpha}^{*}\}$ ▷ proposed risk-averse

(b) $c(\omega,\omega') = \left|z_{\omega}^{WS} - z_{\omega'}^{WS}\right|;\ \forall\omega,\omega' \in \Omega_{\alpha}$ ▷ $\Omega = \Omega_{\alpha}$ and $\Omega_s = \Omega_{\alpha,s}$ for Algorithm C in steps 1-3

Step 1: Select the first scenario as the most equidistant scenario from all other scenarios in the set Ω :

$$\omega_1 = \arg\min_{\omega'\in\Omega}\left\{\sum_{\omega\in\Omega}\pi_{\omega}c(\omega,\omega')\right\} \tag{3.39}$$

$\Omega_s^{[1]} \leftarrow \{\omega_1\}$ ▷ $\Omega_s^{[i]}$ is the set of selected scenarios until step i

$\Omega_J^{[1]} \leftarrow \Omega\backslash\{\omega_1\}$ ▷ $\Omega_J^{[i]}$: the scenarios set not selected in the first i steps

Step *i*: Identify the scenarios ω_i to be added to Ω_s until it reaches a given cardinality N_s based on the distance function between $\Omega_s^{[i-1]}$ and $\Omega_J^{[i-1]}$:

For i in $\{2\ldots N_s\}$:

$$\omega_i = \arg\min_{\omega'\in\Omega_J^{[i-1]}}\left\{\sum_{\omega\in\Omega_J^{[i-1]}\backslash\{\omega'\}}\pi_{\omega}\min_{\omega''\in\Omega_s^{[i-1]}\cup\{\omega\}}c(\omega,\omega'')\right\} \tag{3.40}$$

$\Omega_s^{[i]} \leftarrow \Omega_s^{[i-1]} \cup \{\omega_i\}$, $\Omega_J^{[i]} \leftarrow \Omega_J^{[i-1]}\backslash\{\omega_i\}$ ▷ $\Omega_J^{[i]} \cup \Omega_s^{[i]} = \Omega$

End For

Step $N_s + 1$: Redistribute the probabilities of $\Omega_J^{*} = \Omega_J^{[N_s]}$ over $\Omega_s^{*} = \Omega_s^{[N_s]}$ according to the cost function $c(\omega,\omega')$:

$$\pi_{\omega}^{*} = \pi_{\omega} + \sum_{\omega'\in J(\omega)}\pi_{\omega'},\quad \forall\omega \in \Omega_s^{*} \tag{3.41}$$

with $J(\omega)$ being the set of scenarios $\omega' \in \Omega_J^{*}$ such that $\omega = \arg\min_{\omega''\in\Omega_s^{*}} c(\omega'',\omega')$

all x-, z-, y-, and s-variables corresponding to the index ω. The resulting SP for scenario $\omega \in \Omega_s$—with resilience loss minimization objective—is the linear program:

$$\text{SP}(\overline{\boldsymbol{z}}_\omega): \quad \min \left(1 - \frac{\sum_{t=1}^{t=T}[\sum_{j\in V^-} w_j f_{j\omega}(t) - \varphi(0)]}{T(\sum_{j\in V^-} w_j P_j^- - \varphi(0))}\right) \tag{3.42}$$

$$\text{s.t. } (3.10) - (3.14) \text{ for scenario } \omega \tag{3.43}$$

Because $\text{SP}(\overline{\boldsymbol{z}}_\omega)$ is a linear program in which $\overline{\boldsymbol{z}}_\omega$ appears only in the constraints, the dual of $\text{SP}(\overline{\boldsymbol{z}}_\omega)$ can be formulated as a linear program of the form:

$$\text{DSP}(\overline{\boldsymbol{z}}_\omega): \quad \max \quad (\boldsymbol{b} - \boldsymbol{B}\overline{\boldsymbol{z}}_\omega)\,\boldsymbol{d}_\omega \tag{3.44}$$

$$\text{s.t. } \boldsymbol{d}_\omega \in \mathcal{D} \tag{3.45}$$

where $\boldsymbol{b}$ is the right-hand side vector of (3.43), $\boldsymbol{B}$ is the left-hand side coefficient matrix of (3.43), $\boldsymbol{d}_\omega$ is the dual variable vector corresponding to constraint (3.43), and $\mathcal{D}$ represents the dual feasible region. Let $\mathcal{D}_p$ and $\mathcal{D}_r$ respectively denote the extreme points and extreme rays of $\mathcal{D}$. Then, letting $\mathcal{D}_p^{\omega n} \subseteq \mathcal{D}_p$ and $\mathcal{D}_r^{\omega n} \subseteq \mathcal{D}_r$ respectively denote a subset of the extreme points and extreme rays produced prior to iteration n of Benders decomposition, the restricted master problem (RMP) for iteration n is formulated as:

$$\min \quad \sum_{\omega=1}^{\Omega_s} \pi_\omega v_\omega \tag{3.46}$$

s.t.

$$v_\omega \geq (\boldsymbol{b} - \boldsymbol{B}\boldsymbol{z}_\omega)\,\overline{\boldsymbol{d}}_\omega, \forall \omega \in \Omega_s,\ \overline{\boldsymbol{d}}_\omega \in \mathcal{D}_p^{\omega n} \tag{3.47}$$

$$0 \geq (\boldsymbol{b} - \boldsymbol{B}\boldsymbol{z}_\omega)\,\overline{\boldsymbol{d}}_\omega, \forall \omega \in \Omega_s,\ \overline{\boldsymbol{d}}_\omega \in \mathcal{D}_r^{\omega n} \tag{3.48}$$

$$\text{constraints } (3.15)\text{–}(3.30)$$

where v_ω is a new variable that represents the resilience loss in scenario ω. Constraints (3.47)

and (3.48) are respectively known as *optimality cuts* and *feasibility cuts*.

In the proposed Benders algorithm (Algorithm 2), the first step is to set the upper bound, lower bound and iteration counter at ∞, 0 and 0, respectively. In iteration n, RMP is solved first to obtain an optimal solution $\bar{\boldsymbol{z}}^n$ (note that in iteration 0, RMP has no cuts and any feasible solution to (3.15)–(3.30) is optimal with an objecive value of 0). From $\bar{\boldsymbol{z}}^n$, let $\bar{\boldsymbol{z}}^n_\omega$ denote the partial solution associated with the x-, z-, y-, and s-variables corresponding to the index ω. Then, DSP($\bar{\boldsymbol{z}}^n_\omega$) is solved (note that since the linear program in (3.42)–(3.43) and so its dual (3.44)–(3.45) are scenario indexed, they can be solved in parallel), yielding either an extreme point $\overline{\boldsymbol{d}}_\omega \in \mathcal{D}_p$ (if the model is solved to optimality) or an extreme ray $\overline{\boldsymbol{d}}_\omega \in \mathcal{D}_p$ (if the model is concluded to be unbounded). In the former case, $\overline{\boldsymbol{d}}_\omega$ is added to $\mathcal{D}_p^{\omega n}$ (i.e., $\mathcal{D}_p^{\omega,n+1} \leftarrow \mathcal{D}_p^{\omega n} \cup \{\overline{\boldsymbol{d}}_\omega\}$ and $\mathcal{D}_r^{\omega,n+1} \leftarrow \mathcal{D}_r^{\omega n}$), resulting in a new optimality cut; otherwise, $\overline{\boldsymbol{d}}_\omega$ is added to $\mathcal{D}_r^{\omega n}$ (i.e., $\mathcal{D}_p^{\omega,n+1} \leftarrow \mathcal{D}_p^{\omega n}$ and $\mathcal{D}_r^{\omega,n+1} \leftarrow \mathcal{D}_r^{\omega n} \cup \{\overline{\boldsymbol{d}}_\omega\}$), yielding a new feasibility cut. The RMP objective provides a lower bound to the optimal solution of the original problem (3.9)–(3.30) —under a resilience loss minimization objective—; furthermore, as demonstrated in the following proposition, the dual subproblem DSP($\overline{\boldsymbol{z}}_\omega$) always has an optimal solution, meaning the weighted sum $\sum_{\omega\in\Omega_s} \pi_\omega \left(\boldsymbol{b} - \boldsymbol{B}\overline{\boldsymbol{z}}^n_\omega\right) \overline{\boldsymbol{d}}_\omega$ yields an upper bound. We now state and prove the required result.

Proposition 3.1 *For a given binary variable vector* $\overline{\boldsymbol{z}}_\omega = \left[\overline{x}_{iji'j'k}, \overline{s}_{ij\omega}(t), \overline{y}_{ijk\omega}(t), \overline{z}_{ijk}\right]$ *that satisfies the constraints* (3.15)–(3.30)*, both SP*($\overline{\boldsymbol{z}}_\omega$) *and DSP*($\overline{\boldsymbol{z}}_\omega$) *are always feasible and bounded.*

Proof 3.1 *Observe that setting* $f_{ij\omega}(t) = 0,\ \forall\{i,j\} \in E,\ \forall t \in \{1\dots T\}$, *and* $f_{j\omega}(t) = 0,\ \forall j \in V^+,\ \forall t \in \{1\dots T\}$, *satisfies Constraints* (3.10)–(3.14)*; thus, SP*($\overline{\boldsymbol{z}}_\omega$) *is feasible. To*

show the boundedness of SP($\overline{\boldsymbol{z}}_\omega$), note that $f_{j\omega}(t) \leq P_j^-,\ \forall j \in V^-,\ \forall t \in \{1 \dots T\}$ due to Constraint (3.13)*; therefore, the objective of SP($\overline{\boldsymbol{z}}_\omega$) is bounded to be nonnegative. By duality theory, DSP($\overline{\boldsymbol{z}}_\omega$) must be feasible and bounded because SP($\overline{\boldsymbol{z}}_\omega$) is feasible and bounded.*

Algorithm 2: Benders decomposition algorithm

Step 0: $UB \leftarrow \infty, LB \leftarrow 0$, iteration counter $n = 0$

Step 1: Solve the RMP to obtain its optimal solution $(\overline{\boldsymbol{z}}_\omega, \bar{v}_\omega), \forall \omega \in \Omega_s$ ▷ $\Omega_s = \Omega_{\alpha,s}$ for CVaR model

$LB \leftarrow \max\{LB, \sum_{\omega \in \Omega_s} \pi_\omega \bar{v}_\omega\}$

Step 2: **For** each $\omega \in \Omega_s$:

Solve the DSP($\overline{\boldsymbol{z}}_\omega$) to obtain its optimal solution $\overline{\boldsymbol{d}}_\omega$ and objective value $(\boldsymbol{b} - \boldsymbol{B}\overline{\boldsymbol{z}}_\omega)\,\overline{\boldsymbol{d}}_\omega$

End For

$UB \leftarrow \min\{UB, \sum_{\omega \in \Omega_s} \pi_\omega\,(\boldsymbol{b} - \boldsymbol{B}\overline{\boldsymbol{z}}_\omega)\,\overline{\boldsymbol{d}}_\omega\}$

Step 3: **If** $UB - LB \leq \epsilon$: ▷ ϵ is a predefined tolerance

Stop and report the solution

Else:

(a) Add a total number of $|\Omega_s|$ Benders optimality cuts of the form: $v_\omega \geq (\boldsymbol{b} - \boldsymbol{B}\boldsymbol{z}_\omega)\,\overline{\boldsymbol{d}}_\omega, \forall \omega \in \Omega_s$ to the RMP

(b) $n \leftarrow n + 1$ and go to Step 1

End If

This result additionally shows that feasibility cuts are not needed in the decomposition procedure; therefore, only optimality cuts are generated and added to the RMP in each iteration, and the convergence of the algorithm is accelerated.

3.4 Numerical studies

3.4.1 System description

To test the proposed model and solution approach, the data from the French electrical power network company RTE (D'Electricité, 2019) is utilized in this work. The RTE network

can be modeled as an undirected graph with 172 substations (nodes) and 220 transmission lines (edges) covering up to more than 17,500 miles. There are 26 power generators and 145 distributors in the network. Some of the generators and distributors also transmit power from other generators to distributors. The weights of the edges (i.e., their capacities) are assumed to be identical. Specially, the capacity of each transmission line is 5000 MW, and the total network flow received by demand nodes is 61928 MW. In addition, given that the power network flow does not follow the general flow-based model introduced in this paper (Bienstock & Mattia, 2007), the DC model has been used as a linear approximation of the power flow in the network (see Appendix A.1 for details).

In this study, three possible cases are considered (along with subcases for their travel times) for network failure modes that differ in terms of their spatial coverage and the importance or criticality of the components in the network:

- **Case 1: Random failures -** common failures that occur randomly across the network caused often by weather-related triggers, man-made accidents and operation errors affecting the whole network. In this case, network edges are removed randomly with an equal failure probability for all edges in the network.

- **Case 2: Cascading failures -** failures of initial components that may cause other interconnected components to fail due to increased loads causing a sequence of failures in the network. The cascading failure process was simulated using the ML model (Motter & Lai, 2002).

- **Case 3: Spatial failures -** failures caused generally by natural disasters (e.g., earthquakes and floods) where only a local spatial area of the network is affected,

and thus only components that are spatially close to each other are impacted by the local disruption.

For all these cases, the three subcases of travel times are: (a) without travel time consideration, (b) with deterministic travel time consideration, and (c) with random travel time consideration. Considering these allows for measuring the impact of travel times, uncertainty and risk to be tested under various scenarios of failure propagation and revealing under which circumstances the usage of these additions to system resilience is critical. The distribution of the failed components over the geographic area of the network for each case can be found in Appendix B.1.

3.4.2 Uncertainty representation

The proposed model assumes the time to repair each edge and the travel time between failed edges are uncertain, but the remaining parameters are deterministic. The remainder of this section summarizes the assumed probability distributions for the uncertain parameters.

Let $E' \subseteq E$ denote the set of disrupted edges, and ttr_{ij} denote the time to repair edge $e = \{i, j\} \in E'$. We assume $ttr_{i,j}$ has a Weibull distribution with scale parameter ν_e and shape parameter β_e. Specially, the probability density function of ttr_{ij} is given by:

$$h(t, \beta_e, \nu_e) = \frac{\beta_e}{\nu_e} \left(\frac{t}{\nu_e} \right)^{\beta_e - 1} e^{-\left(\frac{t}{\nu_e}\right)^{\beta_e}}, \; t \geq 0 \tag{3.49}$$

Note that the Weibull distribution is commonly used to model activity times (Abdelkader, 2004).

For $e = \{i, j\} \in E'$ and $e' = \{i', j'\} \in E'$, let $tt_{iji'j'}$ denote the travel time between edge e and e'. A deterministic estimate of the travel time from e to e' is derived using a

separate transportation network. In the transportation network, each edge has an associated length and speed limit, and its traversal time c_l is estimated assuming it will always be possible to travel at the speed limit. The deterministic estimate of $tt_{iji'j'}$, hereafter denoted as $dtt_{iji'j'}$, is obtained by determining the shortest path length between two nodes in the transportation network, namely those that are closest to the midpoint of e and e' (see Figure 3.2 for illustration). To represent the uncertainty of $tt_{iji'j'}$, a distribution for traversal time of edges in the transportation network is populated; given c_l, the random traversal time cr_l is distributed according to the probability mass function:

$$P(cr_l = t) = \begin{cases} 0.3, & t = c_l \\ 0.3, & t = 1.5\ c_l \\ 0.4, & t = 2\ c_l \end{cases} \tag{3.50}$$

and $tt_{iji'j'}$ is found by solving the shortest path problem as explained. This approach follows other disaster relief studies assuming that uncertain traversal times are based on a coefficient multiplication of the deterministic traversal times of the transportation network (de la Torre *et al.*, 2012; Mete & Zabinsky, 2010).

3.4.3 Assumptions and computational information

In this study, the Weibull distributed repair time shape and scale parameters are assumed to be 5 and 2, respectively, for all components. Such assumptions are made following other studies in the literature in terms of the chosen probability distribution and parameters (Fang & Sansavini, 2019). Thus, the mean-time-to-repair (MTTR) used in the deterministic model is 1.84 hours. Without loss of generality, we assume that 10% of the edges are damaged under each failure mode and that the number of available maintenance crews is

three. Table 3.1 shows the decrease in the network performance under each failure mode. In addition, the restoration planning horizon T is chosen as 20 hours, which is sufficient to restore the network performance to its original state under all cases. For the scenario generation process, 1000 scenarios are generated of each failure mode and its included subcases. After that, scenario reduction algorithms (1-A and 1-C) were used to reduce the number of scenarios into a smaller set. For the risk-neutral stochastic optimization model, the total number of scenarios is reduced to 10 scenarios; and for the risk-averse stochastic optimization model (with $\alpha = 80\%$) we reduce the total number of scenarios to 5 given that less probability space is covered (80% less) with the CVaR measure. Solutions to the MILPs used in the scenario reduction procedure and the stochastic optimization models were computed using CPLEX 12.10 (CPLEX, 2020) and programmed using Python 3.7 (Python, 2020) on a 3.2 GHz Intel Core i5 iMac machine with 24 GB of RAM.

Table 3.1. Network performance drop after possible modes of disruption

Case	Random failures	Cascading failures	Spatial failures
Performance drop	9%	13.35%	12.78%

Based on our preliminary analysis, a time limit of 2 hours (7200 seconds) and 1 hour (3600 seconds) was set for each instance of the risk-neutral stochastic optimization model with 10 scenarios and the risk-averse stochastic optimization model with 5 scenarios, respectively. This amount of time allows our implementation of Benders algorithm to solve both problems within 2% adjusted optimality gap (see Appendix A.2 for details) for all subcases. Algorithm 2 was implemented using callbacks with Benders cuts added as lazy constraints. Table 3.2 shows the added value of our proposed solution algorithm compared to CPLEX standard solver, and Table 3.3 summarizes the dimensions of different problem

instances.

Table 3.2. Comparison of Benders decomposition and CPLEX solver solutions for the Risk-neutral stochastic optimization model with 10 reduced scenarios

Case	CPLEX standard solver			Benders decomposition		
	Computational time (s)	Gap(%)	Resilience objective value	Computational time (s)	Gap(%)	Resilience objective value
Random failures	7201.05	5.59	0.3437980	7202.178	0.1444	**0.913716**
Random failures (deterministic travel times)	7201.36	5.99	0.3035116	7200.977	0.7702	**0.844289**
Random failures (random travel times)	7201.18	2.56	0.63019	7200.49	0.7646	**0.82157**
Cascading failures	7200.20	1.13	0.8678093	5300.619	1.0288	**0.875282**
Cascading failures (deterministic travel times)	7201.46	2.26	0.78629732	6000.816	0.9407	**0.881616**
Cascading failures (random travel times)	7200.40	6.52	0.481307	7201.611	1.1633	**0.850502**
Spatial failures	7201.83	4.08	0.6243989	7201.101	1.2052	**0.835887**
Spatial failures (deterministic travel times)	7201.15	4.01	0.6289536	7201.170	1.4432	**0.817396**
Spatial failures (random travel times)	7206.79	6.82	0.41048	7217.37	1.3527	**0.800491**

Table 3.3. Problem sizes of different study instances

Instance	No. of continuous variables	No. of binary variables	No. of constraints	No. of Scenarios	No. of maintenance crews	Max computational time (s)
Risk-neutral	115,320	315,612	377,104	10	3	7200
Risk-averse	57,660	158,532	188,629	5	3	3600
Deterministic	11,532	32,868	37,695	1	3	600

3.4.4 Results

Scenario reduction results

In this section, we compare the results from the adopted risk-neutral scenario reduction algorithm based on the individual WS solutions with the ones from the standard algorithm based on the norm of the difference between pairs of scenarios' random vectors. Figure 3.3 presents a histogram comparison of the WS resilience values of the reduced set of scenarios using the WS metric (Algorithm 1-A) and the standard probability metric (Algorithm 1-B) for one failure mode.

The WS reduced scenarios show more resemblance to the original set of scenarios with

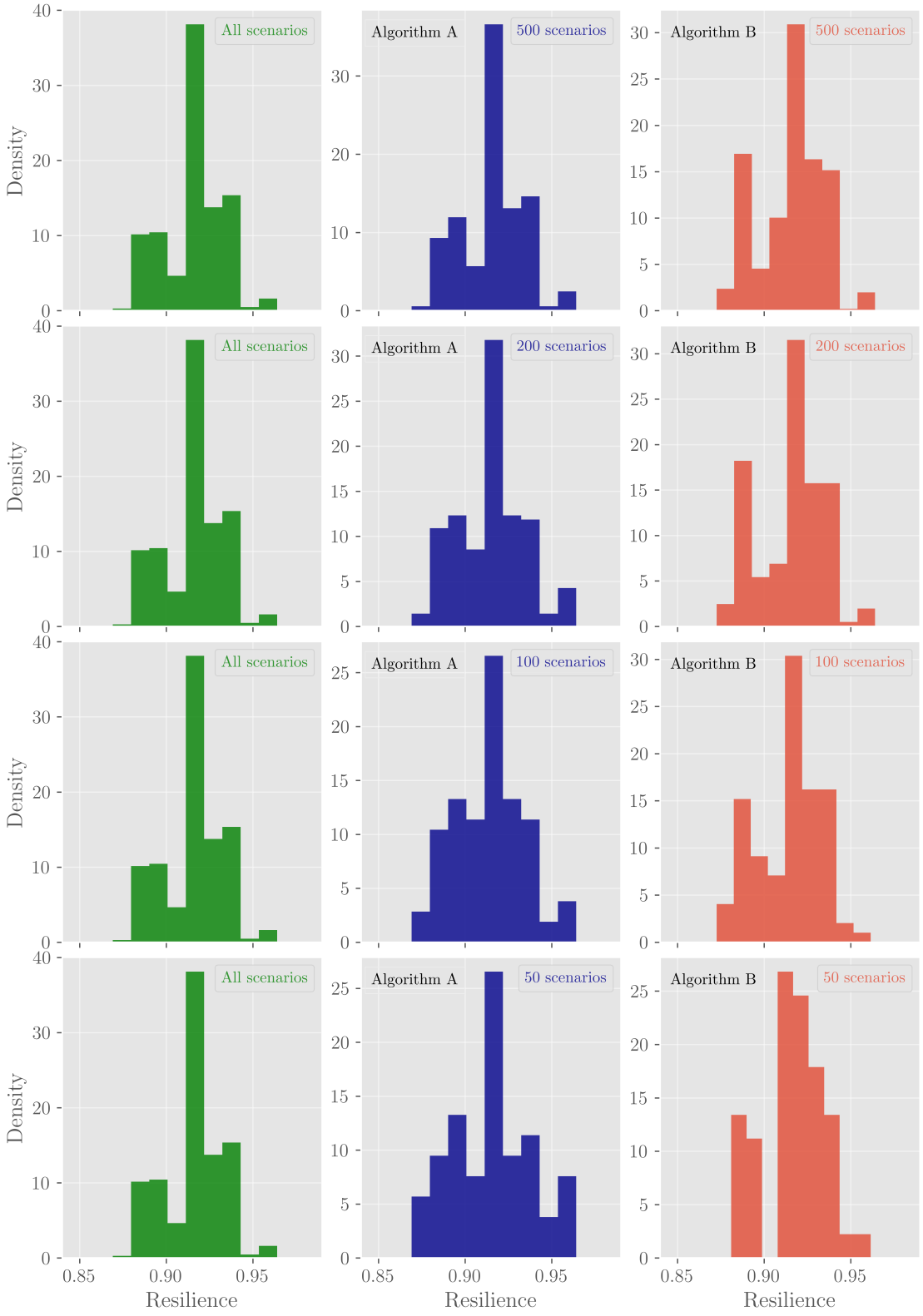

Figure 3.3. WS results of scenario reduction algorithms 1-A and 1-B for different reduced numbers of scenarios

respect to the distribution of objective values. Furthermore, Tables 3.4 and 3.5 present the values of mean and standard deviation of system resilience for the reduced sets using both algorithms under different target numbers of reduced scenarios without/with travel time considerations. It is worth pointing out that the standard probability metric method cannot differentiate between the model with no travel times and the one considering deterministic travel times since the same set of scenarios will be chosen for both cases.

Table 3.4. WS results from scenario reduction algorithms 1-A and 1-B for different reduced numbers of scenarios without travel time consideration

All 1000 scenarios		Algorithm 1-A			Algorithm 1-B		
Resilience mean	Resilience standard deviation	Number of reduced scenarios	Resilience mean	Resilience standard deviation	Number of reduced scenarios	Resilience mean	Resilience standard deviation
0.915831	0.0172952	500	0.915831	0.0172866	500	0.915613	0.0176127
		200	0.915831	0.0172866	200	0.91598	0.0178898
		100	0.915831	0.0172866	100	0.915249	0.0180558
		50	0.915827	0.0172921	50	0.917131	0.0178635

Table 3.5. WS results from scenario reduction algorithms 1-A and 1-B for different reduced numbers of scenarios considering deterministic travel times

All 1000 scenarios		Algorithm 1-A			Algorithm 1-B		
Resilience mean	Resilience standard deviation	Number of reduced scenarios	Resilience mean	Resilience standard deviation	Number of reduced scenarios	Resilience mean	Resilience standard deviation
0.854238	0.0171757	500	0.854238	0.0171671	500	0.853971	0.0174006
		200	0.854238	0.0171671	200	0.854054	0.0177003
		100	0.854239	0.0171649	100	0.853737	0.017949
		50	0.854242	0.0171685	50	0.855148	0.0178526

Table 3.6 shows the benefit of using a warm start setting (supplying the deterministic solution as an initial feasible solution) for each single scenario problem in reducing both computational time and optimality gaps for the WS problems.

Table 3.6. Comparison of computational time and optimality gap for single scenario problems with warm vs. cold start

Instance	Average optimality gap (%)	Max optimality gap (%)	Average computational time per problem (s)	Max computational time per problem (s)
1000 scenario with cold start	0.573	2.27	118.135	120
1000 scenario with warm start	0.13	0.59	108.82	120

Stochastic optimization models results

A key result in this study is the impact of the inclusion of travel times between failed components for each maintenance crew on the system resilience. Figure 3.4 shows a comparison between resilience with and without deterministic travel times for all three failure modes. (The travel time between each pair of failed components is assumed to be $dtt_{ijj'j'}$ for the former and 0 for the latter). For all failure modes, the impact of travel times is significant. The result indicates that the resilience models without considering travel times between failed components might overestimate the actual possible resilience values achieved and the time to restore the system to its undisrupted performance. Note that this occurs even in the spatial failures case in which pairs of failed components are likely to be close to each other. A sample of optimal routing for one failure mode is provided in Appendix B.2.

Risk-neutral stochastic model

To measure the added value of incorporating uncertainty into the model and to compare the stochastic solution (SS) to its deterministic counterpart, we use what is known as the value of stochastic solution (VSS) as our metric for comparison. This measure indicates the difference in the objective values of the stochastic solution and the deterministic

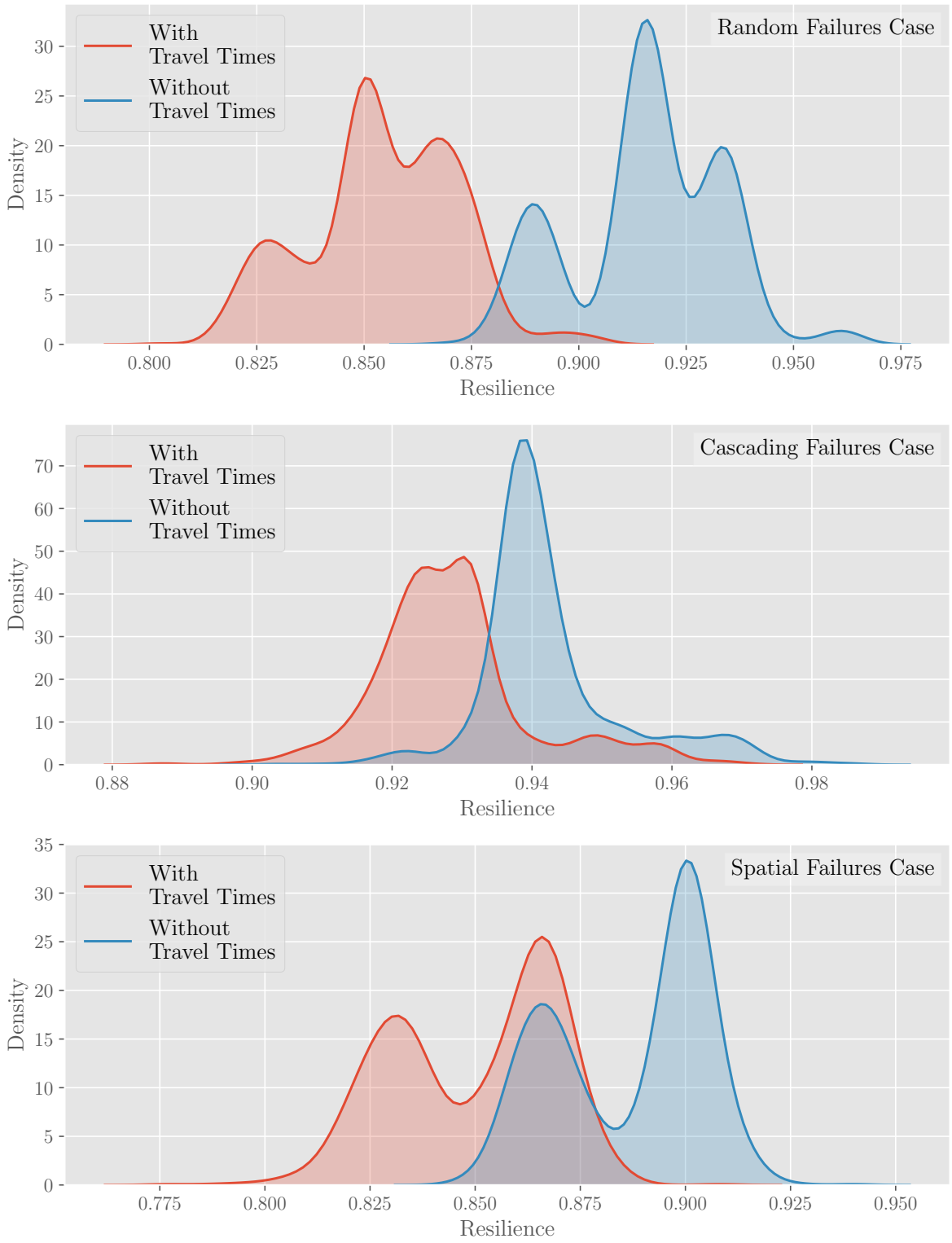

Figure 3.4. Comparison of resilience values for the 1000 scenarios WSs with/without deterministic travel times

counterpart (Birge, 1982). By solving the restoration problems for the different disruption cases (with the subcases of excluding travel times, and including deterministic travel times and random travel times) using the proposed Benders decomposition method, we can find the added value of uncertainty. Figure 3.5 shows the added value of the risk-neutral stochastic model compared to its deterministic counterpart in terms of the value of resilience achieved at the end of the restoration period and in terms of the extra amount of flow (power) received by demand nodes under the cases of random failures and cascading failures. Based on that, if the stochastic solution was used instead of the deterministic one, more flow will be pushed to satisfy more demand by amounts of at least 3000 MWh (3 GWh) for all subcases of the random failures case and 1800 MWh (1.8 GWh) for all subcases of the cascading failures case. Given that the annual electricity consumption per household in France is about 5.425 MWh (Odyssee-Mure, 2020) and the daily consumption is approximately 0.015 MWh, the extra amount of flow gained by the stochastic solution is equivalent to the daily consumption of 200,000–275,000 households for case 1 and 100,000–600,000 households for case 2 (see Figure 3.6). This indicates the significance of incorporating uncertainty into the restoration scheduling tasks.

In contrast to the previous cases, the stochastic solution for the case with spatial failures only shows an improvement over the deterministic solution in the subcase with random travel times. In the other subcases, the deterministic and stochastic solutions are the same. Resilience progress over time curves for cases 1 and 2 can be found under Appendix B.3 showing how the stochastic solution outperforms the deterministic counterpart in almost every scenario.

To validate the solution resulting from the reduced set of scenarios, we compare the

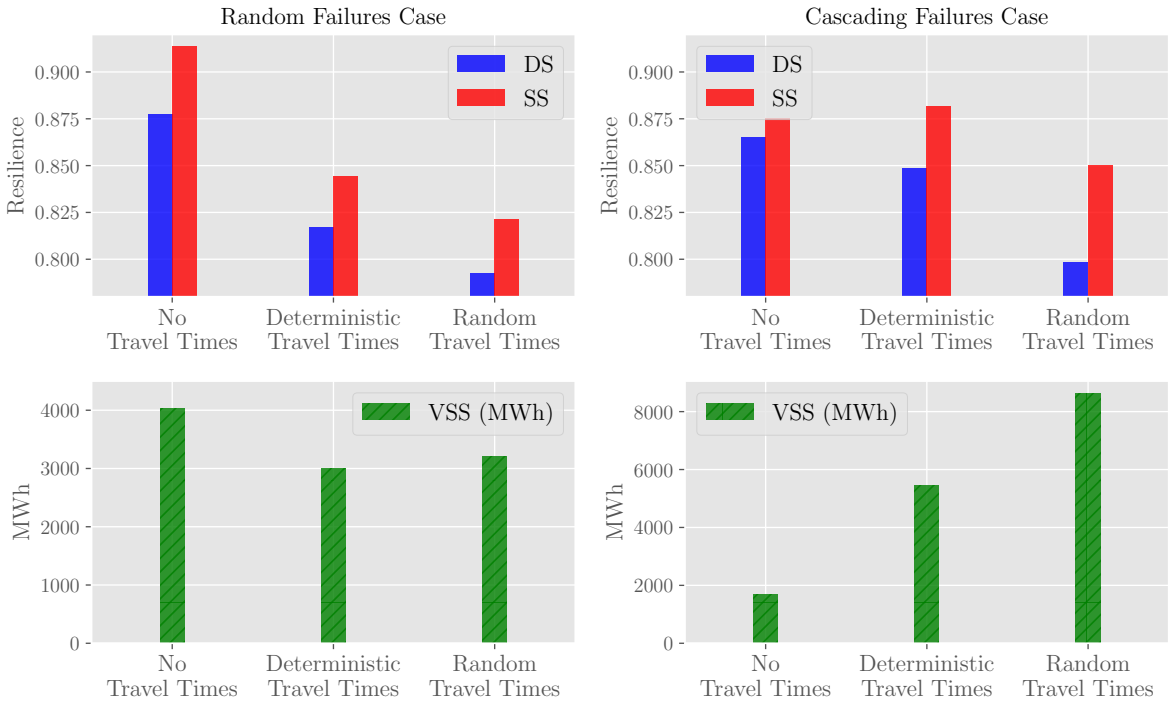

Figure 3.5. Case 1 and 2 (Random Failures and Cascading Failures): Resilience values and VSS (as higher satisfied demand in MWh) under different travel time assumptions

solution for each subcase to the one for the full set of scenarios as shown in Table 3.7. In all subcases, the estimate of the expected resilience value for the small set of scenarios is within about a 0.01 difference from the expected resilience for the full set of scenarios.

Risk-averse stochastic model

For the risk-averse model, five reduced scenarios are chosen to represent the worst 20% cases with $\alpha = 0.8$. Similar to the VSS, we adopt the mean-risk value of stochastic solution (MRVSS) (Noyan, 2012), a measure of the possible gain from solving stochastic models incorporating a mean-risk function, as the method to quantify the gains from solving the CVaR problem. However, given that only a CVaR approach is considered rather than a mean-risk one, we rename the measure to CVaR-VSS, i.e., the mean-risk measure with the

Table 3.7. Validation of solutions for the reduced set of scenarios when applied to the full set of scenarios

Case	Full set of scenarios (1000 scenarios)	Reduced set of scenarios (10 scenarios)
	Resilience objective value	Resilience objective value
Random failures	0.912227	0.913716
Random failures (deterministic travel times)	0.838694	0.844289
Random failures (random travel times)	0.828919	0.82157
Cascading failures	0.881547	0.875282
Cascading failures (deterministic travel times)	0.881711	0.881616
Cascading failures (random travel times)	0.845592	0.850502
Spatial failures	0.848444	0.835887
Spatial failures (deterministic travel times)	0.815873	0.817396
Spatial failures (random travel times)	0.796081	0.800491

weight of the expected resilience of scenarios not in α-CVaR being 0. Figures 3.7, 3.8 and 3.9 compare the CVaR solution and the deterministic solution in terms of resilience values and CVaR-VSS for all cases.

In almost all of these cases, the CVaR solutions outperform the deterministic solutions by achieving higher resilience values accompanied with significant CVaR-VSS values ranging from about 50,000 to 800,000 households daily consumption equivalence in the worst-case scenarios. Note that, in contrast to the risk-neutral case, the case with spatial failures also shows a significant CVaR-VSS under all subcases. Figure 3.10 plots the network performance over time for the high-risk scenarios in Case 3-b (spatial failures with deterministic travel times), showing how the CVaR restoration plan generally achieves full performance in these scenarios faster than either a risk-neutral or deterministic restoration plan.

Table 3.8 compares the CVaR solution and the deterministic and risk-neutral solutions across Cases 1–3. It can be seen that the risk-averse solution performs the best in all the cases by mitigating the risk associated with resilience loss. Moreover, the risk-neutral solution almost always comes second in performance with the deterministic solution classified as the

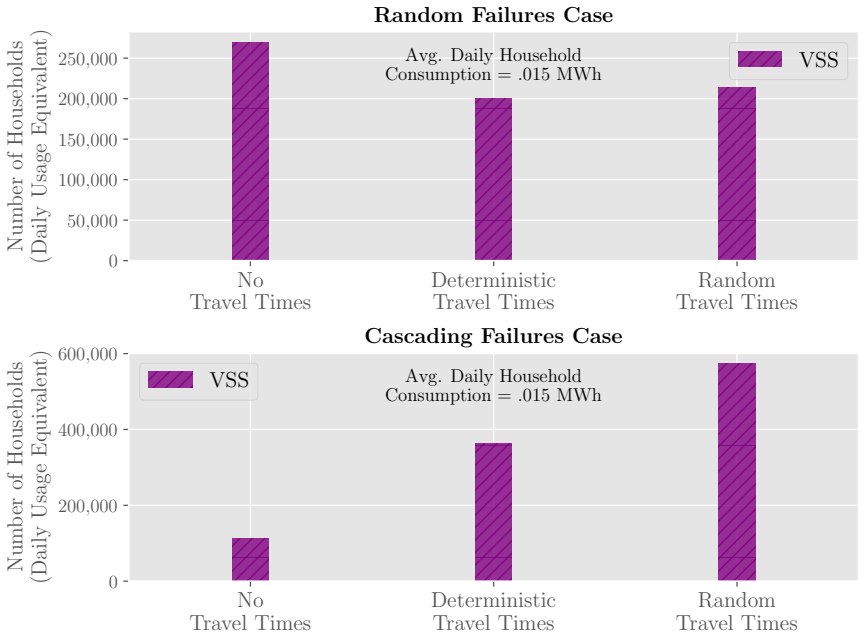

Figure 3.6. Cases 1 and 2 (Random Failures and Cascading Failures): VSS in equivalent number of households consumption related to the extra amount of satisfied demand in MWh under different travel time assumptions

solution involving the highest risk.

In addition, It is of interest to investigate whether the CVaR solution performs well in scenarios other than the high-risk ones. Table 3.9 compares the risk-neutral solution for all cases with the deterministic counterpart and the CVaR solution applied to the reduced set of 10 scenarios associated with the risk-neutral problem. Surprisingly, the CVaR solution in some cases outperforms the risk-neutral solution. One possible reason of this unexpected finding is that the CVaR problems generally use fewer scenarios, given the $1 - \alpha\%$ reduced covered area of possible scenarios allowing the optimal solutions of the problems to be closer to the 0% optimality gap in less amount of computational time. Therefore, two important features of the CVaR approach can be summarized as follows: (1) the CVaR approach covers a fair amount of uncertainty (depending on α value), making its suggested plan more pleasing than the fixed deterministic counterpart, and (2) the CVaR problem is solved with

Figure 3.7. Case 1 (Random Failures): Resilience values and CVaR-VSS in equivalent number of households consumption related to the extra amount of satisfied demand in MWh under different travel time assumptions ($\alpha = 0.8$)

fewer scenarios than its risk-neutral counterpart allowing the optimal solution to be found in less time (50% in our setting) and with lower optimality gaps.

Table 3.8. Solution comparison of the risk-averse resilience values ($\alpha = 0.8$) with deterministic and risk-neutral alternatives

Case	Computational time (s)	Gap(%)	CVaR solution	Deterministic solution	Stochastic solution
Random failures	3600.000	0.0691	**0.887089**	0.846803	0.885704
Random failures (deterministic travel times)	3600.797	0.5549	**0.827217**	0.804466	**0.827217**
Random failures (random travel times)	3600.632	0.833	**0.8103**	0.7876	**0.8103**
Cascading failures	3607.194	0.1988	**0.920725**	0.850712	0.868874
Cascading failures (deterministic travel times)	3600.476	0.8428	**0.880710**	0.860402	0.873507
Cascading failures (random travel times)	3600.035	1.4551	**0.8289**	0.7959	0.8155
Spatial failures	3600.312	0.7766	**0.842965**	0.828520	0.828520
Spatial failures (deterministic travel times)	3600.015	1.4309	**0.804756**	0.800828	0.800828
Spatial failures (random travel times)	3600.896	1.3141	**0.7744**	0.7622	**0.7744**

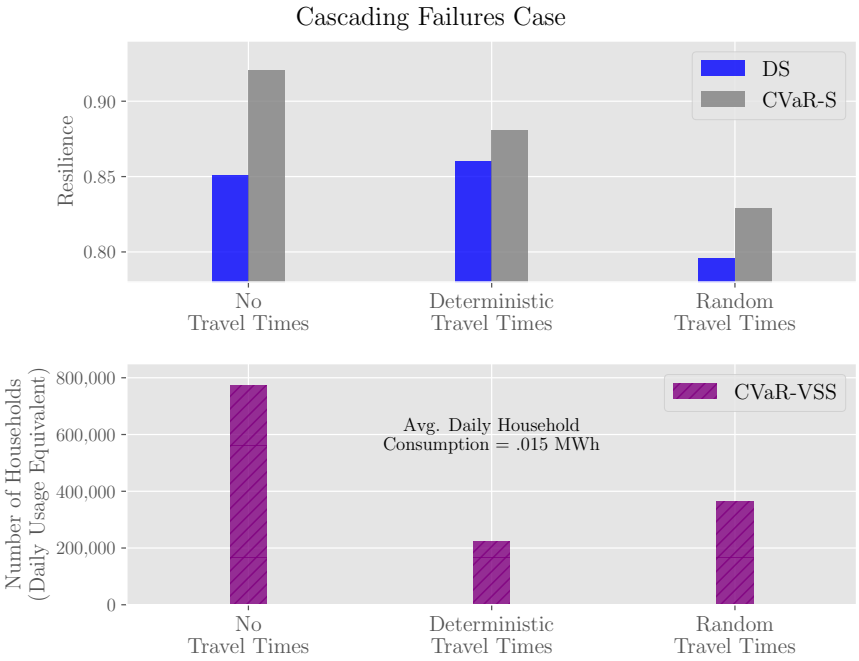

Figure 3.8. Case 2 (Cascading Failures): Resilience values and CVaR-VSS in equivalent number of households consumption related to the extra amount of satisfied demand in MWh under different travel time assumptions ($\alpha = 0.8$)

Table 3.9. Solution comparison of the risk-neutral resilience values with deterministic and risk-neutral alternatives

Case	Computational time (s)	Gap(%)	Stochastic solution	Deterministic solution	CVaR solution
Random failures	7202.178	0.1444	**0.913716**	0.877421	0.912732
Random failures (deterministic travel times)	7200.977	0.7702	**0.844289**	0.817283	**0.844289**
Random failures (random travel times)	7200.49	0.7646	**0.82157**	0.7928	**0.82157**
Cascading failures	5300.619	1.0288	0.875282	0.865170	**0.911292**
Cascading failures (deterministic travel times)	6000.816	0.9407	0.881616	0.848590	**0.882013**
Cascading failures (random travel times)	7200.4	0.9549	**0.8505**	0.7983	0.8314
Spatial failures	7201.101	1.2052	0.835887	0.835887	**0.850345**
Spatial failures (deterministic travel times)	7201.170	1.4432	0.817396	0.817396	**0.818078**
Spatial failures (random travel times)	7217.37	1.3527	**0.800491**	0.7704	**0.800491**

3.5 Conclusion and future work

This chapter proposes risk-neutral and risk-averse two-stage stochastic optimization models for CI restoration planning, where post-disruption restoration tasks occur in a highly dynamic environment and thus subject to a considerable amount of uncertainty. The models

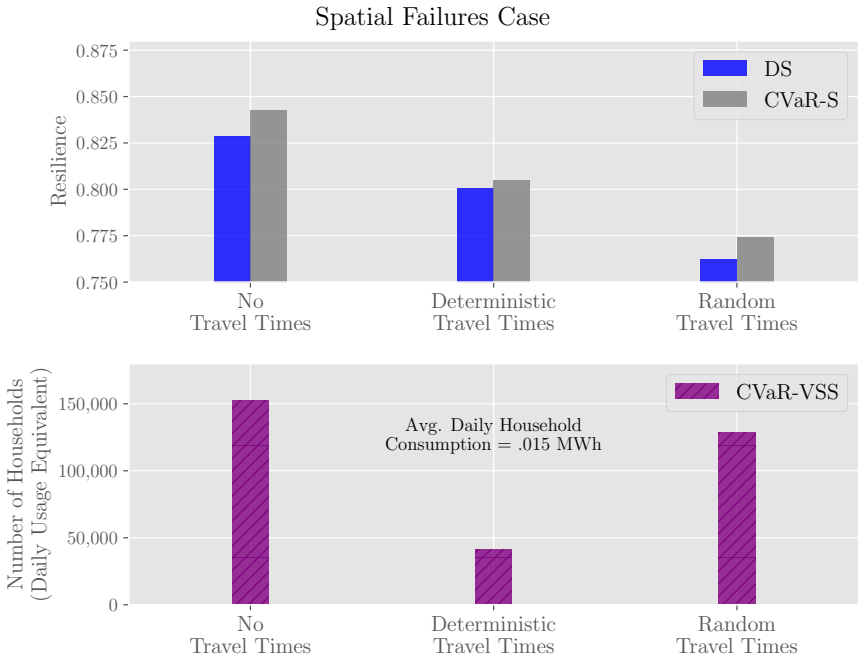

Figure 3.9. Case 3 (Spatial Failures): Resilience values and CVaR-VSS in equivalent number of households consumption related to the extra amount of satisfied demand in MWh under different travel time assumptions ($\alpha = 0.8$)

address two important challenges facing restoration planning, which are the accessibility of failed components and uncertainty associated with restoration task durations and possible starting times. For the former, travel time between components has been added to the model to connect CI restoration models to the state of the underlying transportation network. For the latter, the uncertainty of repair times and travel times is handled by sampling from their suggested probability distributions through a maxi-min Latin hypercube technique, with the number of discrete uncertainty scenarios being reduced to a tractable size by applying an improved risk-neutral and a proposed risk-averse fast forward selection algorithm based on the WS objective values of individual scenarios. The objective of the model is to minimize the expected loss of performance over all possible realizations of the random parameters, and thus to maximize the system's resilience. Three common network failure mechanisms

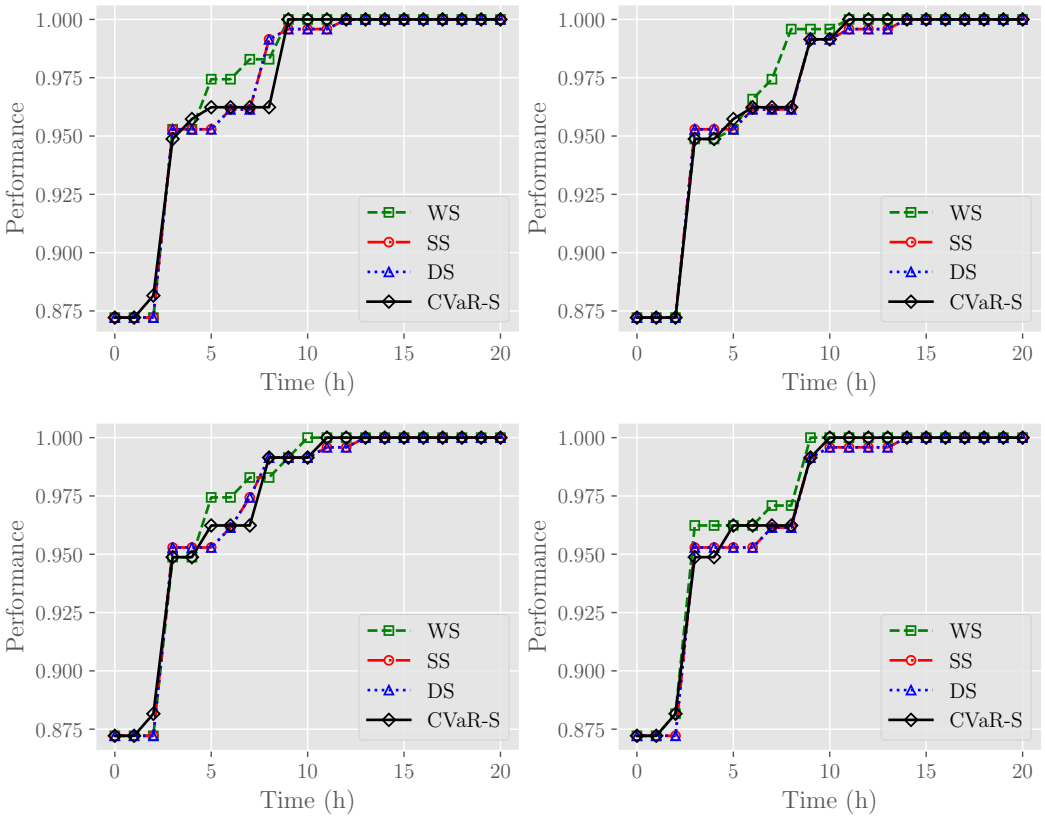

Figure 3.10. Case 3-b (Spatial Failures with Deterministic Travel Times): Comparison of network performance during the restoration period in high-risk scenarios under different solution plans

(i.e., random failures, cascading failures and spatial failures) are tested.

The proposed approach was demonstrated using a real-life case study based on the RTE 400 kV French electric power transmission network. Our first finding was the significant impact of incorporating travel times into resilience modeling. In fact, one can see that resilience models that do not consider travel times are overestimating their expected resilience achieved and the speed of restoring the system to its undisrupted performance level. Furthermore, to assess the added value of incorporating uncertainty, two measures were used to quantify the significance of adapting stochastic models over deterministic counterparts: VSS for the risk-neutral stochastic model and CVaR-VSS for the risk-averse stochastic model.

Both models have resulted in positive values of VSS and CVaR-VSS in 2 out of 3 cases and all three cases, respectively. There is a clear benefit of using stochastic methods that account for uncertainty over deterministic ones that depend on the expected values of the uncertain parameters. In addition, CVaR solutions were generally found with less computational time, and their suggested restoration plans perform on par with the risk-neutral counterparts and sometimes even better under a risk-neutral setting of scenarios selection. However, under high-risk scenarios, CVaR proposed solutions mitigate the risk associated with such scenarios by achieving resilience values close to the wait-and-see solutions of such individual scenarios. In addition, the CVaR solution under this setting performed second to none under all failure modes and their subcases.

The stochastic optimization models proposed in this study are reformulated as deterministic equivalent large MILPs in order to generate methods to solve proposed models efficiently. A Benders decomposition algorithm is proposed in this paper to solve the proposed models in short time settings. In addition, given that the risk-averse stochastic program is modeled by a scenario selection procedure identifying true risks associated with individual scenarios, the Benders decomposition algorithm proposed here is robust to work with both versions of the stochastic model. Thus, a practical framework for solving risk-averse versions of resilience-based optimization models, starting from scenarios generation, risk-averse scenarios reduction and ending with a solution procedure, is shown here to facilitate linking risk measures to current and future resilience optimization models.

The proposed stochastic optimization models present a practical framework for risk-neutral and risk-averse resilience-based applications and possibly other applications with task-scheduling procedures involving fair amount of uncertainty. Nonetheless, possible

additions in terms of planning flexibility to the current framework are adding multi-mode repairs of failed components and allowing for multi-crew restoration of failed components under travel time considerations. Moreover, restoration considering multiple interdependent networks (Gomez *et al.*, 2019) under uncertainty and network-based risk measures along with coordinating the restoration of the transportation network can also be studied as future research directions. Finally, the models in the present study assume that the restoration plan is determined initially and cannot be altered afterwards. Indeed, relaxing this assumption by enabling sequential change of the plan as time goes on will add more flexibility to the models but will significantly increase the computational time by moving the models from the two-stage setting into a more dynamic multi-stage stochastic optimization framework. Such computational differences can be tested using time-consistent risk-averse measures such as Expected CVaR (Homem-de-Mello & Pagnoncelli, 2016) and Expected Conditional Stochastic Dominance (Escudero *et al.*, 2017).

Appendix A

A.1 Model adaptation for the power network

The general flow-based model introduced in this paper assumes that the flow in the network can be directly controlled, which is not the case for power infrastructure networks (Bienstock & Mattia, 2007). The DC model is a commonly used linear approximation of the power grid to model its operations, especially the power transmission network (Bienstock & Mattia, 2007; Nurre *et al.*, 2012). The DC model includes decision variables (i.e., the phase angles) for all the nodes in the network. The flow on edge $\{i, j\}$ is then a function of the phase angles of nodes i and j along with the reactance of the edge $\{i, j\}$. The reactance, b_{ij}, of the edge is dependent on its length and the voltage levels. By defining θ_i for $i \in V$ as the phase angle of node i, the flow on edge $\{i, j\}$ for a given scenario is determined by:

$$b_{ij} f_{ij} = \theta_i - \theta_j \tag{3.51}$$

Note that both the phase angle variables and the edge flow variables are unrestricted in the DC model. A negative flow on edge $\{ij\}$ corresponds to power flowing from node j to node i. Therefore, it is necessary to incorporate the constraints given by Equation (3.51) into the optimization problem (3.9)–(3.30). We define variables $\theta_i(t)$ for $i \in V$ and $t \in \{1 \ldots, T\}$ for the phase angle of node i in time period t. Then, the DC flow is incorporated by adding two constraints controlling flow on each edge along with (3.14):

$$b_{ij} f_{ij\omega}(t) \leq \theta_{i\omega}(t) - \theta_{j\omega}(t) + M\left[1 - s_{ij\omega}(t)\right], \forall ij \in E, \forall t \in \{1, \ldots, T\}, \forall \omega \in \Omega_s \tag{3.52}$$

$$b_{ij} f_{ij\omega}(t) \geq \theta_{i\omega}(t) - \theta_{j\omega}(t) - M\left[1 - s_{ij\omega}(t)\right], \forall ij \in E, \forall t \in \{1, \ldots, T\}, \forall \omega \in \Omega_s \tag{3.53}$$

Therefore, whenever $s_{ij\omega}(t) = 1$, constraints (3.52) and (3.53) will make sure that the DC

flow satisfies Equation (3.51) for edge $\{i, j\}$ in time period t. In addition, Constraints (3.52) and (3.53) are added to the optimization problem (3.9)–(3.30) and to each scenario-related subproblem from the proposed Benders decomposition.

A.2 Optimality gap calculation

Regarding the relative optimality gap of the stochastic optimization models, we note that the optimality gap using the resilience measure (or loss of resilience) by Fang *et al.* (2016) is inflated given a constant term in the objective function's numerator representing either the negative summation of the aggregated system performance measure (flow in our case) in the disrupted state: $-\sum_{t=1}^{t=T} \varphi(0)$ for a maximization problem or the summation of aggregated system flow over time in the nominal state: $\sum_{t=1}^{t=T} \varphi(t_0)$ for a resilience loss minimization problem. For example, if the cumulative sum of flow $\forall t \in \{1 \dots T\}$ is 100, $\sum_{t=1}^{t=T} \varphi(0) = 70$ and $\sum_{t=1}^{t=T} \varphi(t_0) = 120$, the resilience objective function solution ($\widehat{Obj}$) will be 0.60 and if we assume that the upper bound on the cumulative flow is 115, the upper bound on resilience (Obj^{UB}) will be 0.90; thus, if we calculate the optimality gap by: $\left(\frac{Obj^{UB}}{\widehat{Obj}}\right) - 1$, it will be estimated as 50.00% where the gap in terms of the aggregated flow: $\left(\frac{\text{Aggregated Flow}^{UB}}{\widehat{\text{Aggregated Flow}}}\right) - 1$, which is the term to be maximized, is 15.00%. Based on that, we use from this point onward an adjusted optimality gap calculated using: $\left(\frac{Obj^{UB} + \frac{T\varphi(0)}{T(\varphi(t_0) - \varphi(0))}}{\widehat{Obj} + \frac{T\varphi(0)}{T(\varphi(t_0) - \varphi(0))}}\right) - 1$ for a maximization problem and: $\left(\frac{\frac{T\varphi(t_0)}{T(\varphi(t_0) - \varphi(0))} - Obj^{LB}}{\frac{T\varphi(t_0)}{T(\varphi(t_0) - \varphi(0))} - \widehat{Obj}}\right) - 1$ for a minimization objective to eliminate the impact of constant terms on the gap estimation of the aggregated flow. In Table 3.2, we compare the proposed Benders algorithm to the standard CPLEX solver. The optimalty gap for the Benders implementation is found using: $\left(\frac{\frac{T\varphi(t_0)}{T(\varphi(t_0) - \varphi(0))} - LB}{\frac{T\varphi(t_0)}{T(\varphi(t_0) - \varphi(0))} - \widehat{Obj}}\right) - 1$ where LB is the lower bound representing the optimal objective function value of the master problem at the last iteration

of the algorithm before termination. For the CPLEX solver, we use the reported best lower bound on the objective function Obj^{LB}_{solver} and the best available objective value $\widehat{Obj}_{solver}$ reported by CPLEX: $\left(\frac{\frac{T\varphi(t_0)}{T(\varphi(t_0)-\varphi(0))}-Obj^{LB}_{solver}}{\frac{T\varphi(t_0)}{T(\varphi(t_0)-\varphi(0))}-\widehat{Obj}_{solver}}\right)-1$ to calculate the optimality gap.

Appendix B

B.1 Maps of failed components for numerical studies

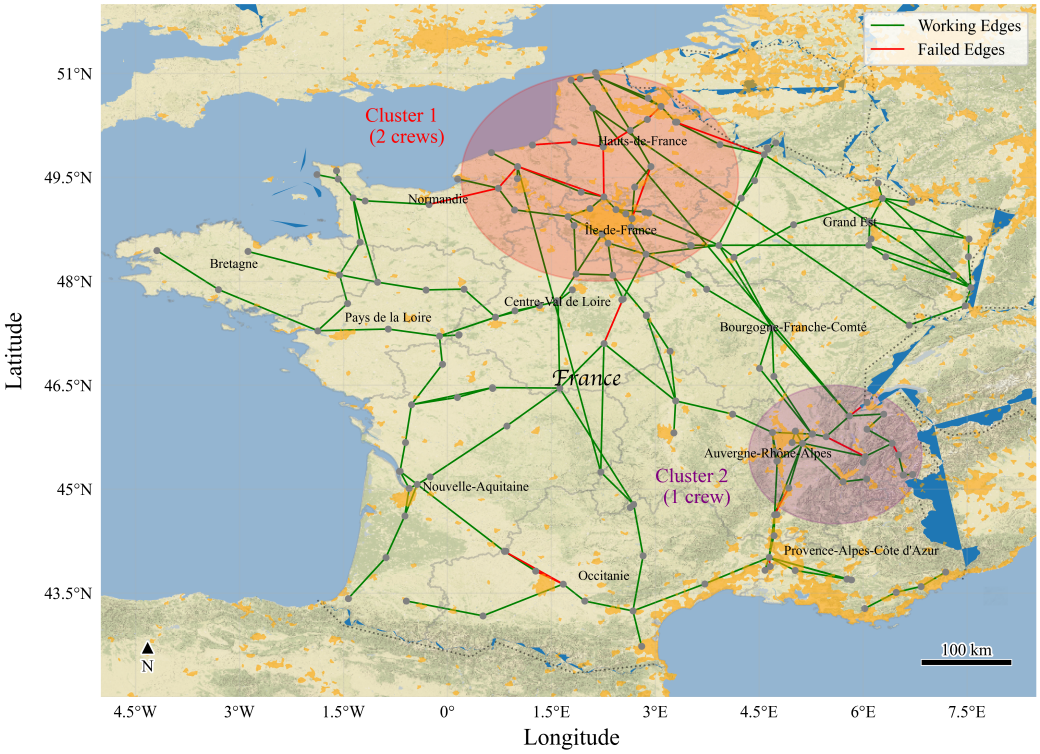

Figure 3.11. Case 1: Distribution of random failures

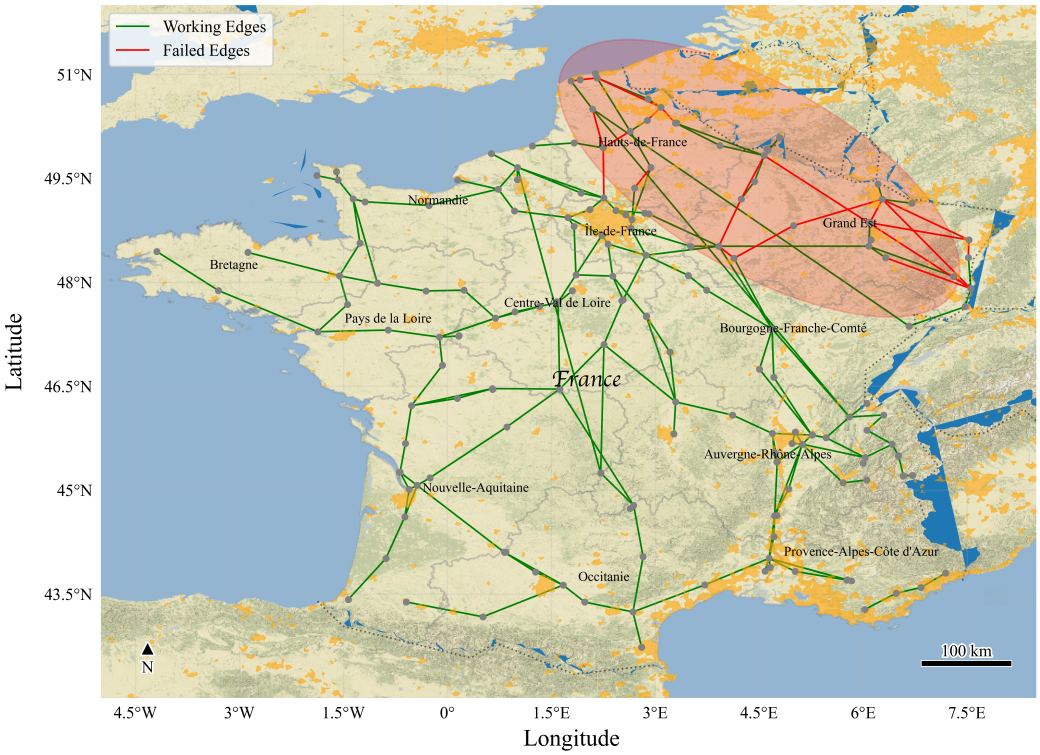

Figure 3.12. Case 2: Distribution of cascading failures

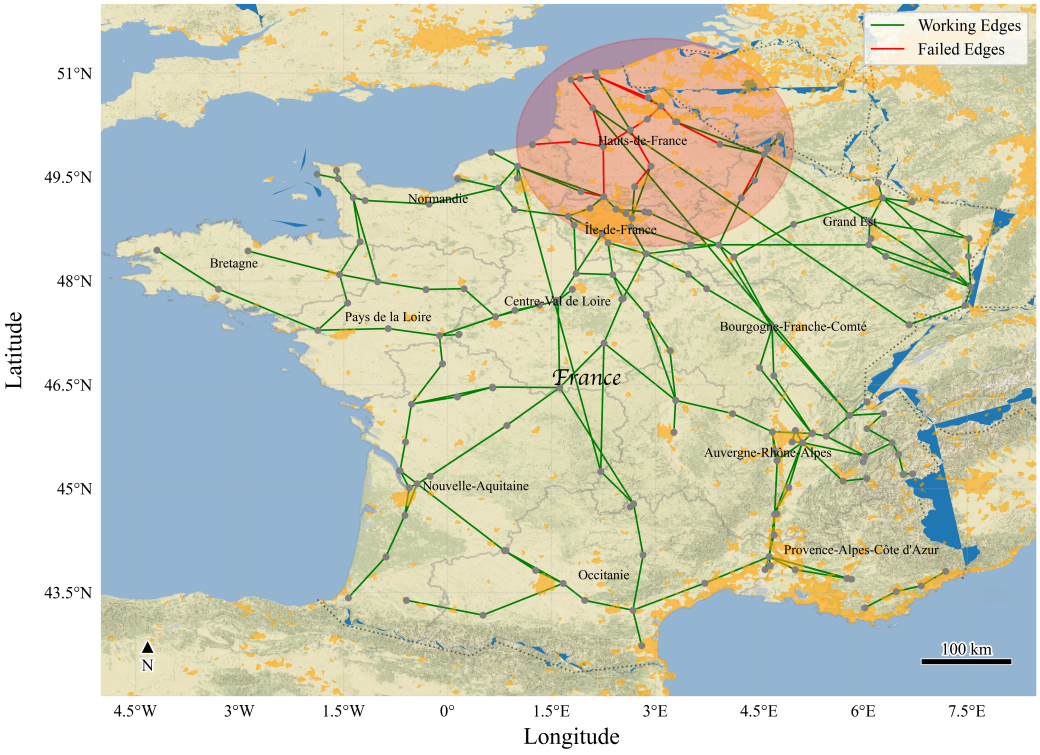

Figure 3.13. Case 3: Distribution of spatial failures

B.2 Sample of optimal solution routing under deterministic travel times

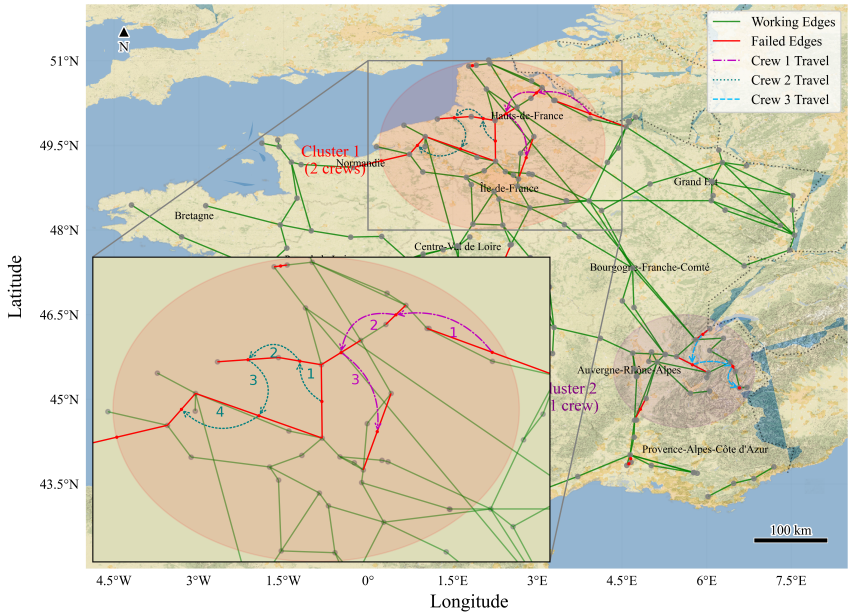

Figure 3.14. Case 1-b (Random Failures with Deterministic Travel Times): Optimal routing for crews 1 and 2

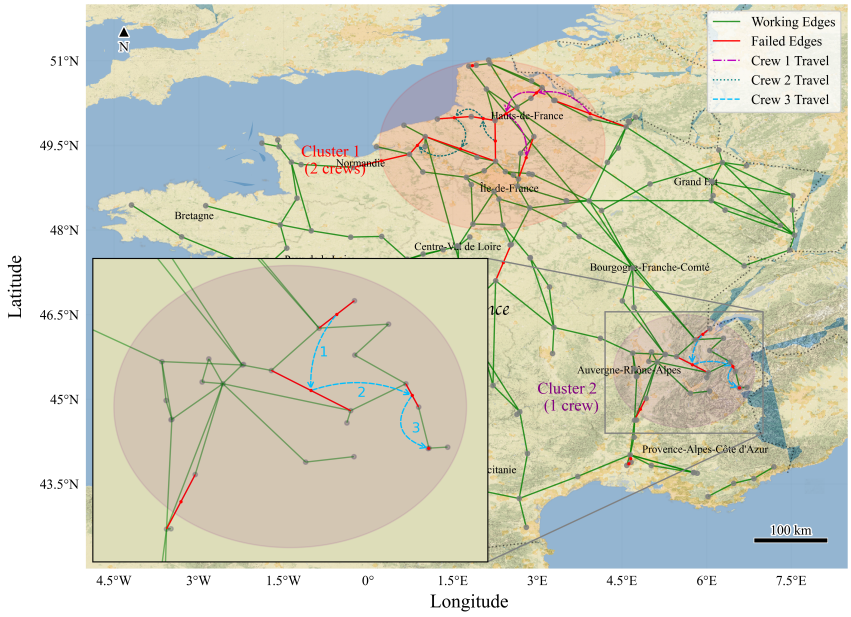

Figure 3.15. Case 1-b (Random Failures with Deterministic Travel Times): Optimal routing for crew 3

B.3 Resilience curves under different considerations of travel times

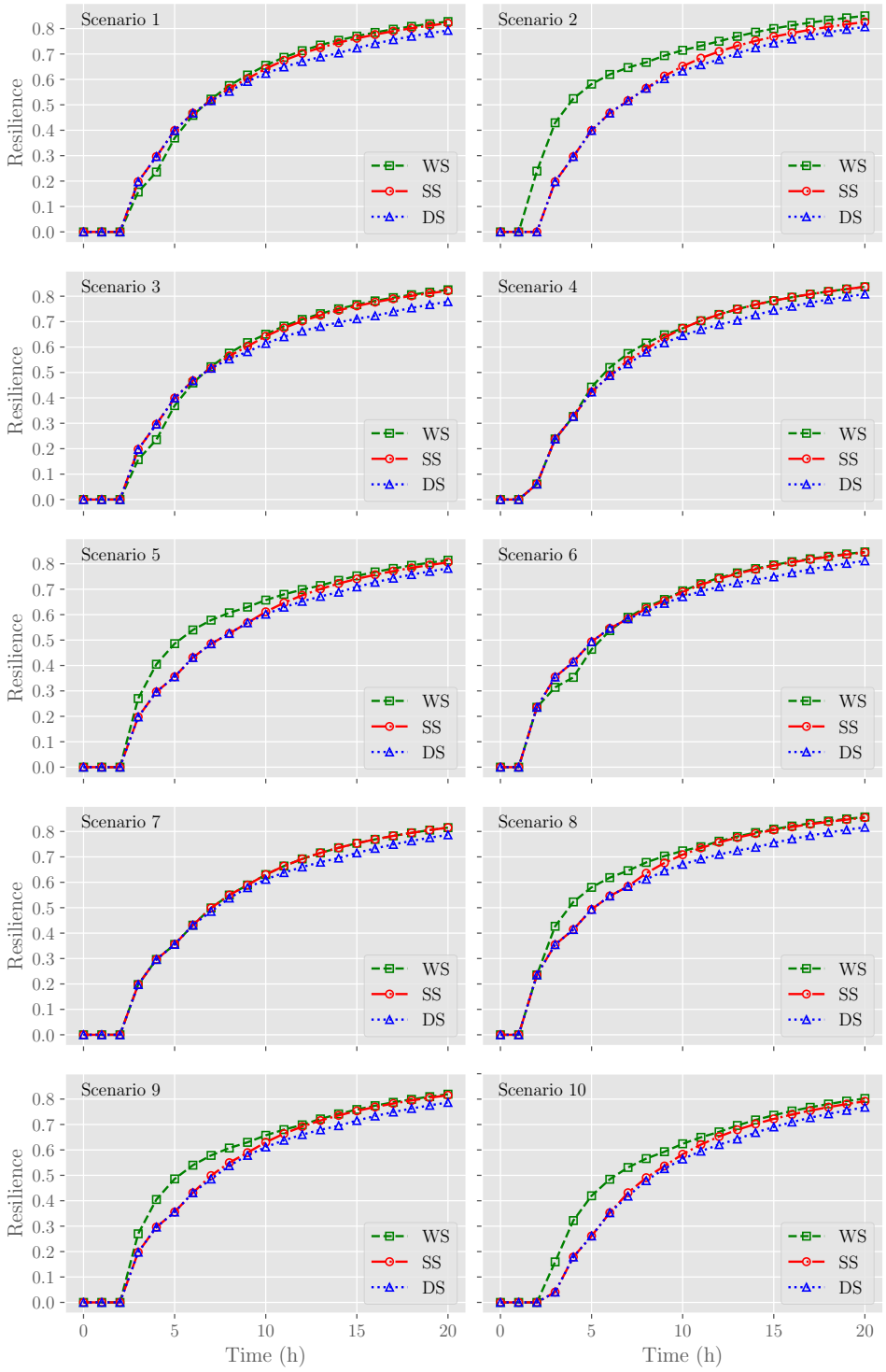

Figure 3.16. Case 1-c (Random Failures with Random Travel Times): Comparison of resilience curves under different solution plans for the reduced 10 scenarios

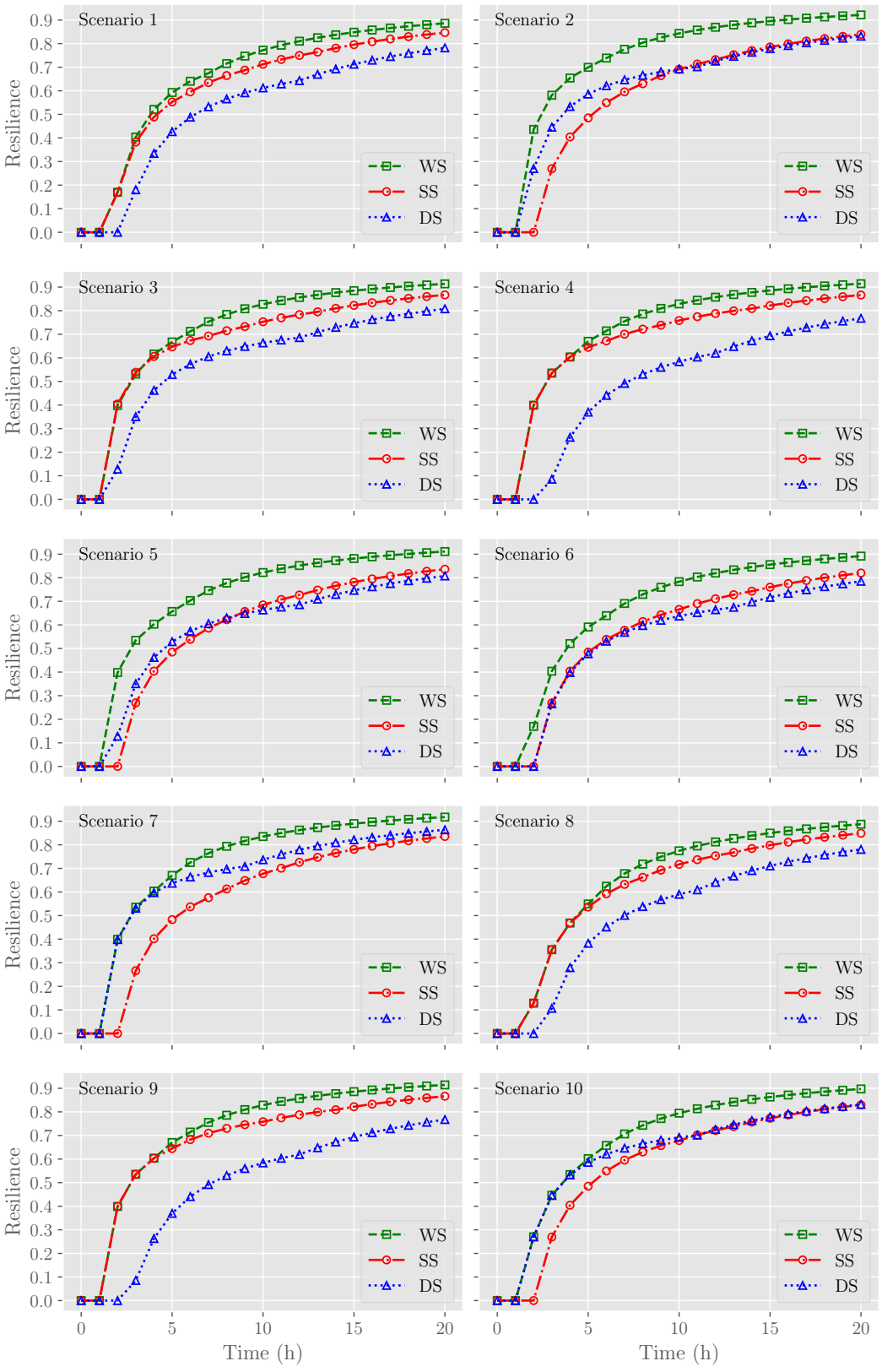

Figure 3.17. Case 2-c (Cascading Failures with Random Travel Times): Comparison of resilience curves under different solution plans for the reduced 10 scenarios

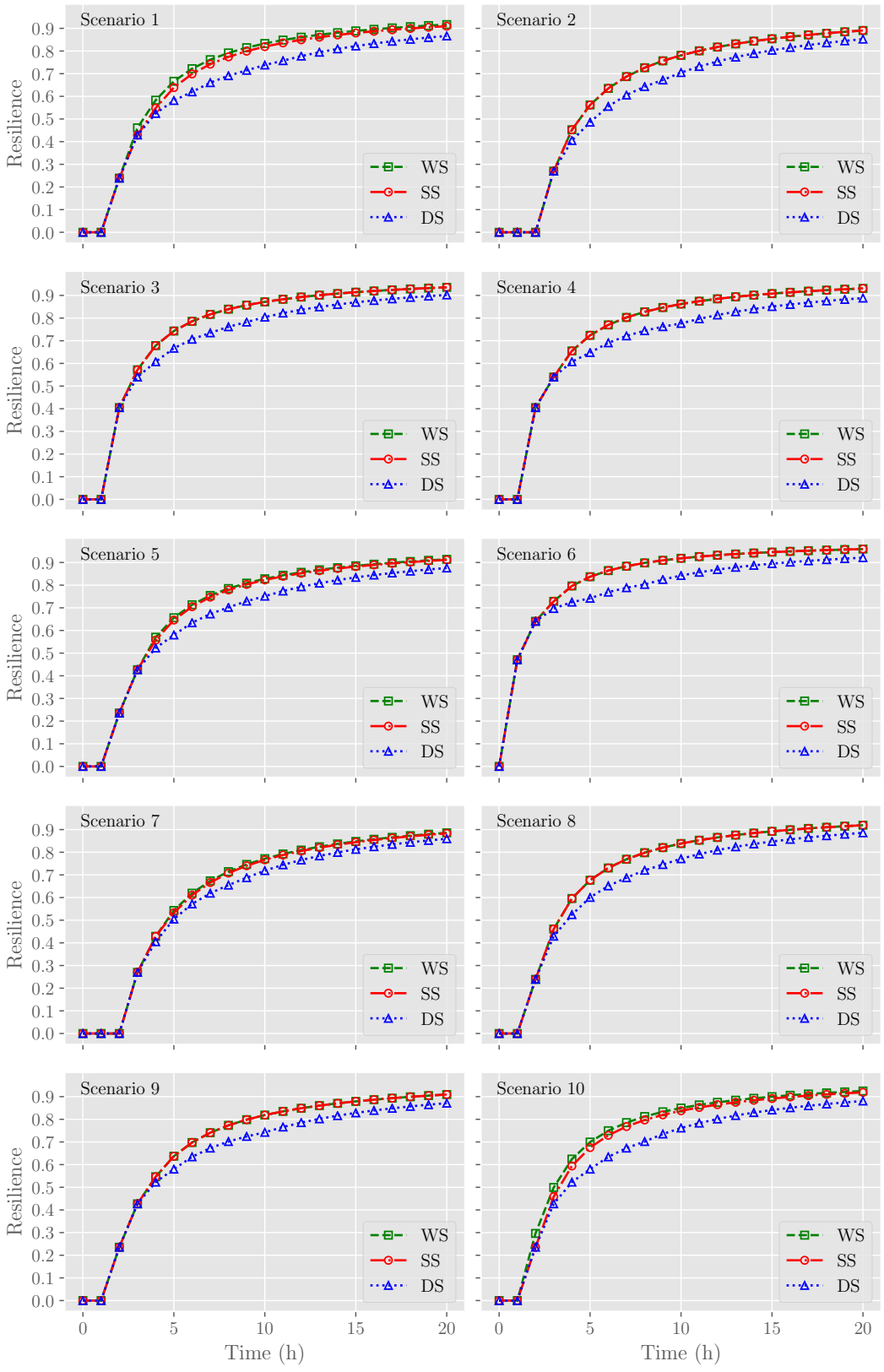

Figure 3.18. Case 1-a (Random Failures without Travel Times): Comparison of resilience curves under different solution plans for the reduced 10 scenarios

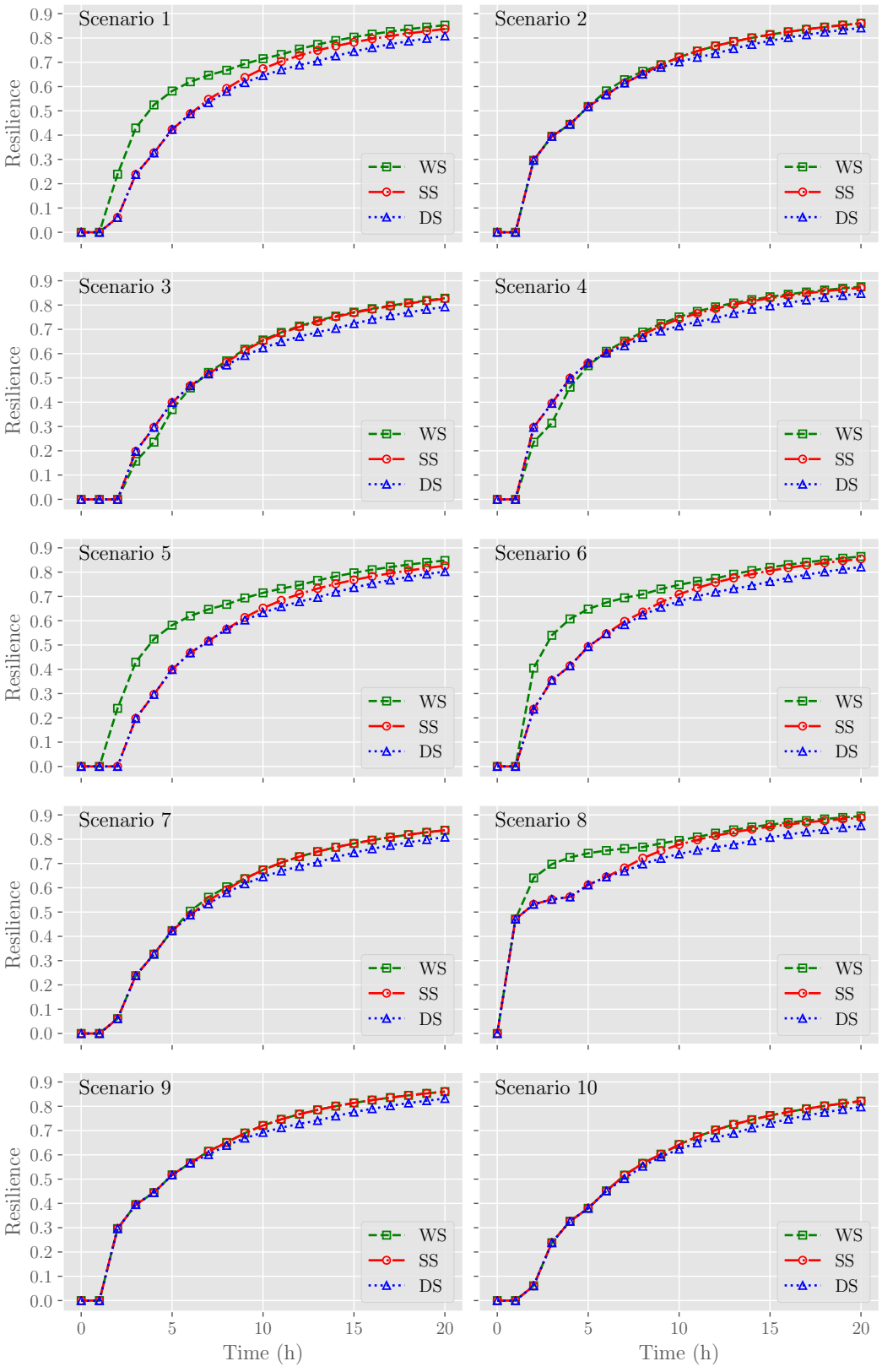

Figure 3.19. Case 1-b (Random Failures with Deterministic Travel Times): Comparison of resilience curves under different solution plans for the reduced 10 scenarios

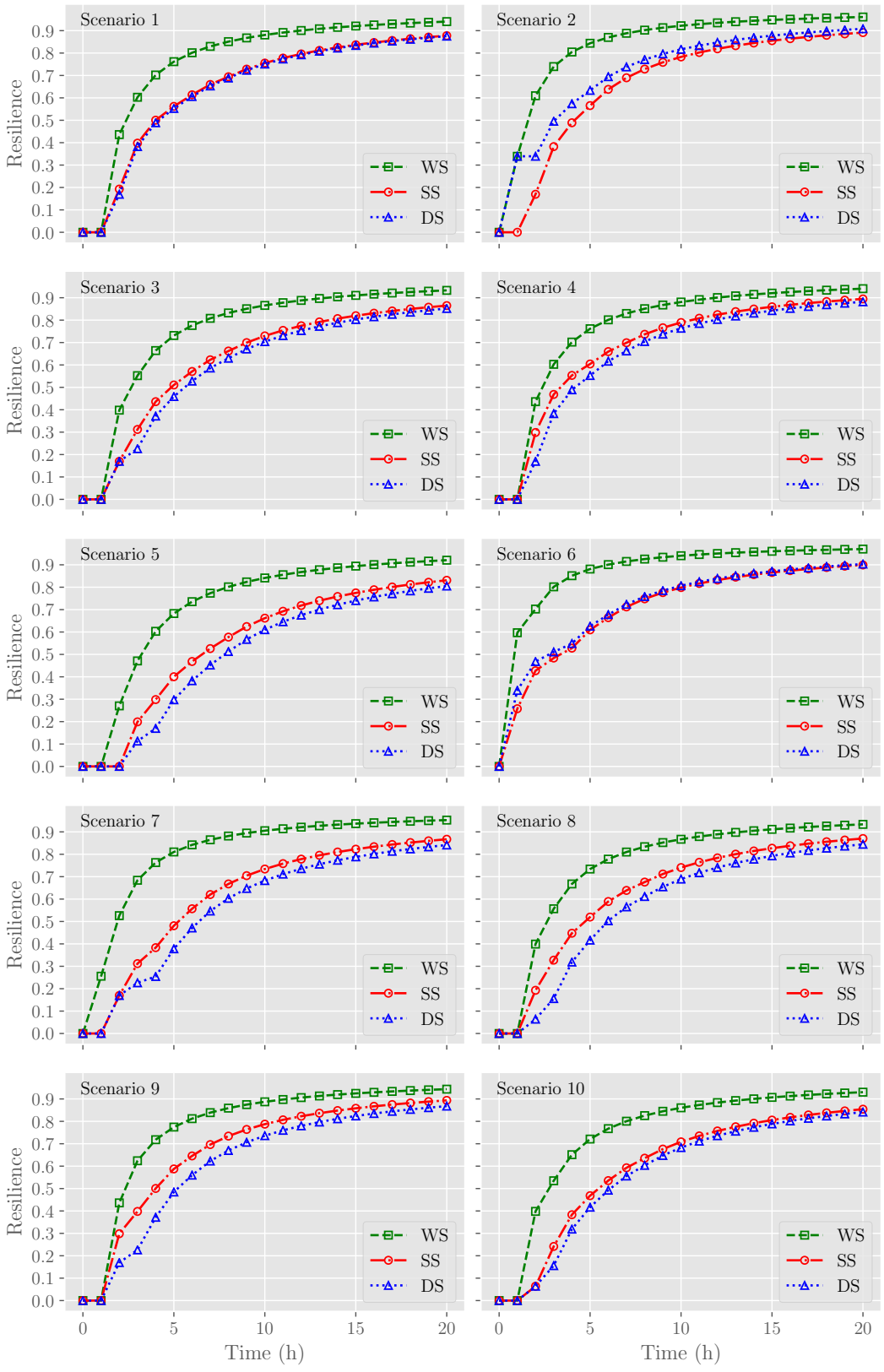

Figure 3.20. Case 2-a (Cascading Failures without Travel Times): Comparison of resilience curves under different solution plans for the reduced 10 scenarios

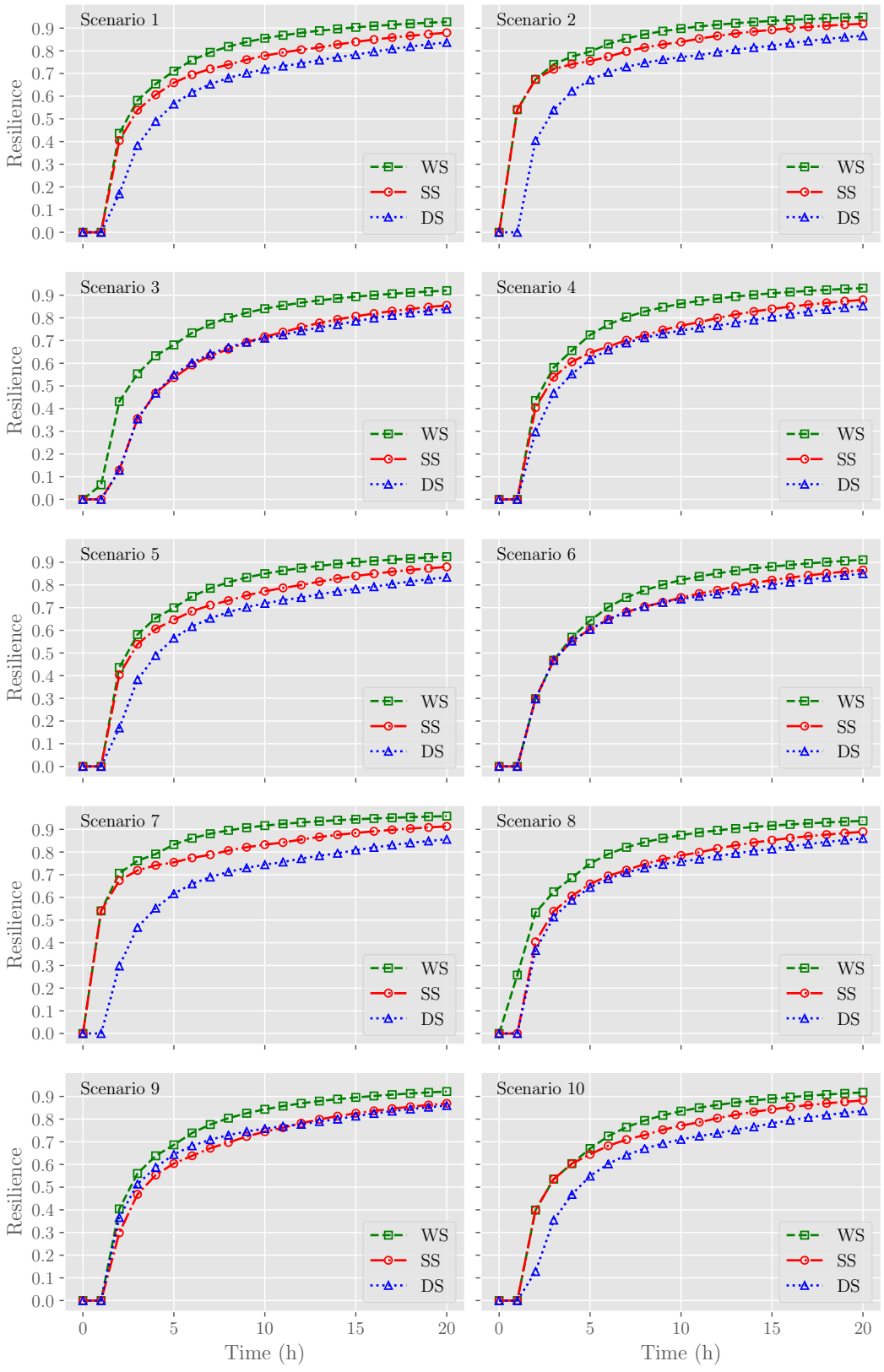

Figure 3.21. Case 2-b (Cascading Failures with Travel Times): Comparison of resilience curves under different solution plans for the reduced 10 scenarios

References

Abdelkader, Y. H. (2004). Evaluating project completion times when activity times are Weibull distributed. *European Journal of Operational Research*, *157*(3), 704–715. doi: 10.1016/S0377-2217(03)00269-8

Aksu, D. T., & Ozdamar, L. (2014). A mathematical model for post-disaster road restoration: Enabling accessibility and evacuation. *Transportation Research Part E: Logistics and Transportation Review*, *61*(1), 56–67. doi: 10.1016/j.tre.2013.10.009

Almoghathawi, Y., Barker, K., & Albert, L. A. (2019). Resilience-driven restoration model for interdependent infrastructure networks. *Reliability Engineering and System Safety*, *185*, 12–23. doi: 10.1016/j.ress.2018.12.006

Anaya-Arenas, A. M., Renaud, J., & Ruiz, A. (2014). Relief distribution networks: a systematic review. *Annals of Operations Research*, *223*(1), 53–79. doi: 10.1007/s10479-014-1581-y

Arpón, S., Homem-de-Mello, T., & Pagnoncelli, B. (2018). Scenario reduction for stochastic programs with conditional value-at-risk. *Mathematical Programming*, *170*(1), 327–356. doi: 10.1007/s10107-018-1298-9

Barker, K., Lambert, J. H., Zobel, C. W., Tapia, A. H., Ramirez-Marquez, J. E., Albert, L., ... Caragea, C. (2017). Defining resilience analytics for interdependent cyber-physical-social networks. *Sustainable and Resilient Infrastructure*, *2*(2), 59–67. doi: 10.1080/23789689.2017.1294859

Benders, J. F. (1962). Partitioning procedures for solving mixed-variables programming problems. *Numerische Mathematik*, *4*, 238–252.

Bienstock, D., & Grebla, G. (2015). *Robust control of cascading power grid failures using stochastic approximation* (arXiv:1504 ed.).

Bienstock, D., & Mattia, S. (2007). Using mixed-integer programming to solve power grid blackout problems. *Discrete Optimization*, *4*(1), 115–141. doi: 10.1016/j.disopt.2006.10.007

Birge, J. R. (1982). The value of the stochastic solution in stochastic linear programs with fixed recourse. *Mathematical Programming*, *24*(1), 314–325. doi: 10.1007/BF01585113

Bruninx, K. (2014). A practical approach on scenario generation and & reduction algorithms for wind power forecast error scenarios..

Bryson, K. M., Millar, H., Joseph, A., & Mobolurin, A. (2002). Using formal MS/OR

modeling to support disaster recovery planning. *European Journal of Operational Research*, *141*(3), 679–688. doi: 10.1016/S0377-2217(01)00275-2

Campbell, R. J., & Lowry, S. (2012). Weather-related power outages and electric system resiliency. Washington, DC: Library of Congress.

Casari, M., & Wilkie, S. J. (2005). Sequencing lifeline repairs after an earthquake: An economic approach. *Journal of Regulatory Economics*, *27*(1), 47–65. doi: 10.1007/S11149-004-4418-9

Çelik, M., Ergun, Ö., & Keskinocak, P. (2015). The post-disaster debris clearance problem under incomplete information. *Operations Research*, *63*(1), 65–85. doi: 10.1287/opre.2014.1342

Chang, L., & Wu, Z. (2011). Performance and reliability of electrical power grids under cascading failures. *International Journal of Electrical Power and Energy Systems*, *33*(8), 1410–1419. doi: 10.1016/j.ijepes.2011.06.021

Chen, J., Lim, C. H., Qian, P. Z., Linderoth, J., & Wright, S. J. (2014). Validating sample average approximation solutions with negatively dependent batches.

CNBC. (2017). *Harvey and Irma economic hit could total $200 billion: Moody's.* (Available at: https://www.cnbc.com/2017/09/11/harvey-and-irma-economic-hit-could-total-200-billion-moodys.html)

CPLEX, IBM. (2020). *CPLEX Optimizer — IBM.* https://www.ibm.com/analytics/cplex-optimizer.

de la Torre, L. E., Dolinskaya, I. S., & Smilowitz, K. R. (2012). Disaster relief routing: Integrating research and practice. *Socio-Economic Planning Sciences*, *46*(1), 88–97. (Special Issue: Disaster Planning and Logistics: Part 1) doi: 10.1016/j.seps.2011.06.001

D'Electricité, Le Réseau de Transport. (2019). *RTE - Generation forecast.* (Available at: https://clients.rte-france.com/lang/an/visiteurs/vie/prod/prevision{_}production.jsp?t=solaire)

Dupačová, J., Gröwe-Kuska, N., & Römisch, W. (2003). Scenario reduction in stochastic programming. *Mathematical Programming*, *95*(3), 493–511. doi: 10.1007/s10107-002-0331-0

Ellis, J., Fisher, D., Longstaff, T., Pesante, L., & Pethia, R. (1997). *Report to the president's commission on critical infrastructure protection.* (Tech. Rep.). Pittsburgh, PA: Carnegie Mellon University Software Engineering Institute. (Available at: https://apps.dtic.mil/docs/citations/ADA324232) doi: 10.21236/ada324232

Escudero, L. F., Garín, M. A., & Unzueta, A. (2017). Scenario cluster Lagrangean decomposition for risk averse in multistage stochastic optimization. *Computers and Operations Research*, *85*, 154–171. doi: 10.1016/j.cor.2017.04.007

Executive Office of the President. (2011). *A policy framework for the 21st century grid: Enabling our secure energy future*. Washington, D.C.: National Science and Technology Council.

Executive Office of the President, Council of Economic Advisers. (2013). *Economic benefits of increasing electric grid resilience to weather outages*. Washington, D.C.: The Council.

Fairbrother, J., Turner, A., & Wallace, S. W. (2019). Problem-driven scenario generation: an analytical approach for stochastic programs with tail risk measure. *Mathematical Programming*, *0*, 1–42. doi: 10.1007/s10107-019-01451-7

Fang, Y., Pedroni, N., & Zio, E. (2016). Resilience-Based Component Importance Measures for Critical Infrastructure Network Systems. *IEEE Transactions on Reliability*, *65*(2), 502–512. doi: 10.1109/tr.2016.2521761

Fang, Y., Pedroni, N., & Zio, E. (2017). Comparing network-centric and power flow models for the optimal allocation of link capacities in a cascade-resilient power transmission network. *IEEE Systems Journal*, *11*(3), 1632–1643. doi: 10.1109/jsyst.2014.2352152

Fang, Y., & Sansavini, G. (2017). Emergence of antifragility by optimum postdisruption restoration planning of infrastructure networks. *Journal of Infrastructure Systems*, *23*(4), 04017024. doi: 10.1061/(ASCE)IS.1943-555X.0000380

Fang, Y., & Sansavini, G. (2019). Optimum post-disruption restoration under uncertainty for enhancing critical infrastructure resilience. *Reliability Engineering and System Safety*, *185*(January 2019), 1–11. doi: 10.1016/j.ress.2018.12.002

FEMA. (2017). *Historic disaster response to hurricane harvey in texas.* (Available at: https://www.fema.gov/news-release/2017/09/22/historic-disaster-response-hurricane-harvey-texas)

Force, Hurricane Sandy Rebuilding Task Force. (2013). *Hurricane Sandy rebuilding strategy* (US). Washington, DC: Department of Housing and Urban Development,.

Garay-Sianca, A., & Pinkley, S. G. N. (2021, feb). Interdependent integrated network design and scheduling problems with movement of machines. *European Journal of Operational Research*, *289*(1), 297–327. doi: 10.1016/j.ejor.2020.07.013

García-Bertrand, R., & Mínguez, R. (2012). Iterative scenario based reduction technique for stochastic optimization using conditional value-at-risk. *Optimization and Engineering*, *15*(2), 355–380. doi: 10.1007/s11081-012-9201-7

Gasser, P., Lustenberger, P., Cinelli, M., Kim, W., Spada, M., Burgherr, P., ... Sun, T. Y. (2019). A review on resilience assessment of energy systems. *Sustainable and Resilient Infrastructure*, 1–27. doi: 10.1080/23789689.2019.1610600

Gomez, C., González, A. D., Baroud, H., & Bedoya-Motta, C. D. (2019). Integrating operational and organizational aspects in interdependent infrastructure network recovery. *Risk Analysis*, *39*(9), 1913–1929. doi: 10.1111/risa.13340

González, A. D., Dueñas-Osorio, L., Sánchez-Silva, M., & Medaglia, A. L. (2016). The Interdependent Network Design Problem for Optimal Infrastructure System Restoration. *Computer-Aided Civil and Infrastructure Engineering*, *31*(5), 334–350. doi: 10.1111/mice.12171

Heitsch, H., & Römisch, W. (2003). Scenario reduction algorithms in stochastic programming. *Computational Optimization and Applications*, *24*(2/3), 187–206. doi: 10.1023/a:1021805924152

Helbing, D. (2013). Globally networked risks and how to respond. *Nature*, *497*(7447), 51–59. doi: 10.1038/nature12047

Henry, D., & Ramirez-Marquez, J. E. (2012). Generic metrics and quantitative approaches for system resilience as a function of time. *Reliability Engineering and System Safety*, *99*, 114–122. doi: 10.1016/j.ress.2011.09.002

Hollnagel, E., Woods, D. D., & Leveson, N. (2006). *Resilience engineering: Concepts and precepts*. Aldershot, UK: Ashgate Publishing, Ltd.

Homem-de-Mello, T., & Pagnoncelli, B. K. (2016, feb). Risk aversion in multistage stochastic programming: A modeling and algorithmic perspective. *European Journal of Operational Research*, *249*(1), 188–199. doi: 10.1016/j.ejor.2015.05.048

Horejšová, M., Vitali, S., Kopa, M., & Moriggia, V. (2020, jun). Evaluation of scenario reduction algorithms with nested distance. *Computational Management Science*, *17*(2), 241–275. doi: 10.1007/s10287-020-00375-4

Hosseini, S., Barker, K., & Ramirez-Marquez, J. E. (2016). A review of definitions and measures of system resilience. *Reliability Engineering and System Safety*, *145*, 47–61. doi: 10.1016/j.ress.2015.08.006

Iloglu, S., & Albert, L. A. (2020). A maximal multiple coverage and network restoration problem for disaster recovery. *Operations Research Perspectives*, *7*, 100132. doi: 10.1016/j.orp.2019.100132

Karagiannis, G. M., Chondrogiannis, S., Krausmann, E., & Turksezer, Z. I. (2017). *Power grid recovery after natural hazard impact* (Tech. Rep. No. EUR 28844 EN).

Luxembourg: Publications Office of the European Union. doi: 10.2760/87402

Kasaei, M., & Salman, F. S. (2016). Arc routing problems to restore connectivity of a road network. *Transportation Research Part E: Logistics and Transportation Review*, *95*, 177–206. doi: 10.1016/j.tre.2016.09.012

Kleywegt, A. J., Shapiro, A., & Homem-de-Mello, T. (2002, jan). The sample average approximation method for stochastic discrete optimization. *SIAM Journal on Optimization*, *12*(2), 479–502. doi: 10.1137/s1052623499363220

Krokhmal, P., Palmquist, J., & Uryasev, S. (2002). Portfolio optimization with conditional value-at-risk objective and constraints. *Journal of risk*, *4*, 43–68.

Lee II, E. E., Mitchell, J. E., & Wallace, W. A. (2007). Restoration of services in interdependent infrastructure systems: A network flows approach. *IEEE Transactions on Systems, Man, and Cybernetics, Part C (Applications and Reviews)*, *37*(6), 1303–1317. doi: 10.1109/TSMCC.2007.905859

Li, Y., & Lence, B. J. (2007). Estimating resilience for water resources systems. *Water Resources Research*, *43*(7), 1–11. doi: 10.1029/2006wr005636

Luo, H., Alkhaleel, B. A., Liao, H., & Pascual, R. (2020). Resilience improvement of a critical infrastructure via optimal replacement and reordering of critical components. *Sustainable and Resilient Infrastructure*, 1–21. doi: 10.1080/23789689.2019.1710072

Manuel, J. (2013). *The long road to recovery: Environmental health impacts of hurricane sandy* (Vol. 121) (No. 5). Environmental Health Perspectives. doi: 10.1289/ehp.121-a152

Matisziw, T. C., Murray, A. T., & Grubesic, T. H. (2010). Strategic network restoration. *Networks and Spatial Economics*, *10*(3), 345–361. doi: 10.1007/s11067-009-9123-x

Mete, H. O., & Zabinsky, Z. B. (2010). Stochastic optimization of medical supply location and distribution in disaster management. *International Journal of Production Economics*, *126*(1), 76–84. (Improving Disaster Supply Chain Management – Key supply chain factors for humanitarian relief) doi: 10.1016/j.ijpe.2009.10.004

Morales, J. M., Pineda, S., Conejo, A. J., & Carrión, M. (2009). Scenario reduction for futures market trading in electricity markets. *IEEE Transactions on Power Systems*, *24*(2), 878–888. doi: 10.1109/TPWRS.2009.2016072

Morshedlou, N. (2018). *Adaptive and Restorative Capacity Planning for Complex Infrastructure Networks: Optimization Algorithms and Applications* (Unpublished doctoral dissertation). University of Oklahoma.

Motter, A. E., & Lai, Y.-C. (2002). Cascade-based attacks on complex networks. *Physical Review E*, *66*(6). doi: 10.1103/physreve.66.065102

Noyan, N. (2012). Risk-averse two-stage stochastic programming with an application to disaster management. *Computers and Operations Research*, *39*(3), 541–559. doi: 10.1016/j.cor.2011.03.017

Nurre, S. G., Cavdaroglu, B., Mitchell, J. E., Sharkey, T. C., & Wallace, W. A. (2012). Restoring infrastructure systems: An integrated network design and scheduling (INDS) problem. *European Journal of Operational Research*, *223*(3), 794–806. doi: 10.1016/j.ejor.2012.07.010

Nurre, S. G., & Sharkey, T. C. (2014). Integrated network design and scheduling problems with parallel identical machines: Complexity results and dispatching rules. *Networks*, *63*(4), 306–326. doi: 10.1002/net.21547

O'Donnell, K. (2013). Critical infrastructure resilience: Resilience thinking in australia's federal critical infrastructure protection policy. *Salus Journal*, *1*(3), 13.

Odyssee-Mure. (2020). *EU household energy consumption.* (Available at: https://www.odyssee-mure.eu/publications/efficiency-by-sector/households/household-eu.pdf)

Ouyang, M., & Wang, Z. (2015). Resilience assessment of interdependent infrastructure systems: With a focus on joint restoration modeling and analysis. *Reliability Engineering and System Safety*, *141*, 74–82. doi: 10.1016/j.ress.2015.03.011

Özdamar, L., & Ertem, M. A. (2015). Models, solutions and enabling technologies in humanitarian logistics. *European Journal of Operational Research*, *244*(1), 55–65. doi: 10.1016/j.ejor.2014.11.030

Pineda, S., & Conejo, A. (2010). Scenario reduction for risk-averse electricity trading. *IET Generation, Transmission & Distribution*, *4*(6), 694. doi: 10.1049/iet-gtd.2009.0376

Python. (2020). *Python.org.* https://www.python.org/.

Rachev, S. T. (1991). *Probability metrics and the stability of stochastic models, scenario.* Chichester New York: Wiley.

Rahmaniani, R., Crainic, T. G., Gendreau, M., & Rei, W. (2017). The benders decomposition algorithm: A literature review. *European Journal of Operational Research*, *259*(3), 801–817. doi: 10.1016/j.ejor.2016.12.005

Rockafellar, R. T., & Uryasev, S. (2000). Optimization of conditional value-at-risk. *The Journal of Risk*, *2*(3), 21–41. doi: 10.21314/jor.2000.038

Rose, A. (2007). Economic resilience to natural and man-made disasters: Multidisciplinary origins and contextual dimensions. *Environmental Hazards*, *7*(4), 383–398. doi: 10.1016/j.envhaz.2007.10.001

Sharkey, T. C., Cavdaroglu, B., Nguyen, H., Holman, J., Mitchell, J. E., & Wallace, W. A. (2015, jul). Interdependent network restoration: On the value of information-sharing. *European Journal of Operational Research*, *244*(1), 309–321. doi: 10.1016/j.ejor.2014.12.051

Vugrin, E. D., Turnquist, M. A., & Brown, N. J. (2014). Optimal recovery sequencing for enhanced resilience and service restoration in transportation networks. *International Journal of Critical Infrastructures*, *10*(3/4), 218–246. doi: 10.1504/IJCIS.2014.066356

White House. (2013). *Presidential Policy Directive/PPD-21 : Critical Infrastructure Security and Resilience. Office of the Press Secretary: Washington, DC.* [Administration of Barack Obama]. Washington, DC..

Wyss, G. D., & Jorgensen, K. H. (1998). A User ' s Guide to LHS : Sandia's Latin Hypercube Sampling Software Acknowledgments. *Distribution*(February), 88. doi: 98-0210

Xu, N., Guikema, S. D., Davidson, R. A., Nozick, L. K., Çağnan, Z., & Vaziri, K. (2007). Optimizing scheduling of post-earthquake electric power restoration tasks. *Earthquake Engineering and Structural Dynamics*, *36*(2), 265–284. doi: 10.1002/eqe.623

Zamuda, C., Mignone, B., Bilello, D., Hallett, K., Lee, C., Macknick, J., ... Steinberg, D. (2013). U.S. energy sector vulnerabilities to climate change and extreme weather.

Zhang, C., Kong, J.-j., & Simonovic, S. P. (2018). Restoration resource allocation model for enhancing resilience of interdependent infrastructure systems. *Safety Science*, *102*, 169–177. doi: 10.1016/j.ssci.2017.10.014

Zio, E. (2016). Challenges in the vulnerability and risk analysis of critical infrastructures. *Reliability Engineering and System Safety*, *152*, 137–150. doi: 10.1016/j.ress.2016.02.009

Chapter 4

Model and Solution Method for Mean-Risk Cost-Based Post-Disruption Restoration of Interdependent Critical Infrastructure Networks

Basem A. Alkhaleel, Haitao Liao, Kelly M. Sullivan

Abstract

Critical infrastructure networks (CINs), such as power grids, water distribution systems, and telecommunication networks, are essential for the functioning of society and the economy. As these infrastructure networks are not isolated from each other, their functions are not independent and may be vulnerable to disruptive events (e.g., component failures, terrorist attacks, natural disasters). For decision makers, how to restore the functions of CINs while accounting for interdependencies and various uncertainties becomes a challenging task. In this work, we study the post-disruption restoration problem for a system of interdependent CINs under uncertainty. We propose a two-stage mean-risk stochastic restoration model using mixed-integer linear programming (MILP) with the goal of minimizing the total cost associated with unsatisfied demands, repair tasks, and flow of interdependent infrastructure networks. The restoration model considers the availability of limited time and resources and provides a prioritized list of components to be restored along with assigning and scheduling them to the available network-specific work crews. Additionally, the model features flexible restoration strategies including multicrew assignment for a single component and a multimodal repair setting along with the consideration of full and partial functioning and dependencies between the multi-network components. The proposed model is illustrated

using the power and water networks in Shelby County, Tennessee, United States, under two hypothetical earthquake scenarios.

4.1 Introduction

4.1.1 Background

Modern societies rely on the proper functioning and sustainability of critical infrastructure networks (CINs) such as electric power systems, water supply systems, transportation, and telecommunications (Karakoc *et al.*, 2019). Therefore, maintaining secure and resilient critical infrastructures (CIs) has become one of the most demanding challenges for governments around the globe, especially in the last three decades (Humphreys, 2019; Karagiannis *et al.*, 2017; White House, 2013). For instance, the United States (U.S.) federal planning documents suggest the importance of addressing CI resilience in such a way that reflects its "interconnectedness and interdependency" (White House, 2013). Planning for disruptions to CINs has shifted recently from emphasizing prevention and protection to capturing the CIs' ability to withstand disruptions and quickly recover their functions (Hosseini *et al.*, 2016; Humphreys, 2019). This ability to withstand, adapt to, and recover from disruptions is referred to as *resilience* (Almoghathawi *et al.*, 2019; Barker *et al.*, 2017; Humphreys, 2019).

CINs are often vulnerable and subject to natural and/or man-made disruption events (e.g., earthquakes, hurricanes, and malevolent attacks), which could impact the CINs' performance unpredictably and result in severe socioeconomic consequences (Alkhaleel *et al.*, 2021; Almoghathawi *et al.*, 2019). Indeed, such disruptions become inevitable in a modern world featuring growing dynamic and hazardous operating environments (Helbing, 2013). Economically, they have caused huge economic losses around the globe. In the past 50 years, more than 22,500 disasters occurred globally impacting about 8 million people and costing

approximately (in 2019 dollar-adjusted value) $3.7 trillion (CRED, 2021). Annually, only weather-related outages (excluding malevolent attacks and non-weather natural hazards) are estimated to have cost the U.S. economy an inflation-adjusted annual average of $18 billion up to $70 billion (Campbell & Lowry, 2012; Executive Office of the President, 2013).

Interdependencies among infrastructure networks have become more frequent and complex due to the increasing trend of globalization and technological developments (Karakoc *et al.*, 2019; Rinaldi *et al.*, 2001; Saidi *et al.*, 2018). However, although interdependencies can improve the efficiency of networks functionality, this type of complex coordination often causes them to become more vulnerable to disruptions (e.g., random failures, malevolent attacks, and natural disasters). As a result, a disruption in some components of one of the infrastructure networks could cause a malfunction in the undisrupted components of other dependent networks, resulting in a series of cascading failures affecting the whole infrastructure network system (Buldyrev *et al.*, 2010; Danziger *et al.*, 2016; Eusgeld *et al.*, 2011; Karakoc *et al.*, 2019; Little, 2002; Ouyang, 2014; Wallace *et al.*, 2003). Rinaldi *et al.* (2001) stated in a seminal paper on infrastructure interdependencies that "critical infrastructures are highly interconnected and mutually dependent in complex ways, both physically and through a host of information and communications technologies." Although the interdependent nature of "lifeline" infrastructures was acknowledged two decades ago (Amin, 2002), the literature on the study of interdependent networks has only recently started appearing and has become a trending topic in resilience engineering applications (Almoghathawi *et al.*, 2019; Buldyrev *et al.*, 2010, 2011; Cavdaroglu *et al.*, 2011; Danziger *et al.*, 2016).

The high vulnerability of infrastructure networks against disruptions and the

associated risks of such events have become a critical concern for decision makers, especially with the need to account for the interdependencies through recovery planning to obtain a realistic analysis of their performance (Holden *et al.*, 2013). Moreover, scheduling the restoration processes separately for interdependent critical infrastructure networks (ICINs) without considering their interdependencies could cause misutilization of resources, waste of time and funds, and even might trigger additional inefficiency of distribution systems (Baidya & Sun, 2017). However, functional connectivity among these CIs is not the only dependency that should be taken into account; spatial, cyber, social, and logical interdependencies are other interdependency forms that could impact restoration and recovery planning (Min *et al.*, 2007; Rinaldi *et al.*, 2001; Sharkey *et al.*, 2015).

Recent events such as Hurricane Harvey (Force, 2013) and the 2016 Ecuador earthquake (Meltzer *et al.*, 2019) suggest that not all undesired events can be prevented. In these events and many others, multiple networked systems including the transportation, power, and water networks are impacted (Manuel, 2013; Meltzer *et al.*, 2019; Mendonca *et al.*, 2004). Hence, improving recovery planning actions after disruptions is an essential part of CIs resilience. That is, resilience can be effectively improved by developing optimized plans for promptly restoring the disrupted service after the occurrence of a disruptive event. In planning ICINs restoration, prioritizing components is key in improving the recovery process and system resilience. It is also necessary to consider the practical significant challenges that face recovery actions such as repair times uncertainty and poor access to damaged facilities when developing restoration plans (Karagiannis *et al.*, 2017). To this end, the development of effective restoration strategies and scheduling approaches for CIs post-disruption restoration is typically accomplished through optimization approaches. In the literature, there are

numerous studies in the context of post-disruption CI restoration under a mathematical programming framework (Alkhaleel *et al.*, 2021; Fang & Sansavini, 2017; Nurre & Sharkey, 2014; Vugrin *et al.*, 2014; Zhang *et al.*, 2018). Of course, the main goal of such studies is to optimize the scheduling process of restoration tasks in order to accelerate the recovery process and improve the overall resilience (Vugrin *et al.*, 2014).

4.1.2 CIs interdependencies classification

Infrastructure networks are not isolated from each other, but rather they rely on one another in different ways for their proper functioning. Hence, they exhibit interdependency, where a pair of infrastructure networks are said to be interdependent if there is a bidirectional relationship between them through which the state of each infrastructure depends on the state of the other (Peerenboom *et al.*, 2002; Rinaldi *et al.*, 2001). Interdependencies play a critical role in the resilience of CIs by not only contributing to the widespread of failure propagation (e.g., cascading failures), but also by either facilitating or complicating the entire recovery process (Guidotti *et al.*, 2016). The recovery rate of ICIs components depends on several factors which are often difficult to understand, model, and predict; hence, this uncertainty is reflected on planning the recovery strategy and utilizing related resources (Bruneau *et al.*, 2003; Franchin & Cavalieri, 2015; Guidotti *et al.*, 2016; Sharma *et al.*, 2017). The need to describe the relationships among infrastructure systems, and the corresponding propagation of system disruptions led to the definition of several classifications of the nature of infrastructure interdependencies (e.g., Lee II *et al.* (2007); Rinaldi *et al.* (2001); Wallace *et al.* (2003); Zhang and Peeta (2011); Zimmerman (2001)). The classification of Rinaldi *et al.* (2001) is described as a "self-contained classification" that is capable of capturing the

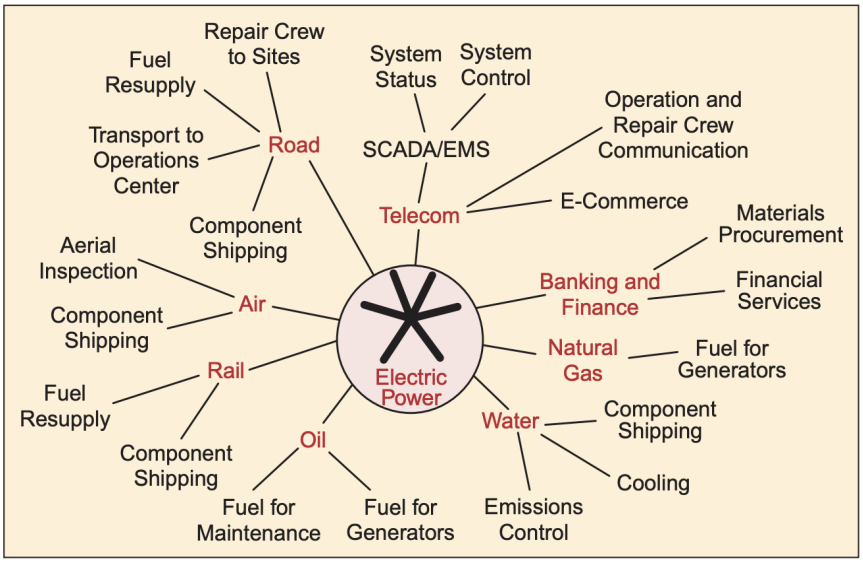

Figure 4.1. Examples of electric power infrastructure dependencies (adapted from Rinaldi *et al.* (2001))

different nature of interdependencies (Ouyang, 2014).

Rinaldi *et al.* (2001) classified the interdependencies between infrastructure networks into four categories: (i) *physical interdependency*, an output from an infrastructure network is an input to another one and vice versa, (ii) *cyber interdependency*, if an infrastructure network depends on information transmitted through an information infrastructure, (iii) *geographical interdependency*, if two infrastructure networks are affected by the same local disruptive event, and (iv) *logical interdependency*, all other types of interdependencies (e.g., the social or legal link between two CIs). Figure 4.1 shows some examples of the interdependencies between electric power networks and different infrastructure networks. Throughout this article, we focus on the physical interdependency among different CINs. This physical interdependency defined by Rinaldi *et al.* (2001) is equivalent to the so-called functional or input interdependency in other interdependency classifications (Lee II *et al.*, 2007).

4.1.3 Related literature

There are several modeling, optimization, and simulation techniques proposed in the literature that consider interdependencies between infrastructure networks (see Ouyang (2014) for a detailed review). Such techniques can be classified into six categories (Rinaldi, 2004): (i) aggregate supply and demand tools, where infrastructures are linked by their demand for commodities (or services) supplied by other infrastructures (e.g., Enayaty Ahangar *et al.* (2020)), (ii) dynamic simulations, which examines infrastructures operations, the effects of disruptions, and the associated consequences (e.g., Zhang *et al.* (2016) (iii) agent-based models, where physical components of infrastructures can be modeled as agents allowing the analyses of the operational characteristics, the physical states of infrastructures, and the decision-making policies involved with infrastructure operations (e.g., Azucena *et al.* (2021)). (iv) physics-based models, where physical characteristics of CIs can be analyzed with standard engineering techniques such as power flow in electric power grids (e.g., Unsihuay *et al.* (2007)) (v) population mobility models, where this class of models examines the movement of entities (e.g., people following their daily routines) through urban regions (e.g., Casalicchio *et al.* (2009)). (vi) Leontief input-output models, where Leontief's model of economic flows can be applied to CIs studies (Haimes & Jiang, 2001). Throughout this article, the focus will be on the first category with aggregated supply and demand tools.

Post-disruption restoration and recovery problems considering interdependent critical infrastructures (ICIs) have been addressed in the literature through different approaches. Almoghathawi *et al.* (2021) classifies these approaches into two broad categories: (i)

infrastructure-specific approaches, which consider the physics of different infrastructures (e.g., DC power flow model) and hence could be applied on these infrastructure networks only, and (ii) general approaches, which could be applied to any system of interdependent infrastructure networks. Both approaches often fall under the area of combining network design and scheduling problems following the lead of Nurre *et al.* (2012) who introduced the integrated network design and scheduling problem (INDS) for restoring a single infrastructure network with the goal of maximizing the cumulative maximum flow over time. Other goals and problem types of post-disruption recovery can be found in the survey article by Çelik (2016) who summarized the work on recovering networks for humanitarian operations and the different problems (decision-making processes) associated with this field of research.

Regarding the infrastructure-specific approaches for interdependent networks restoration, Coffrin *et al.* (2012) proposed a randomized adaptive decomposition approach to solve the problem of restoring two physically interdependent infrastructure networks, namely power and gas networks. They integrated two network-specific flow models (i.e., a linearized DC flow model for the power network and a maximum flow model for the gas network) using a mixed-integer programming (MIP) approach with the objective of maximizing the weighted sum of interdependent demand over the restoration time horizon. However, their proposed model did not consider different restoration durations for the disrupted components of both networks. Baidya and Sun (2017) presented an optimized restoration strategy with the goal of prioritizing the restoration activities between two physically interdependent infrastructure networks –power and communication networks– considering their physical properties. The proposed approach is formulated using MIP with the objective of activating every node in both networks with the minimum number of activation/energization of branches. Tootaghaj

et al. (2017) studied the impact of cascading disruption on the physically interdependent power grid and communication network by considering only disruptions in power networks. As a result, they proposed a two-step recovery approach. The first step is to avoid further cascades, for which they formulated the minimum cost flow assignment problem using linear programming with the objective of finding a DC power flow setting that stops the cascading failure at minimum cost. The second step is to provide a recovery schedule, for which they formulated the recovery problem using MIP—with the goal of maximizing the total amount of delivered power over the recovery horizon—and solved the problem using heuristic approaches.

Regarding the general approaches for interdependent infrastructure networks restoration, Lee II *et al.* (2007) proposed an MIP model for interdependent layer networks accounting for different interdependencies between the infrastructure networks. The objective of the model is to minimize the flow costs along with the costs of unmet demand. Moreover, the model focuses only on determining the set of disrupted components (i.e., edges) of the interdependent infrastructure networks that need to be recovered to restore the performance of each of the infrastructure networks to its pre-disruption functionality level. Hence, the proposed model does not specify a threshold time at which edges need to be restored nor the assignment of each work crew to restore which disrupted component. On the other hand, Gong *et al.* (2009) focused only on the scheduling problem of a predetermined set of disrupted components for ICINs with predefined due dates for them. They provided an MIP multi-objective restoration planning model to find the optimal restoration schedule for disrupted components. They proposed a logic-based benders decomposition approach to solve the model, whose objective is to minimize the weighted sum of cost, tardiness, and

makespan associated with the restoration process. Cavdaroglu *et al.* (2011) integrated the two approaches by Lee II *et al.* (2007) and Gong *et al.* (2009) by providing an MIP model that: (i) determines the set of disrupted components (i.e., edges) to be restored, (ii) assigns and schedules them to work crews. The model was solved using a suggested heuristic solution method. The objective of the model is to minimize the total cost of flow, unsatisfied demand, and installation and assignment associated with the full restoration of a set of infrastructure networks accounting for their interdependencies. In addition, Holden *et al.* (2013) proposed an extended network flow approach to simulate the performance of infrastructure networks at a local scale (i.e., community scale) considering the physical interdependency among them. They provided a linear programming optimization model with the goal of finding the optimal performance of the infrastructure networks such that the total cost associated with production, storage, commodity flow, discharge, and shortage (i.e., unsatisfied demand) is minimized. However, the proposed approach by Holden *et al.* (2013) does not explicitly discuss what is the set of disrupted networks components, their restoration durations, their restoration priorities, and the availability of work crews. Ouyang and Wang (2015) compared the effectiveness of five strategies for joint restoration of interdependent infrastructures and applied a Genetic Algorithm (GA) to generate recovery sequences. Sharkey *et al.* (2015) studied the restoration of multiple ICINs under a centralized decision-making framework and proposed an MIP model to solve the problem. Additionally, González *et al.* (2016) proposed an MIP model for optimizing infrastructure systems joint restoration considering geographical and physical interdependencies between multiple CI systems. Di Muro *et al.* (2016) studied the recovery problem of the system of ICINs in the presence of cascading failures to mitigate its breakdown. They considered the restoration of disrupted network

components (i.e., nodes) located at the boundary of the largest connected component in the functional networks. In their study, they tried to reconnect the boundary nodes to the largest connected component considering the probability of recovery that halts the cascade.

In recent years, Zhang *et al.* (2018) optimized the allocation of restoration resources for a set of physically interdependent infrastructure networks to enhance their resilience. A genetic algorithm was developed to allocate limited resources to interdependent infrastructure networks and to determine the optimal restoration budget following a disruptive event. Mooney *et al.* (2019) proposed a multi-objective MIP model that integrates a facilities location problem, that determines where resources should be stationed following a disruption, and a recovery scheduling problem to optimize the restoration process of a system of ICIs. Karakoc *et al.* (2019) proposed a community resilience-driven multi-objective MIP model to schedule the restoration process of disrupted components of a system of ICIs with emphasis on social vulnerability of communities. Almoghathawi *et al.* (2019) proposed a multi-objective MIP restoration model for systems of interdependent infrastructure networks. Their goal was to find the minimum-cost restoration strategy of a system of interdependent networks that achieves a certain level of resilience. Ghorbani-Renani *et al.* (2020) proposed a tri-level pre- and post-disruption optimization problem integrating protection, interdiction, and restoration of a system of interdependent networks to improve both vulnerability and recoverability of the system. Garay-Sianca and Pinkley (2021) optimized the restoration of ICIs considering the movement of work crews (machines) through a damaged transportation network being restored by formulating and solving an MIP model.

It is noticeable that the studies on post-disruption restoration and recovery of ICINs are based on deterministic assumptions such as complete information on the restoration

resources and full knowledge of the activities durations (Alkhaleel *et al.*, 2021). However, the restoration of ICINs is complicated by numerous decisions that need to be made in a highly uncertain environment (Fang & Sansavini, 2019). Such uncertainty is linked to several factors including the availability of restoration resources, the time duration for repairing failed components and the accessibility to failed components through the underlying transportation network (Alkhaleel *et al.*, 2021). Moreover, existing optimization approaches do not account for risk measures related to the uncertainty associated with the execution of the optimal plan. Just recently, Alkhaleel *et al.* (2021) explored integrating risk to resilience-based restoration models; this work showed that it is essential to consider risk-averse decision-making, especially in *one-shot* applications such as post-disruption restoration of ICINs. This paper builds upon the previous work by the authors (Alkhaleel *et al.*, 2021); however, here, we extend the previous work to ICINs with an underlying transportation network, explore flexible restoration strategies (i.e., multimode repair and multicrew assignments), and integrate costs of unsatisfied demand (resilience loss equivalent), repair, and flow into the model; with such modifications, we address some of the limitations of the previous work such as: (i) the need to choose between either a risk-neutral approach or a risk-averse one to implement (cannot be combined), (ii) assuming binary functional status of components (either fully functional or disrupted), (iii) preventing concurrent restoration of a single component by multiple crews (a single component can only be restored by one crew), (iv) lack of an economic measure of developed plans (e.g., using only a resilience measure can cause extra hidden cost in the repair process), (v) unavailability of different repair modes for failed components (failed components need to be fully restored).

4.1.4 Overview and research contribution

In this article, we study the interdependent critical infrastructure networks restoration problem (ICINRP), which seeks to minimize the total cost associated with unsatisfied demand (resilience loss), repair tasks, and network flow by improving the restoration strategy of a system of interdependent networks following the occurrence of a disruptive event considering limited time and resources availability. The goal of this paper is to help decision makers plan for ICIs recovery following the occurrence of a disruptive event not only by improving the speed of system recovery, but by also linking risk and its importance level, assessed by the decision maker, to the restoration plan decisions. Accordingly, a two-stage stochastic optimization model using mixed-integer linear programming was proposed to solve the ICINRP under a mean-risk measure. The primary objective of the proposed model is to determine (i) the set of failed components to be restored, (ii) the repair mode for each failed component, (iii) the set of failed components for each crew to restore individually or concurrently, (iv) the baseline restoration sequence across scenarios for each crew in order to minimize the total cost associated with the restoration process (i.e., disruption, repair, and flow costs).

The main contributions of this paper are four-fold. (1) This is the first paper that incorporates a mean-risk approach into ICIs post-disruption restoration models allowing decision makers to choose a risk-averse optimal plan related to a risk importance factor; (2) it explores flexible restoration strategies, and partial functioning and dependencies under uncertainty; (3) it provides an efficient solution approach for solving mean-risk restoration models compared to standard solvers; and (4) the proposed model, solution approach, and

flexible restoration strategies are tested using a realistic case study of a system of ICINs in Shelby County, Tennessee (TN), U.S. under two hypothetical earthquake scenarios.

The remainder of this paper is organized as follows. Section 4.2 presents the background and methodology pertinent to the developed model and summarizes the proposed mathematical formulations. Section 4.3 provides the solution approach used in this paper. Section 4.4 presents a case study on the system of ICINs in Shelby County, TN, U.S. to illustrate the use and advantage of the suggested model. Finally, concluding remarks and future research directions are provided in Section 4.5.

4.2 Methodology and model development

4.2.1 Risk measure

Before introducing the risk measure approach used in developing the mean-risk two-stage stochastic model, we first define the general form of two-stage stochastic models.

Definition 4.1 *Given a probability space denoted by* $(\Omega, \mathcal{F}, \mathcal{P})$, *where* Ω *is the sample space,* $\mathcal{F}$ *is a* σ*-algebra on* Ω *and* $\mathcal{P}$ *is a probability measure on* Ω*; for a finite probability space, where* $\Omega = \{\omega_1, \ldots, \omega_N\}$ *with corresponding probabilities* $\pi_1, \ldots, \pi_N$*, the general form of the two-stage stochastic linear programming problem is defined as (Birge & Louveaux, 2011):*

$$\min_{\boldsymbol{x} \in X} \mathbb{E}(f(\boldsymbol{x}, \omega)) = \min_{\boldsymbol{x} \in X} c^T \boldsymbol{x} + \mathbb{E}(Q(\boldsymbol{x}, \xi(\omega))) \tag{4.1}$$

where $f(\boldsymbol{x}, \omega) = \boldsymbol{c}^T \boldsymbol{x} + Q(\boldsymbol{x}, \xi(\omega))$ *is the cost function of the first-stage problem and:*

$$Q\left(\boldsymbol{x}, \xi^i\right) = \min_{\boldsymbol{y}^i} \left\{ \left(\boldsymbol{q}^i\right)^T \boldsymbol{y}^i : \boldsymbol{L}^i \boldsymbol{x} + \boldsymbol{W}^i \boldsymbol{y}^i = \boldsymbol{h}^i, \boldsymbol{y}^i \geq 0 \right\} \tag{4.2}$$

is the second-stage problem corresponding to the realization of the random data $\xi(\omega)$ *for*

event ω_i, denoted by $\xi^i = \left(\boldsymbol{q}^i, \boldsymbol{L}^i, \boldsymbol{W}^i, \boldsymbol{h}^i\right)$ where $\boldsymbol{x}$ and $\boldsymbol{y}$ are the vectors of first-stage and second-stage decision variables, respectively.

The general two-stage stochastic optimization model is risk-neutral (i.e., there is no accounting for risk in the objective function). The main goal of such models is to show the effect of incorporating uncertainty compared to deterministic ones. However, although solutions to risk-neutral models often perform better than deterministic solutions, both solutions may be subject to poor performance for certain realizations in practice. Such realizations are known as worst-case scenarios in the stochastic optimization literature (Birge & Louveaux, 2011). Given the one-shot nature of CI restoration and its significant socioeconomic impact, it is of interest to consider stochastic models that account for both uncertainty and risk when planning restoration; such models are known as mean-risk models (Noyan, 2012). Mean-risk models are defined as in Definition 4.2:

Definition 4.2 *For a specific risk measure $\rho : \mathcal{Z} \rightarrow \mathbb{R}$, where ρ is a functional and $\mathcal{Z}$ is a linear space of $\mathcal{F}$-measurable functions on the probability space $(\Omega, \mathcal{F}, \mathcal{P})$, a mean-risk function is defined as (Noyan, 2012):*

$$\min_{\boldsymbol{x} \in X} \{\mathbb{E}(f(\boldsymbol{x}, \omega)) + \zeta \rho(f(\boldsymbol{x}, \omega))\} \tag{4.3}$$

where ζ is a non-negative trade-off coefficient representing the exchange rate of mean cost for risk.

The change rate of risk ζ, hereafter referred to as the risk coefficient, is specified by the decision maker according to the assessment of the associated risk. Toward stating a mean-risk restoration optimization model in Section 4.2.2, we now summarize the Conditional Value

at Risk (CVaR) as the risk measure (Krokhmal *et al.*, 2002; Rockafellar & Uryasev, 2000) and recap some results pertinent to the developed optimization model.

Definition 4.3 *Let Z denote a* loss *random variable (the term "loss" is used here to indicate that larger values are undesirable) with cumulative distribution function (CDF) $F(\cdot)$. For a given risk level $\alpha \in (0, 1]$, the Value at Risk (VaR) of Z is defined as:*

$$\mathrm{VaR}_\alpha(Z) = \min\{t | F(t) \geq \alpha\} = \min\{t | P(Z \leq t) \geq \alpha\} \tag{4.4}$$

Thus, for a continuous random variable Z, $\mathrm{VaR}_\alpha[Z]$ is the quantile of Z that exceeds the loss with probability α. The CVaR for Z with risk level $\alpha \in [0, 1]$ is the expected loss given that the loss is at least $\mathrm{VaR}_\alpha(Z)$, i.e.:

$$\mathrm{CVaR}_\alpha(Z) = \mathbb{E}\left(Z | Z \geq \mathrm{VaR}_\alpha(Z)\right) \tag{4.5}$$

It is known that CVaR can also be expressed as the optimal solution to the optimization problem:

$$\mathrm{CVaR}_\alpha[Z] = \min_{\eta \in \mathbb{R}} \left\{ \eta + \frac{1}{1-\alpha} \mathbb{E}\left[(Z - \eta)_+\right] \right\} \tag{4.6}$$

where $(a)_+ := \max(a, 0)$ (Rockafellar & Uryasev, 2000). Combining Equations (4.3) and (4.5), the mean-risk model with a CVaR risk measure can be formulated as:

$$\min_{\boldsymbol{x} \in X} \left\{ \mathbb{E}(f(\boldsymbol{x}, \omega)) + \zeta \, \mathrm{CVaR}_\alpha(f(\boldsymbol{x}, \omega)) \right\} \tag{4.7}$$

Using the result from Equation (4.6), Equation (4.7) can be rewritten as:

$$\min_{\boldsymbol{x} \in X, \eta \in \mathbb{R}} \left\{ \mathbb{E}(f(\boldsymbol{x}, \omega)) + \zeta \left(\eta + \frac{1}{1-\alpha} \mathbb{E}\left[(f(\boldsymbol{x}, \omega)) - \eta)_+\right] \right) \right\} \tag{4.8}$$

4.2.2 Mean-risk two-stage stochastic program formulation

This section formulates a mean-risk two-stage stochastic program for the ICINRP in which the first-stage schedules the restoration of failed components for each network using multiple network-specific repair crews, chooses the repair mode for each failed component (e.g., perfect or imperfect), and determines the fixed restoration cost of failed components; and the second-stage determines the resulting costs associated with unmet demand and flow for networks under a given realization of the random variables (i.e., repair time for each component and travel times between components). Rather than to optimize explicitly over all random variables, it is common to sample scenarios from their joint distribution. Let Ω and Ψ denote the set of scenarios and networks, respectively. For a given scenario $\omega \in \Omega$, let $ttr^{\psi}_{c\omega}$ denote the time to repair component (either node or arc) $c \in C'^{\psi}$. Note that throughout this article we refer to directed (unidirectional) edges as *arcs* and bidirectional ones as *edges*. For travel times, let $tt^{\psi}_{cc'}$ denote the travel time from component $c \in C'^{\psi}$ to component $c' \in C'^{\psi}$ in the same network. It will also be convenient to define $\xi(\omega)$ as a vector specifying the realized values of all random variables in scenario ω.

An equivalent optimization problem to the mean-risk problem in Equation (4.8) can be proposed for a finite probability space $\Omega = \{\omega_1, \ldots, \omega_N\}$ with corresponding probabilities $\pi_1, \ldots, \pi_N$ as shown in Remark 4.1:

Remark 4.1 *For a finite probability space* $\Omega = \{\omega_1, \ldots, \omega_N\}$ *with* $|\Omega| = N$ *and corresponding probabilities* $\pi_1, \ldots, \pi_N$*, an equivalent formulation of the mean-risk problem*

in Equation (4.8)*:*

$$\min_{\boldsymbol{x}\in X,\eta\in\mathbb{R}} \left\{ \mathbb{E}(f(\boldsymbol{x},\omega)) + \zeta \left(\eta + \frac{1}{1-\alpha}\mathbb{E}\left[(f(\boldsymbol{x},\omega)) - \eta)_+\right] \right) \right\}$$

is the following optimization problem:

$$\min_{\boldsymbol{x}\in X,\boldsymbol{y},\eta\in\mathbb{R}} \quad (1+\zeta)\boldsymbol{c}^T\boldsymbol{x} + \sum_{\omega=1}^{|\Omega|} \pi_\omega \left(\boldsymbol{q}_\omega\right)^T \boldsymbol{y}_\omega + \zeta \left(\eta + \frac{1}{1-\alpha} \sum_{\omega=1}^{|\Omega|} \pi_\omega v_\omega \right) \tag{4.9}$$

s.t.

$$\boldsymbol{W}_\omega \boldsymbol{y}_\omega = \boldsymbol{h}_\omega - \boldsymbol{L}_\omega \boldsymbol{x}, \quad \omega = 1, \ldots, |\Omega|, \tag{4.10}$$

$$\boldsymbol{x} \in X, \tag{4.11}$$

$$\boldsymbol{y}_\omega \geq 0, \quad \omega = 1, \ldots, |\Omega| \tag{4.12}$$

$$v_\omega \geq \left(\boldsymbol{q}_\omega\right)^T \boldsymbol{y}_\omega - \eta, \quad \omega = 1, \ldots, |\Omega| \tag{4.13}$$

$$\eta \in \mathbb{R}, v_\omega \geq 0, \quad \omega = 1, \ldots, |\Omega| \tag{4.14}$$

The proof of Remark 4.1 can be found in Noyan (2012). This result will be used to formulate the ICINs mean-risk two-stage stochastic programming problem following the notation.

Assumptions

There are several assumptions and considerations for the proposed mean-risk optimization model to solve the ICINRP:

- Each supply node, demand node, and arc in each infrastructure network has a known supply capacity, demand, and flow capacity, respectively.
- Each disrupted component in each infrastructure network can be restored under

different possible repair modes (e.g., perfect and imperfect), where each repair mode is related proportionally to the restored capacity of the failed component and the restoration time.

- Imperfect node repair proportionally adjusts a restored node's ability to generate supply or consume demand but assumes nodes are uncapacitated for incoming and outgoing flow (transshipment nodes are only restored in perfect repair mode).

- Each disrupted component in each network can be restored with a different restoration time under each scenario.

- The flow costs through each arc, unmet demand costs, and restoration costs for disrupted components in each infrastructure network are known and fixed.

- The number of available network-specific work crews for each infrastructure network is known.

Notation

A summary of notation follows. In addition to the notation already defined, the summary defines (i) first-stage binary variables $x^{\psi}_{cc'k}$ and o^{ψ}_{cy} in order to encode a restoration plan and choose repair modes for different components (i.e., some disrupted critical components need to be fully repaired to restore the performance of the system while only imperfect repair is needed for other components), (ii) second-stage binary variables $\kappa^{\psi}_{cky\omega}(t)$ and $s^{\psi}_{c\omega}(t)$ in order to resolve the status of each disrupted component and each crew restoration rate for each time period and realized scenario, (iii) second-stage continuous

variables $p^{\psi}_{ck y\omega}$ and $\iota^{\psi}_{ck y\omega}(t)$ to mange the assigned restoration task proportion of each component to crews and check the completion of these tasks under each realized scenario, and (iv) flow variables $f^{\psi}_{ij\omega}(t)$ in order to facilitate determining the maximum weighted flow for each time period and realized scenario. The feasible region of the optimization problem is denoted by X, and the set of decision variables is represented as $\{x, o, f, u, s, \kappa, st, p, \iota, \eta, v\}$.

Parameters & Sets

Ψ	Set of infrastructure networks
Υ	Set of interdependent nodes i and i' between networks ψ and ψ' $(\psi \neq \psi')$ where node $i \in V^{\psi}$ requires node $i' \in V^{\psi'}$ to be operational $((i,\psi) \neq (i',\psi'))$
$G^{\psi}(V^{\psi}, A^{\psi})$	Directed graph consisting of nodes V^{ψ} and arcs A^{ψ} for each network $\psi \in \Psi$
$\{V^{\psi}_{+}, V^{\psi}_{*}, V^{\psi}_{-}\}$	Set of {supply, transshipment, demand} nodes for each network $\psi \in \Psi$
T	The number of time periods in restoration planning
A'^{ψ}	Set of failed arcs before restoration $(A'^{\psi} \subset A^{\psi})$ for each network $\psi \in \Psi$
V'^{ψ}	Set of failed nodes before restoration $(V'^{\psi} \subset V^{\psi})$ for each network $\psi \in \Psi$
C^{ψ}	Set of all components $(C^{\psi} = A^{\psi} \cup V^{\psi})$ in network $\psi \in \Psi$
C'^{ψ}	Set of all failed components $(C'^{\psi} = A'^{\psi} \cup V'^{\psi})$ in network $\psi \in \Psi$
K^{ψ}	Set of repair crews for each network $\psi \in \Psi$
Y^{ψ}	Set of repair modes for each network $\psi \in \Psi$

$P_{+}^{i\psi}$	Supply of node $i \in V_{+}^{\psi}$ per time period for each network $\psi \in \Psi$
$P_{-}^{i\psi}$	Demand of node $i \in V_{-}^{\psi}$ per time period for each network $\psi \in \Psi$
P_{ij}^{ψ}	Flow capacity of arc $(i,j) \in A^{\psi}$ per time period for each network $\psi \in \Psi$
χ_{y}^{ψ}	Capacity proportion associated with each repair mode $y \in Y^{\psi}$
$tt_{cc'\omega}^{\psi}$	Travel time between component $c \in C'^{\psi}$ and $c' \in C'^{\psi}$ for each network ψ in scenario ω
$ttr_{c\omega}^{\psi}$	Time to repair component $c \in C'^{\psi}$ for each network ψ under each scenario ω
c_{r}^{ψ}	Fixed restoration cost for component $c \in C'^{\psi}$ for each network ψ
c_{d}^{ψ}	Penalty cost of unmet demand in node $j \in V_{-}^{\psi}$ for each network ψ
c_{f}^{ψ}	Unitary flow cost through arc $(i,j) \in A^{\psi}$ for each network ψ
ζ	Risk coefficient value representing the risk weighted importance chosen by the modeler
α	Risk level chosen by the modeler

Decision Variables

$f_{ij\omega}^{\psi}(t)$	Flow on arc $(i,j) \in A^{\psi}$ in time $t \in \{1 \dots T\}$ for each scenario ω for each network ψ
$f_{j\omega}^{\psi}(t)$	Total flow reaching demand node $j \in V_{-}^{\psi}$ in time $t \in \{1 \dots T\}$ for each scenario ω

$u^{\psi}_{i\omega}(t)$	Amount of unmet demand at node $i \in V^{\psi}_{-}$ in time $t \in \{1 \dots T\}$ for each scenario ω
o^{ψ}_{cy}	Binary variable indicating whether ($o^{\psi}_{cy} = 1$) or not ($o^{\psi}_{cy} = 0$) component $c \in C'^{\psi}$ will be repaired under mode $y \in Y^{\psi}$
$s^{\psi}_{c\omega}(t)$	Binary variable indicating whether ($s^{\psi}_{c\omega} = 1$) or not ($s^{\psi}_{c\omega} = 0$) component $c \in C^{\psi}$ is functioning at time $t \in \{0 \dots T\}$
$st^{\psi}_{ck\omega}$	Time at which crew $k \in K^{\psi}$ begins repairing component $c \in C'^{\psi}$ in scenario ω
$p^{\psi}_{cky\omega}$	Continuous variable $\in [0, 1]$ indicating the proportional repair task for each crew $k \in K^{\psi}$ in restoring component $c \in C'^{\psi}$ under repair mode $y \in Y^{\psi}$; 0 for no contribution and 1 for full restoration by a single crew $k \in K^{\psi}$
$\kappa^{\psi}_{cky\omega}(t)$	Binary variable that equals 1 if component $c \in C'^{\psi}$ is assigned to crew $k \in K^{\psi}$ under repair mode $y \in Y^{\psi}$ and crew $k \in K^{\psi}$ restored the assigned $p^{\psi}_{cky\omega}$ by time $t \in \{0 \dots T\}$; 0 otherwise
$x^{\psi}_{cc'k}$	Binary variable that equals 1 if crew $k \in K^{\psi}$ repairs component $c \in C'^{\psi}$ before component $c' \in C'^{\psi} \setminus \{c\}$
$\iota^{\psi}_{cky\omega}(t)$	Continuous variable $\in [0, 1]$ indicating whether the proportional restoration task assigned to each crew $k \in K^{\psi}$ for component $c \in C'^{\psi}$ under repair mode $y \in Y^{\psi}$ is accomplished by time $t \in \{1 \dots T\}$
η	Auxiliary variable representing the VaR_{α}
υ_{ω}	Continuous variable representing the second-stage costs in scenario ω

The two-stage mean-risk stochastic optimization model for minimizing the expected total cost of the ICINRP follows:

$$\min_{\{x,o,f,u,s,\kappa,st,p,\iota,\eta,v\}\in X}(1+\zeta)\Bigg(\sum_{\psi\in\Psi}\sum_{y\in Y^{\psi}} c_r^{\psi} o_{cy}^{\psi}\chi_y^{\psi}\Bigg) + \sum_{\omega=1}^{|\Omega|}\pi_\omega \sum_{\psi\in\Psi}\sum_{t\in\{1..T\}}\Bigg(\sum_{ij\in A^{\psi}} c_f^{\psi} f_{ij\omega}^{\psi}(t) + \sum_{j\in V_-^{\psi}} c_d^{\psi} u_{j\omega}^{\psi}(t)\Bigg) + \zeta\Bigg(\eta + \frac{1}{1-\alpha}\sum_{\omega=1}^{|\Omega|}\pi_\omega v_\omega\Bigg) \tag{4.15}$$

s.t.

$$\sum_{ij\in A^{\psi}} f_{ij\omega}^{\psi}(t) - \sum_{ji\in A^{\psi}} f_{ji\omega}^{\psi}(t) \le P_+^{i\psi},\ \forall i\in V_+^{\psi},\ \forall t\in\{1\dots T\},\ \forall\omega\in\Omega,\forall\psi\in\Psi \tag{4.16}$$

$$\sum_{ij\in A^{\psi}} f_{ij\omega}^{\psi}(t) - \sum_{ji\in A^{\psi}} f_{ji\omega}^{\psi}(t) = 0,\ \forall i\in V_*^{\psi},\ \forall t\in\{1\dots T\},\ \forall\omega\in\Omega,\forall\psi\in\Psi \tag{4.17}$$

$$\sum_{ij\in A^{\psi}} f_{ij\omega}^{\psi}(t) - \sum_{ji\in A^{\psi}} f_{ji\omega}^{\psi}(t) - u_{i\omega}^{\psi}(t) = -P_-^{i\psi}\ ,\ \forall i\in V_-^{\psi},\ \forall t\in\{1\dots T\},\ \forall\omega\in\Omega,\forall\psi\in\Psi \tag{4.18}$$

$$0 \le u_{i\omega}^{\psi}(t) \le P_-^{i\psi},\ \forall i\in V_-^{\psi},\ \forall t\in\{1\dots T\},\ \forall\omega\in\Omega,\forall\psi\in\Psi \tag{4.19}$$

$$0 \le f_{ij\omega}^{\psi}(t)\ \le s_{ij\omega}^{\psi}(t)P_{ij}^{\psi},\ \forall ij\in A^{\psi},\ \forall t\in\{1\dots T\},\ \forall\omega\in\Omega,\forall\psi\in\Psi \tag{4.20}$$

$$0 \le f_{ij\omega}^{\psi}(t)\ \le s_{i\omega}^{\psi}(t)P_{ij}^{\psi},\ \forall ij\in A^{\psi},\forall i\in V^{\psi},\forall t\in\{1\dots T\},\forall\omega\in\Omega,\forall\psi\in\Psi \tag{4.21}$$

$$0 \le f_{ij\omega}^{\psi}(t)\ \le s_{j\omega}^{\psi}(t)P_{ij}^{\psi},\ \forall ij\in A^{\psi},\forall j\in V^{\psi},\forall t\in\{1\dots T\},\forall\omega\in\Omega,\forall\psi\in\Psi \tag{4.22}$$

$$0 \le f_{ij\omega}^{\psi}(t) \le \sum_{y\in Y^{\psi}} o_{ijy}^{\psi}\chi_y^{\psi}P_{ij}^{\psi},\ \forall ij\in A'^{\psi},\ \forall t\in\{1\dots T\},\ \forall\omega\in\Omega,\forall\psi\in\Psi \tag{4.23}$$

$$\sum_{ij\in A^{\psi}} f^{\psi}_{ij\omega}(t) - \sum_{ji\in A^{\psi}} f^{\psi}_{ji\omega}(t) \leq \sum_{y\in Y^{\psi}} o^{\psi}_{iy}\chi^{\psi}_{y}P^{i\psi}_{+}, \forall i \in V^{\psi}_{+} \cap V^{'\psi}, \forall t \in \{1\dots T\}, \forall \omega \in \Omega, \forall \psi \in \Psi$$

(4.24)

$$\sum_{ij\in A^{\psi}} f^{\psi}_{ij\omega}(t) - \sum_{ji\in A^{\psi}} f^{\psi}_{ji\omega}(t) \geq -\sum_{y\in Y^{\psi}} o^{\psi}_{iy}\chi^{\psi}_{y}P^{i\psi}_{-}, \forall i \in V^{\psi}_{-} \cap V^{'\psi}, \forall t \in \{1\dots T\}, \forall \omega \in \Omega, \forall \psi \in \Psi$$

(4.25)

$$s^{\psi}_{c\omega}(0) = 0, \forall c \in C^{'\psi},\ \forall \omega \in \Omega, \forall \psi \in \Psi \tag{4.26}$$

$$s^{\psi}_{c\omega}(0) = 1, \forall c \in C^{\psi}\backslash C^{'\psi},\ \forall \omega \in \Omega, \forall \psi \in \Psi \tag{4.27}$$

$$\kappa^{\psi}_{cky\omega}(0) = 0,\ \forall c \in C^{'\psi}, \forall k \in K^{\psi}, \forall y \in Y^{\psi},\ \forall \omega \in \Omega, \forall \psi \in \Psi \tag{4.28}$$

$$\sum_{y\in Y^{\psi}} o^{\psi}_{cy} \leq 1, \forall c \in C^{'\psi}, \forall \psi \in \Psi \tag{4.29}$$

$$o^{\psi}_{cy}t \geq st^{\psi}_{ck\omega} + p^{\psi}_{cky\omega}\chi^{\psi}_{y}ttr^{\psi}_{c\omega} - M(1-\kappa^{\psi}_{cky\omega}(t)), \forall c \in C^{'\psi}, \forall t \in \{1\dots T\}, \forall k \in K^{\psi},$$

$$\forall y \in Y^{\psi}, \forall \psi \in \Psi \tag{4.30}$$

$$\sum_{k\in K^{\psi}} p^{\psi}_{cky\omega} = o^{\psi}_{cy}, \forall c \in C^{'\psi}, \forall y \in Y^{\psi}, \forall \omega \in \Omega, \forall \psi \in \Psi \tag{4.31}$$

$$s^{\psi}_{c\omega}(t)\ \leq s^{\psi}_{c\omega}(t+1)\ ,\ \forall c \in C^{\psi},\ \forall t \in \{0\dots T-1\},\ \forall \omega \in \Omega, \forall \psi \in \Psi \tag{4.32}$$

$$\kappa^{\psi}_{cky\omega}(t)\ \leq \kappa^{\psi}_{cky\omega}(t+1)\ ,\ \forall c \in C^{'\psi}, \forall t \in \{0\dots T-1\}, \forall k \in K^{\psi}, \forall y \in Y^{\psi},\ \forall \omega \in \Omega, \forall \psi \in \Psi$$

(4.33)

$$st^{\psi}_{ck\omega} + \sum_{y\in Y^{\psi}} p^{\psi}_{cky\omega}\chi^{\psi}_{y}ttr^{\psi}_{c\omega} + tt^{\psi}_{cc'\omega} \leq st^{\psi}_{c'k\omega} + Mx^{\psi}_{cc'k},\ \forall c, c'\ \in C^{'\psi}\ :\ c \neq c',$$

$$\forall k \in K^{\psi},\ \forall \omega \in \Omega, \forall \psi \in \Psi \tag{4.34}$$

$$st^{\psi}_{c'k\omega} + \sum_{y\in Y^{\psi}} p^{\psi}_{c'ky\omega}\chi^{\psi}_{y}ttr^{\psi}_{c'\omega} + tt^{\psi}_{c'c\omega} \leq st^{\psi}_{ck\omega} + M(1-x^{\psi}_{cc'k}), \forall c, c'\ \in C^{'\psi}\ :\ c \neq c',$$

$$\forall k \in K^{\psi}, \forall \omega \in \Omega, \forall \psi \in \Psi \tag{4.35}$$

$$st^{\psi}_{ck\omega} \geq (1 - \sum_{y \in Y^{\psi}} o^{\psi}_{cy})T, \forall c \in C'^{\psi}, \forall k \in K^{\psi}, \forall \omega \in \Omega, \forall \psi \in \Psi \tag{4.36}$$

$$s^{\psi}_{c\omega}(t) \leq \sum_{k \in K^{\psi}} \sum_{y \in Y^{\psi}} \iota^{\psi}_{cky\omega}(t), \forall c \in C'^{\psi}, \ \forall t \in \{1 \dots T\}, \ \forall \omega \in \Omega, \forall \psi \in \Psi \tag{4.37}$$

$$\iota^{\psi}_{cky\omega}(t) \leq \kappa^{\psi}_{cky\omega}(t), \forall c \in C'^{\psi}, \forall t \in \{1 \dots T\}, \forall k \in K^{\psi}, \forall y \in Y^{\psi}, \forall \omega \in \Omega, \forall \psi \in \Psi \tag{4.38}$$

$$\iota^{\psi}_{cky\omega}(t) \leq p^{\psi}_{cky\omega}, \forall c \in C'^{\psi}, \forall t \in \{1 \dots T\}, \forall k \in K^{\psi}, \forall y \in Y^{\psi}, \forall \omega \in \Omega, \forall \psi \in \Psi \tag{4.39}$$

$$\iota^{\psi}_{cky\omega}(t) \geq p^{\psi}_{cky\omega} - (1 - \kappa^{\psi}_{cky\omega}(t)), \forall c \in C'^{\psi}, \forall t \in \{1 \dots T\}, \forall k \in K^{\psi}, \forall y \in Y^{\psi}, \forall \omega \in \Omega, \forall \psi \in \Psi \tag{4.40}$$

$$s^{\psi}_{i\omega}(t) - s^{\psi'}_{i'\omega}(t) \leq 0 \ , \forall (i, i') \in \Upsilon \colon (i, \psi) \neq (i', \psi'), \forall t \in \{1 \dots T\} \tag{4.41}$$

$$\sum_{ij \in A^{\psi}} f^{\psi}_{ij\omega}(t) - \sum_{ji \in A^{\psi}} f^{\psi}_{ji\omega}(t) \leq \sum_{y \in Y^{\psi}} o^{\psi}_{i'y} \chi^{\psi}_{y} P^{i\psi}_{+}, \forall (i, i') \in \Upsilon \colon (i, \psi) \neq (i', \psi'), i \in V^{\psi}_{+},$$

$$\forall t \in \{1 \dots T\}, \forall \omega \in \Omega, \forall \psi \in \Psi \tag{4.42}$$

$$\sum_{ij \in A^{\psi}} f^{\psi}_{ij\omega}(t) - \sum_{ji \in A^{\psi}} f^{\psi}_{ji\omega}(t) \geq - \sum_{y \in Y^{\psi}} o^{\psi}_{i'y} \chi^{\psi}_{y} P^{i\psi}_{-}, \forall (i, i') \in \Upsilon \colon (i, \psi) \neq (i', \psi'), \forall i \in V^{\psi}_{-},$$

$$\forall t \in \{1 \dots T\}, \forall \omega \in \Omega, \forall \psi \in \Psi \tag{4.43}$$

$$v_{\omega} \geq \sum_{\psi \in \Psi} \sum_{t \in \{1 \dots T\}} \left(\sum_{ij \in A^{\psi}} c^{\psi}_{f} f^{\psi}_{ij\omega}(t) + \sum_{j \in V^{\psi}_{-}} c^{\psi}_{d} u^{\psi}_{j\omega}(t) \right) - \eta \tag{4.44}$$

$$x^{\psi}_{cc'k} \in \{0, 1\}, \ \forall c \in C'^{\psi}, \forall c' \in C'^{\psi} \setminus \{c\}, \ \forall k \in K^{\psi}, \forall \psi \in \Psi \tag{4.45}$$

$$o^{\psi}_{cy} \in \{0, 1\}, \forall c \in C'^{\psi}, \forall y \in Y^{\psi}, \forall \psi \in \Psi \tag{4.46}$$

$$\kappa^{\psi}_{cky\omega}(t) \in \{0, 1\}, \forall c \in C'^{\psi}, \ \forall t \in \{0 \dots T\}, \forall k \in K^{\psi}, \forall y \in Y^{\psi}, \forall \omega \in \Omega, \forall \psi \in \Psi \tag{4.47}$$

$$s^{\psi}_{c\omega}(t) \in \{0, 1\}, \forall c \in C^{\psi}, \ \forall t \in \{1 \dots T\}, \forall \omega \in \Omega, \forall \psi \in \Psi \tag{4.48}$$

$$p^{\psi}_{cky\omega} \in [0, 1], \forall c \in C'^{\psi}, \forall k \in K^{\psi}, \forall y \in Y^{\psi}, \forall \omega \in \Omega, \forall \psi \in \Psi \tag{4.49}$$

$$\iota^{\psi}_{cky\omega}(t) \in [0, 1], \forall c \in C'^{\psi}, \ \forall t \in \{1 \dots T\}, \forall k \in K^{\psi}, \forall y \in Y^{\psi}, \forall \omega \in \Omega, \forall \psi \in \Psi \tag{4.50}$$

$$\eta \in \mathbb{R} \tag{4.51}$$

$$v_\omega \geq 0, \forall \omega \in \Omega \tag{4.52}$$

The goal of model (4.15)–(4.52) is to determine (i) the set of failed components to be restored, (ii) the repair mode for each failed component, (iii) the set of failed components for each crew to restore individually or concurrently, and (iv) the baseline restoration sequence across scenarios for each crew in order to minimize the total cost associated with unsatisfied demand (loss of resilience): $\sum_{j \in V_-^\psi} c_d^\psi u_{j\omega}^\psi(t)$, restoration: $\sum_{y \in Y^\psi} c_r^\psi o_{cy}^\psi \chi_y^\psi$, and flow: $\sum_{ij \in A^\psi} c_f^\psi f_{ij\omega}^\psi(t)$ for each network $\psi \in \Psi$. Constraints (4.16)–(4.18) are flow balance constraints for each network ψ. Constraint (4.19) ensures that the unsatisfied demand $u_{i\omega}^\psi(t)$ for each demand node $j \in V_-^\psi$ does not exceed demand $P_-^{i\psi}$ in every time period. Constraints (4.20)–(4.22) ensure that the flow on each arc $(i,j) \in A^\psi$ in each time period does not exceed its capacity if the arc and both of its end nodes i, j are functioning (flow is 0 if the arc or one of its nodes is failed). Constraint (4.23) ensures that the flow on each arc $(i,j) \in A'^\psi$ in each time period does not exceed its capacity associated with the chosen repair mode $\chi_y^\psi P_{ij}^\psi$, where χ_y^ψ is the percentage of capacity restored for each component under repair mode $y \in Y^\psi$. Similarly, Constraints (4.24)–(4.25) limit the outgoing flow from each failed supply node $i \in V_+^\psi \cap V'^\psi$ and the incoming flow to each failed demand node $i \in V_-^\psi \cap V'^\psi$ to the capacities of the nodes associated with the chosen repair modes. Constraints (4.26) and (4.27) set the initial state of components to be 0 for failed components and 1 for other components. Similarly, Constraint (4.28) prevents the completion of failed components restoration by time 0. Constraint (4.29) prevents assigning more than one

repair mode for each failed component. Constraint (4.30) ensures that crew $k \in K^{\psi}$ has completed its task of restoring failed component $c \in C'^{\psi}$ under repair mode $y \in Y^{\psi}$ the assigned proportion $p^{\psi}_{cky\omega}$ by time $t \in \{1 \dots T\}$ if and only if the restoration start time added to the task repair time is no more than t. Note that the restoration time of a component as well as its restored capacity depends on the repair mode $y \in Y^{\psi}$; that is, for a repair mode $y \in Y^{\psi}$ with percentage $\chi^{\psi}_{y} = \%q$, both capacity and repair time are reduced by $\%(1-q)$. Constraint (4.31) ensures that restoration assignments for each failed component $c \in C'^{\psi}$ to all crews do not exceed the restoration task for that component under repair mode $y \in Y^{\psi}$. Constraint (4.32) ensures that components for each network ψ in C'^{ψ} remain functioning after being restored, and components in $C^{\psi} \backslash C'^{\psi}$ are functioning for the entire restoration period. Constraint (4.33) imposes a similar restriction on the $\kappa^{\psi}_{cky\omega}(t)$-variables; that is, if crew $k \in K^{\psi}$ completed the task of repairing component $c \in C'^{\psi}$ by time period $t \in \{1 \dots T-1\}$, where $\kappa^{\psi}_{cky\omega}(0) = s^{\psi}_{c\omega}(0)$ at $t = 0$ by Constraint (4.28), then this task remains completed by time period $t+1$. Constraints (4.34)–(4.35) manage the restoration scheduling process by ensuring that each crew $k \in K^{\psi}$ can work on repairing at most one component at a time, according to the schedule specified by the $x^{\psi}_{cc'k}$-variables. Relative to Constraints (4.34)–(4.35), Constraint (4.36) prevents scheduling non-selected failed components for repair throughout the restoration total time T. Defining $ttr^{\psi\max}_{ij\omega}$ and $tt^{\psi\max}_{iji'j'\omega}$ as the maximum repair time parameter of any failed component in each network under all scenarios and the maximum travel time parameter between any two failed components in each network under all scenarios, $M = |A'^{\psi}|(ttr^{\psi\max}_{ij\omega} + tt^{\psi\max}_{iji'j'\omega})$ is sufficiently large in Constraint (4.30) and Constraints (4.34)–(4.35). Constraints (4.37)–(4.40) ensure the completion of the restoration process for each selected component $c \in C'^{\psi}$ under repair mode

$y \in Y^{\psi}$ by checking the functional status of each failed component at time $t \in \{1 \dots T\}$ in Constraint (4.37) based on the completion of each crew $k \in K^{\psi}$ its assigned task in restoring the failed component in Constraints (4.38)–(4.40). Specifically, Constraints (4.38)–(4.40) impose that $\iota^{\psi}_{cky\omega}(t) = p^{\psi}_{cky\omega}\kappa^{\psi}_{cky\omega}(t)$ and Constraint (4.37) imposes that component $c \in C'^{\psi}$ is only functioning at time $t \in \{1 \dots T\}$ if the cumulative restoration proportion (across all crews) under the selected repair mode $y \in Y^{\psi}$ is 1. Note how Constraint (4.37) represents the sum of the products of $p^{\psi}_{cky\omega}$ and $\kappa^{\psi}_{cky\omega}(t)$ decision variables via $\iota^{\psi}_{cky\omega}(t)$, and that Constraints (4.38)–(4.40) are introduced to linearize the bilinear terms of the sum. Constraints (4.41)–(4.43) are the interdependence constraints across networks Υ; such constraints ensure that interdependencies between networks given by a set of interdependent nodes across networks Υ are respected. In particular, Constraint (4.41) ensures that a node i in network ψ that is dependent on node i' in network ψ', where $\psi \neq \psi'$, cannot function before the functioning of node i'. Similarly, Constraints (4.42)–(4.43) restrict the capacity of node i in network ψ that depends on failed node i' in network ψ', where $\psi \neq \psi'$, which is restored under repair mode $y \in Y^{\psi}$ to the proportional capacity χ^{ψ}_{y} associated with the chosen repair mode of node i'. Constraint (4.44) sets $\eta = \text{VaR}_{\alpha}$ based on the second-stage costs associated with unmet demand and flow costs. Constraints (4.45)–(4.48) require the $x^{\psi}_{cc'k}$-, o^{ψ}_{cy}-, $\kappa^{\psi}_{cky\omega}(t)$-, and $s^{\psi}_{c\omega}(t)$ variables to be binary. Constraints (4.49)–(4.47) require the $p^{\psi}_{cky\omega}$- and $\iota^{\psi}_{cky\omega}(t)$ variables to be bounded between 0 and 1. Finally, Constraints (4.51)–(4.52) require η to be a real number and v_{ω} variables to be positive real numbers.

Model Variants

I *Flexible restoration strategies*

Compared to a previous work (Alkhaleel *et al.*, 2021), the proposed optimization model (4.15)–(4.52), referred to as the *standard model* hereafter, addresses some limitations (i.e., restricting the restoration of each component to a single crew and allowing only a single maximal repair mode) by considering different flexible recovery strategies including multicrew (MC) and multimode (MM) restoration options. In the former, multiple work crews are allowed to restore a single component of the network $\psi \in \Psi$ in time $t \in \{1 \dots T\}$. Compared to a single crew (SC) setting where only one crew is allowed to work on a single component (i.e., each component is restored by at most one crew), it is expected that the MC approach would improve the resilience of the system via minimizing the unsatisfied demand cost, especially when critical components are disrupted. Indeed, changing between an MC setting and an SC setting in the standard model is fairly an easy task. We only need to change the nature of the $p^{\psi}_{cky\omega}$ decision variables from a continuous space $\in [0, 1]$ for the MC setting to a binary space $\in \{0, 1\}$ for the SC setting. In the latter strategy, each failed component is restored to a certain level of capacity associated with a repair mode (i.e., for a repair mode with percentage $\%q$, both capacity and repair time are reduced by $\%(1 - q)$). Compared to a single mode (SM) repair setting, this strategy can help reduce the repair time of components, especially the ones which do not operate at full capacity before disruption. In Section 4.4, we compare these restoration strategies and show the added benefit of incorporating such flexible strategies in restoration planning of ICINs under uncertainty.

II *Partial functioning and interdependency*

In addition to the flexible restoration strategies adapted in the standard model, partial

functioning and interdependency (PFI) can be implemented by changing the nature of the $s^{\psi}_{c\omega}(t)$ decision variables from binary to continuous variables bounded between 0 and 1. When partial functioning is implemented, components can operate at any capacity in time $t \in \{1 \dots T\}$ below either the full capacity (for a perfect repair mode) or the proportional capacity (for an imperfect repair mode). That is, the binary status assumption of components of the interdependent networks (i.e., either fully functional or failed) is relaxed. Similarly, partial dependence between nodes allows a dependent node to be partially functioning if the node or nodes it depends on are partially functioning as well. However, if the operational nature of the component prevents it from being functional at any partial capacity but instead at only a few possible steps (e.g., a power supply station has four generators and can only function partially depending on the number of working generators at 25%, 50%, 75%, and 10%0), then the model can accommodate this change by slight modifications. First, define m^{ψ}_{c} and $m'^{\psi}_{c\omega}(t)$ as an integer parameter representing the number of units per component and an integer decision variable representing the number of operational units per component at time $t \in \{1 \dots T\}$ under scenario $\omega \in \Omega$, respectively. Then, by adding a set of constraints of the form:

$$m^{\psi}_{c} s^{\psi}_{c\omega}(t) \geq m'^{\psi}_{c\omega}(t) \tag{4.53}$$

for each component composed of several units and replacing associated $s^{\psi}_{c\omega}(t)$ decision variables in Constraints (4.20)–(4.22) with $\frac{m'^{\psi}_{c\omega}(t)}{m^{\psi}_{c}}$, we allow stepwise partial functioning linked to the number of operational units. For a system of ICINs that features PFI, it is expected for the system to be more resilient than a counterpart the does not feature PFI due to the reduction in time between the failed state and the first time the disrupted component

starts functioning. We compare the PFI setting against the binary status of components in Section 4.4 to show how PFI affects restoration planning of ICINs under uncertainty.

4.2.3 ICIs resilience metric

The resilience of a single CI is commonly characterized with respect to a measure of performance (e.g., flow, connectivity, amount of demand satisfied) $\varphi(t)$ that evolves over time (Henry & Ramirez-Marquez, 2012; Hosseini *et al.*, 2016). In this study, the focus is on the recovery period after disruption, for which a model that optimizes a restoration plan over a finite planning horizon is proposed. Here, we consider the resilience metric proposed by Fang *et al.* (2016) as the resilience measure of the restoration plans resulting from the standard model. Fang *et al.* (2016) defines system performance as the maximum amount of weighted flow consumed by the demand nodes. Let weights $w_j^\psi \in \mathbb{Z}^+$ be assigned to each demand node $j \in V_-^\psi$ for network $\psi \in \Psi$. These weights are incorporated to enable prioritizing certain types of demand nodes (e.g., it is more important to deliver power to a hospital than to a residential household). Formally, the performance for network $\psi \in \Psi$ is defined as:

$$\varphi^\psi(t) = \sum_{j \in V_-^\psi} w_j^\psi f_j^\psi(t) \tag{4.54}$$

where $f_j^\psi(t)$ is the total flow reaching demand node j in time period $t \in \{1 \dots T\}$.

Based on that, the resilience $R^\psi(T)$ for network $\psi \in \Psi$ is defined as the cumulative performance restored during the restoration horizon normalized by dividing by the cumulative performance that would be restored over the same horizon if the system could be restored to pre-disruption performance instantaneously. That is, network resilience

is given by (Fang *et al.*, 2016):

$$R^{\psi}(T) = \frac{\sum_{t=1}^{t=T}[\sum_{j\in V_{-}^{\psi}} w_j f_j^{\psi}(t) - \varphi^{\psi}(0)]}{T(\sum_{j\in V_{-}^{\psi}} w_j P_{-}^{j\psi} - \varphi^{\psi}(0))}, \quad T \geq 1 \tag{4.55}$$

where $\sum_{j\in V_{-}^{\psi}} w_j P_{-}^{j\psi} = \varphi^{\psi}(t_0)$ denotes the network performance if not affected by the disruption. For one realization $\omega \in \Omega$, $f_{j\omega}^{\psi}$ denotes the flow into demand node $j \in V_{-}^{\psi}$ in network ψ under scenario $\omega \in \Omega$; hence, we can define the resilience $R^{\psi}(T, \xi(\omega))$ of network ψ under scenario $\omega \in \Omega$ as:

$$R^{\psi}(T, \xi(\omega)) = \frac{\sum_{t=1}^{t=T}[\sum_{j\in V_{-}^{\psi}} w_j^{\psi} f_{j\omega}^{\psi}(t) - \varphi^{\psi}(0)]}{T(\sum_{j\in V_{-}^{\psi}} w_j^{\psi} P_{-}^{j\psi} - \varphi^{\psi}(0))}, \quad T \geq 1 \tag{4.56}$$

Hence, ICIs system resilience is defined by combining each network resilience in a total resilience term $R(T, \xi(\omega))$ as follows:

$$R(T, \xi(\omega)) = \sum_{\psi\in\Psi} \gamma^{\psi} R^{\psi}(T, \xi(\omega)) \tag{4.57}$$

where γ^{ψ} is the weight of importance for each network ψ such that $\sum_{\psi\in\Psi} \gamma^{\psi} = 1$.

4.3 Solution approach

4.3.1 Scenario generation and reduction

To ensure a representative set of scenarios for the developed optimization model, a maxi-min Latin hypercube sampling (LHS) technique (Wyss & Jorgensen, 1998) is adapted to generate a large set of scenarios Ω. Using LHS ensures a fair amount of coverage of each random variable's range, and it has been shown to be advantageous when incorporated within a sample average approximation approach (Alkhaleel *et al.*, 2021; Chen *et al.*, 2014; Kleywegt *et al.*, 2002). However, stochastic optimization models tend to be intractable when the number of generated scenarios is large (Morales *et al.*, 2009). One method often used to

overcome this obstacle is to reduce the number of scenarios such that the resulting problem's optimal solution remains close to the solution of the original optimization problem (Fang & Sansavini, 2019; Heitsch & Römisch, 2003; Horejšová *et al.*, 2020). To apply a reduction of scenarios, it is common to select scenarios based upon a *probability distance* between the original and reduced set of scenarios (Dupačová *et al.*, 2003). The most common probability distance used in stochastic optimization is the Kantorovich distance, $D_K(\cdot)$, defined between two probability distributions Q and Q' on Ω by the following problem (Dupačová *et al.*, 2003; Rachev, 1991):

$$D_K\left(Q, Q'\right) = \inf_{\theta} \Big\{ \int_{\Omega\times\Omega} c\left(\omega, \omega'\right) \theta\left(d\omega, d\omega'\right) : \int_{\Omega} \theta\left(\cdot, d\omega'\right) = Q \quad \int_{\Omega} \theta(d\omega, \cdot) = Q' \Big\} \tag{4.58}$$

Problem (4.58) is known as the Monge–Kantorovich mass transportation problem (Rachev, 1991), where $c\left(\omega, \omega'\right)$ is a nonnegative, continuous, and symmetric function, often referred to as cost function. The infimum is taken over all joint probability distributions defined on $\Omega\times\Omega$ represented by $\theta\left(\omega, \omega'\right)$ in (4.58). Note that $D_K(\cdot)$ can only be properly called Kantorovich distance if function $c(\cdot)$ is given by a norm. When Q and Q' are finite distributions corresponding to the initial set of scenarios Ω and the reduced set of scenarios $\Omega_s \subseteq \Omega$, the Kantorovich distance can be determined (see Dupačová *et al.* (2003) for details) by:

$$D_K\left(Q, Q'\right) = \sum_{\omega\in\Omega\setminus\Omega_s} \pi_\omega \min_{\omega'\in\Omega_s} c\left(\omega, \omega'\right) \tag{4.59}$$

where π_ω represents the probability of scenario ω in Ω (Dupačová *et al.*, 2003). Expression (4.59) can be used to derive several heuristics for generating reduced scenario sets that are close to an original set (Dupačová *et al.*, 2003; Morales *et al.*, 2009). One well-known algorithm is the fast forward selection algorithm (Heitsch & Römisch, 2003). This

algorithm is an iterative greedy process that starts with an empty set; and in each step of the algorithm, a scenario that minimizes the Kantorovich distance between the reduced and original sets is selected from the set of non-selected scenarios ($\Omega \backslash \Omega_s$), where Ω_s represents the set of selected scenarios. Then, this scenario is included in the reduced set Ω_s. The algorithm terminates either when a pre-specified number of scenarios is found or by reaching a pre-defined Kantorovich distance threshold (Morales *et al.*, 2009).

In the fast forward selection algorithm, as described by Heitsch and Römisch (2003), the distance between two scenarios ω and ω' is expressed by the function $c(\omega, \omega')$ representing the difference between pairs of random vectors. The function $c(\omega, \omega')$ can be defined based upon probability metrics (Dupačová *et al.*, 2003), optimal objective function values where first-stage decision variables are fixed (Morales *et al.*, 2009), or the wait-and-see objective value for each scenario, which has been shown to practically outperform the other two methods in restoration modeling (Alkhaleel *et al.*, 2021) and other applications (Bruninx, 2014). Here, we use the objective function value z_ω^{WS} of the *wait-and-see solution* (WS) for each scenario $\omega \in \Omega$ (i.e., the objective function resulting from solving model (4.15)–(4.52) when it is populated with ω as its only scenario) to define $c(\cdot, \cdot)$ as follows:

$$c(\omega, \omega') = \left| z_\omega^{WS} - z_{\omega'}^{WS} \right| \tag{4.60}$$

The resulting fast forward selection algorithm can be found in Alkhaleel *et al.* (2021).

4.3.2 Decomposition algorithm

Decomposition algorithms are often used for solving continuous and mixed-integer large-scale two-stage and multi-stage optimization problems (Escudero *et al.*, 2017;

Rahmaniani *et al.*, 2017). One of those types of algorithms is the well-known Benders decomposition (Benders, 1962), which is commonly used in the stochastic optimization literature to solve the scenario-based resulting mixed-integer linear programs (MILPs). Benders decomposition is a variable partitioning technique in which a restricted master problem is solved considering only the complicating variables of the problem. Such variables are temporarily fixed, and the resulting individual or multiple subproblems are solved to identify cuts to be added to the restricted master problem. In this context, the mean-risk model separates into one linear program per scenario ω—forming the subproblem (SP)—in the reduced scenario set Ω_s after fixing the binary o^{ψ}_{cy}- and $s^{\psi}_{c\omega}(t)$-variables.

Formally, for each scenario $\omega \in \Omega_s$, let $\overline{\boldsymbol{z}}_\omega$ denote a fixed assignment of values to all o- and s-variables corresponding to the index ω. The resulting SP for scenario $\omega \in \Omega_s$ is the linear program:

$$\text{SP}(\overline{\boldsymbol{z}}_\omega): \quad \min \sum_{\psi \in \Psi} \sum_{t \in \{1 \dots T\}} \left(\sum_{ij \in A^{\psi}} c^{\psi}_{f} f^{\psi}_{ij\omega}(t) + \sum_{j \in V^{\psi}_{-}} c^{\psi}_{d} u^{\psi}_{j\omega}(t) \right) \tag{4.61}$$

$$\text{s.t. (4.16)–(4.25) and (4.42)–(4.43) for scenario } \omega \tag{4.62}$$

Because $\text{SP}(\overline{\boldsymbol{z}}_\omega)$ is a linear program in which $\overline{\boldsymbol{z}}_\omega$ appears only in the constraints, the dual of $\text{SP}(\overline{\boldsymbol{z}}_\omega)$ can be formulated as a linear program of the form:

$$\text{DSP}(\overline{\boldsymbol{z}}_\omega): \quad \max \quad (\boldsymbol{b}_\omega - \boldsymbol{B}_\omega \overline{\boldsymbol{z}}_\omega)\, \boldsymbol{d}_\omega \tag{4.63}$$

$$\text{s.t. } \boldsymbol{d}_\omega \in \mathcal{D} \tag{4.64}$$

where $\boldsymbol{b}_\omega$ is the right-hand side vector of (4.62), $\boldsymbol{B}_\omega$ is the left-hand side coefficient matrix of (4.62), $\boldsymbol{d}_\omega$ is the dual variable vector corresponding to constraint (4.62), and $\mathcal{D}$ represents the dual feasible region. Let $\mathcal{D}_p$ and $\mathcal{D}_r$ respectively denote the extreme points and extreme

rays of $\mathcal{D}$, and let $\mathcal{D}_p^{\omega n} \subseteq \mathcal{D}_p$ and $\mathcal{D}_r^{\omega n} \subseteq \mathcal{D}_r$ respectively denote a subset of the extreme points and extreme rays produced prior to iteration n of Benders decomposition. Using the optimal solutions of DSP($\bar{\boldsymbol{z}}_\omega^n$) from previous iterations $\{0 \dots n-1\}$, the restricted master problem (RMP) for iteration n can be formulated as:

$$\min\ (1+\zeta)\left(\sum_{\psi\in\Psi}\sum_{y\in Y^\psi} c_r^\psi o_{cy}^\psi \chi_y^\psi\right) + \lambda_1 + \zeta\lambda_2 \tag{4.65}$$

s.t.

$$\lambda_1 \geq \sum_{\omega=1}^{|\Omega_s|} \pi_\omega \left(\boldsymbol{b}_\omega - \boldsymbol{B}_\omega \boldsymbol{z}_\omega\right) \overline{\boldsymbol{d}}_\omega^i,\ i = 0 \dots n-1 \tag{4.66}$$

$$\lambda_2 \geq \eta^i + \frac{1}{1-\alpha}\sum_{\omega=1}^{|\Omega_s|} \pi_\omega v_\omega^i,\ i = 0 \dots n-1 \tag{4.67}$$

$$v_\omega^i \geq \left(\boldsymbol{b}_\omega - \boldsymbol{B}_\omega \boldsymbol{z}_\omega\right) \overline{\boldsymbol{d}}_\omega^i - \eta^i, \forall \omega \in \Omega_s,\ i = 0 \dots n-1 \tag{4.68}$$

$$0 \geq \left(\boldsymbol{b}_\omega - \boldsymbol{B}_\omega \boldsymbol{z}_\omega\right) \overline{\boldsymbol{d}}_\omega^i, \forall \omega \in \Omega_s,\ i = 0 \dots n-1 \tag{4.69}$$

constraints (4.26)–(4.41) and (4.45)–(4.52)

where i denotes the ith iteration cut generated prior to the current iteration related to $\mathcal{D}_p^{\omega n}$ for Constraints (4.66)–(4.67) and $\mathcal{D}_r^{\omega n}$ for Constraint (4.69). Note that Constraint (4.68) is equivalent to Constraint (4.44) in the standard model. Constraints (4.66)–(4.67) and (4.69) are respectively known as *optimality cuts* and *feasibility cuts*.

In the proposed Benders algorithm (Algorithm 1), the first step is to set the upper bound, lower bound, and iteration counter at ∞, 0 and 0, respectively. In iteration n, RMP is solved first to obtain an optimal solution $\bar{\boldsymbol{z}}^n$. Letting $\bar{\boldsymbol{z}}_\omega^n$ denote the partial solution associated with the o- and s-variables corresponding to the index ω, DSP($\bar{\boldsymbol{z}}_\omega^n$) is solved (note that since the linear program in (4.61)–(4.62) and so its dual (4.63)–(4.64) are scenario indexed, they can be solved in parallel providing multicuts), yielding either an extreme point $\overline{\boldsymbol{d}}_\omega \in \mathcal{D}_p$ (if

the model is solved to optimality) or an extreme ray $\overline{\boldsymbol{d}}_\omega \in \mathcal{D}_p$ (if the model is concluded to be unbounded). In the former case, $\overline{\boldsymbol{d}}_\omega$ is added to $\mathcal{D}_p^{\omega n}$ (i.e., $\mathcal{D}_p^{\omega,n+1} \leftarrow \mathcal{D}_p^{\omega n} \cup \{\overline{\boldsymbol{d}}_\omega\}$ and $\mathcal{D}_r^{\omega,n+1} \leftarrow \mathcal{D}_r^{\omega n}$), resulting in a new optimality cut; otherwise, $\overline{\boldsymbol{d}}_\omega$ is added to $\mathcal{D}_r^{\omega n}$ (i.e., $\mathcal{D}_p^{\omega,n+1} \leftarrow \mathcal{D}_p^{\omega n}$ and $\mathcal{D}_r^{\omega,n+1} \leftarrow \mathcal{D}_r^{\omega n} \cup \{\overline{\boldsymbol{d}}_\omega\}$), yielding a new feasibility cut. The RMP objective provides a lower bound to the optimal solution of the original problem (4.15)–(4.52); furthermore, the dual subproblem DSP($\overline{\boldsymbol{z}}_\omega$) always has an optimal solution due to the feasibility and boundedness of the SP($\overline{\boldsymbol{z}}_\omega$), which can be easily proven by showing that the restricting the flow under each scenario to 0 provides a feasible solution and that the flow is bounded by the capacities of the demand nodes (see Alkhaleel *et al.* (2021) for details). This remark shows that feasibility cuts are not needed in the decomposition procedure; therefore, only optimality cuts are generated and added to the RMP in each iteration (as shown in Algorithm 1) and the convergence of the algorithm is accelerated. The optimality gap for this algorithm can be estimated using the upper and lower bounds found at each step. That is, the optimality gap is calculated as $\text{Gap}(\%) = \dfrac{UB - LB}{UB} = \dfrac{\hat{\mu} + \lambda^* - (\hat{\mu} + \overline{\lambda})}{\hat{\mu} + \lambda^*} = \dfrac{\lambda^* - \overline{\lambda}}{\hat{\mu} + \lambda^*}$.

4.4 Case study

In this section, we test the proposed mean-risk optimization model and solution algorithm, and explore the introduced flexible restoration strategies and PFI using a realistic, well-known case in the literature on the system of ICINs in Shelby County, TN, U.S. This county, containing the city of Memphis, is continually under earthquake hazard due to its proximity to the New Madrid Seismic Zone (NMSZ) (Almoghathawi *et al.*, 2021; González *et al.*, 2016). Here, we consider two cases similar to the hypothetical earthquake scenarios

with magnitudes $M_w \in \{6, 7\}$ presented by González *et al.* (2016).

Algorithm 1: Benders decomposition algorithm

Step 0: $UB \leftarrow \infty, LB \leftarrow 0$, iteration counter $n = 0$

Step 1: Solve the RMP (4.65)–(4.69) to obtain its optimal solution $\left(\overline{\boldsymbol{z}}, \overline{\lambda}_1, \overline{\lambda}_2\right)$ and let $\hat{\mu}$ be the optimal first-stage cost and $\overline{\lambda} = \overline{\lambda}_1 + \zeta\overline{\lambda}_2$, $LB \leftarrow \max\{LB, \hat{\mu} + \overline{\lambda}\}$

Step 2: **For** each $\omega \in \Omega_s$:
Solve the DSP($\overline{\boldsymbol{z}}_\omega$) to obtain its optimal solution $\overline{\boldsymbol{d}}_\omega^n$ and objective value $(\boldsymbol{b}_\omega - \boldsymbol{B}_\omega\overline{\boldsymbol{z}}_\omega)\,\overline{\boldsymbol{d}}_\omega^n$
End For

Step 3: Find the α-quantile $\overline{\eta}$ across all DSP($\overline{\boldsymbol{z}}_\omega$) and associated CVaR_α function, denoted as $\hat{\lambda}_2$:
$\hat{\lambda}_2 = \overline{\eta} + \frac{1}{1-\alpha}\left(\sum_{\omega=1}^{|\Omega_s|}\pi_\omega[(\boldsymbol{b}_\omega - \boldsymbol{B}_\omega\overline{\boldsymbol{z}}_\omega)\,\overline{\boldsymbol{d}}_\omega^n - \overline{\eta}]_+\right)$

Step 4: Let $(\eta^n, v_\omega^n) = (\overline{\eta},\, [(\boldsymbol{b}_\omega - \boldsymbol{B}_\omega\overline{\boldsymbol{z}}_\omega)\,\overline{\boldsymbol{d}}_\omega^n - \overline{\eta}]_+)$

Step 5: Find the mean-risk function value, denoted as λ^*, of the current recourse cost solution:
$\lambda^* = \sum_{\omega=1}^{|\Omega_s|}\pi_\omega\,(\boldsymbol{b}_\omega - \boldsymbol{B}_\omega\overline{\boldsymbol{z}}_\omega)\,\overline{\boldsymbol{d}}_\omega^n + \zeta\ \hat{\lambda}_2$
$UB \leftarrow \min\{UB, \hat{\mu} + \lambda^*\}$

Step 6: **If** $UB - LB \leq \epsilon$: ▷ ϵ is a predefined tolerance
Stop and report solution
Else:
(a) Add optimality cuts of the form:
$\lambda_1 \geq \sum_{\omega\in\Omega_s}\pi_\omega\,(\boldsymbol{b}_\omega - \boldsymbol{B}_\omega\boldsymbol{z}_\omega)\,\overline{\boldsymbol{d}}_\omega^n$
$\lambda_2 \geq \eta^n + \frac{1}{1-\alpha}\sum_{\omega=1}^{|\Omega_s|}\pi_\omega v_\omega^n$ to the RMP
(b) Add a total number of $|\Omega_s|$ Benders optimality cuts of the form:
$v_\omega^n \geq (\boldsymbol{b}_\omega - \boldsymbol{B}_\omega\boldsymbol{z}_\omega)\,\overline{\boldsymbol{d}}_\omega^n - \eta^n, \forall\omega \in \Omega_s$ to the RMP
(c) $n \leftarrow n + 1$ and go to Step 1
End If

4.4.1 System description

The system of interdependent networks considered in this study consists of two ICINs located in Shelby County, TN: power and water as depicted in Figure 4.2 (González *et al.*, 2016). The system of networks contains 256 network components divided into 109 nodes and 147 edges. The power network is composed of 60 nodes and 76 edges, and the water

network is composed of 49 nodes and 71 edges. For the water system, storage tanks and large pumps are modeled as generation (supply) nodes and pipe intersections are modeled as water distribution (demand) nodes (Kim *et al.*, 2007). Moreover, gate stations are modeled as power generation (supply) nodes and substations are modeled as power distribution (demand) nodes for the power network. The actual system, managed by the Memphis Light, Gas, and Water (MLGW), is a heterogeneous mix of unidirectional arcs and bidirectional edges (Kim *et al.*, 2007). However, it can be modeled either as a system of directed networks or undirected networks using network flow approaches (Ahuja *et al.*, 1993). In this study, we model the utility networks as directed networks where directed arcs are modeled to send flow in one direction and bidirectional edges are modeled as two directed arcs. Additionally, the functional dependency considered in this study is unidirectional (i.e., only the water network depends on the power network) where each water generation node is dependent on at least one power distribution node. Flow units per hour are in MWh for the power network and million gallons hourly (MGh)$\times 10^2$ or 10kGh for the water network.

4.4.2 Uncertainty representation

The proposed model assumes that the time to repair each component and the travel time between failed components are uncertain, but the remaining parameters are deterministic. The remainder of this section summarizes the assumed probability distributions for the uncertain parameters.

Let $C' \subseteq C$ denote the set of disrupted components, and ttr_c denote the time to repair of component $c \in C'^{\psi}$. We assume ttr_c has a Weibull distribution—commonly used to model activity times (Abdelkader, 2004)—with scale parameter ν_c and shape parameter

β_c. The probability density function of ttr_c is given by:

$$h(t, \beta_c, \nu_c) = \frac{\beta_c}{\nu_c} \left(\frac{t}{\nu_c} \right)^{\beta_c - 1} e^{-\left(\frac{t}{\nu_c}\right)^{\beta_c}}, \; t \geq 0 \tag{4.70}$$

As for travel times, for $c \in C'^{\psi}$ and $c' \in C'^{\psi}$, let $tt^{\psi}_{cc'}$ denote the travel time between components c and c' in network ψ. We derive a deterministic estimate of the travel time from c to c' using a separate transportation network.

In the transportation network, each edge has an associated length and speed limit, and its traversal time d_l is estimated assuming it will always be possible to travel at the speed limit. The deterministic estimate of $tt^{\psi}_{cc'}$, hereafter denoted as $dtt^{\psi}_{cc'}$, is obtained by determining the shortest path length between two nodes in the transportation network, namely those that are the closest to the midpoint of failed arcs and to failed nodes in the utility networks. To represent the uncertainty of $tt^{\psi}_{cc'}$, we populate a distribution for traversal time of edges in the transportation network; given d_l, the random traversal time dr_l is distributed according to the probability mass function:

$$P(dr_l = t) = \begin{cases} 0.3, & t = d_l \\ 0.3, & t = 1.5 \; d_l \\ 0.4, & t = 2 \; d_l \end{cases} \tag{4.71}$$

and each scenario-indexed $tt^{\psi}_{cc'\omega}$ is found by solving the shortest path problem as explained. This approach follows other disaster relief and emergency response studies with the assumption that random traversal times are based on a coefficient multiplication of the transportation network constant traversal times (Alkhaleel *et al.*, 2021; de la Torre *et al.*, 2012; Mete & Zabinsky, 2010).

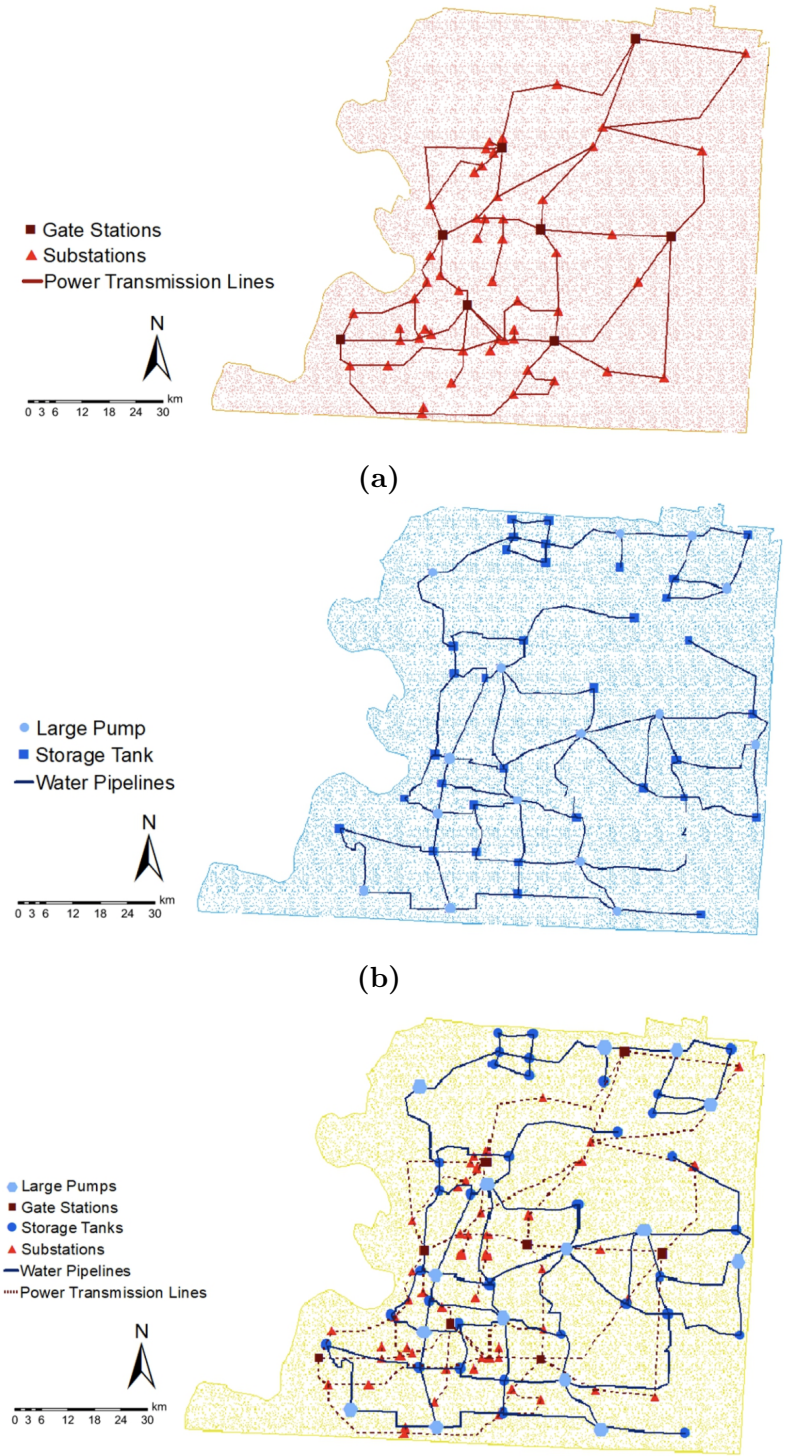

Figure 4.2. Graphical representations of the, (a) power, (b) water, and (c) combined water and power networks in Shelby County, TN (adapted from González *et al.* (2016))

4.4.3 Parameters and computational information

Among the hypothetical earthquake scenarios in Shelby County, TN presented by González *et al.* (2016) with different magnitudes, assuming different failure probabilities of system components with each hypothetical earthquake scenario, we consider two possible scenarios with magnitudes $M_w \in \{6, 7\}$ and a similar number of disrupted components chosen randomly. Additionally, we consider four different risk coefficients (i.e., $\zeta \in \{0, 0.5, 1, 2\}$) associated with each scenario. The number of disrupted components for each network, the percentage of the total number of components for each network, and the associated performance drop for each network in the system under each hypothetical earthquake scenario are summarized in Table 4.1.

Table 4.1. Disruption size and performance drop considering the two magnitudes of hypothetical earthquake scenarios

Case	No. of disrupted components			Disruption percentage			Performance drop		
	Power	Water	System	Power	Water	System	Power	Water	System
Case 1 ($M_w = 6$)	10	6	16	7.35%	5.00%	6.25%	18.64%	20.00%	19.27%
Case 2 ($M_w = 7$)	19	10	29	13.97%	8.33%	11.33%	22.13%	85.64%	50.87%

Regarding the repair parameters, the Weibull distributed repair time shape and scale parameters are assumed to be 2 and 5, respectively, for all components. Such assumptions are made following other studies in the literature in terms of probability distribution chosen and parameters (Fang & Sansavini, 2019). Hence, the mean-time-to-repair (MTTR) used in the deterministic model is about 4.43 hours. In addition, the restoration planning horizon T is chosen as 20 hours, which is sufficient to restore the network performance to its original state under both cases with the chosen number of work crews for each case (total of 4 for case 1 and 5 for case 2 as illustrated in Table 4.3). For possible repair modes for each network, it

is assumed that there are two repair modes for each network ($Y^{\psi} = \{1, 2\}$): (1) perfect repair mode (i.e., the component is restored to its full capacity), and (2) imperfect repair mode (i.e., the component is restored to 50% of its full capacity). Regarding cost parameters, it is assumed that unitary flow cost, unitary unsatisfied demand cost, and fixed repair cost per component are the same for both networks. For unitary flow cost, we use an estimated flow cost of \$30 per flow unit, which is equivalent to the approximate cost of transmission and distribution of 1 MWh of electricity (Fares & King, 2017). For the unsatisfied demand cost, referred to as disruption cost hereafter, the average residential cost of one MWh of electricity in Shelby County, TN is approximately \$97.2; and for the water network, the cost per 10k gallon is about \$30 (MLGW, 2021). However, the economic impact of unsatisfied demand is significantly higher than the cost of services. That is, estimates of service interruption vary significantly with estimated numbers ranging from \$100 up to \$100,000 per demand unit (Wolfram, 2021). Here, it is estimated to be about \$10,000 per demand unit based on the the Interruption Cost Estimate (ICE) tool funded by the Energy Resilience Division of the U.S. Department of Energy's Office of Electricity (OE) for the examined case study area (ICE, 2021). Regarding restoration costs, we assume a fixed repair cost per component. However, repair cost per CI component can vary significantly from thousand dollars to hundreds of million dollars (Assad *et al.*, 2020; HDR, 2012). Nonetheless, a fixed repair cost of \$500,000 per component was estimated to keep both the flow and restoration costs combined lower than the disruption costs to prioritize resilience improvement as the main objective. Table 4.2 summarizes the parameters of cost, risk, and repair for each case.

For the scenario generation process of random variables (i.e., repair and travel times), 1000 scenarios are generated for each case. After that, the scenario reduction algorithm was

Table 4.2. Parameters of cost, risk, and repair for each case of the hypothetical earthquake scenarios

Case	Cost parameters			Risk parameters		Repair parameters	
	Disruption cost (per demand unit)	Repair cost (per component)	Flow cost (per flow unit)	α	ζ	χ_y^ψ	ν_c, β_c
Case 1 ($M_w = 6$) Case 2 ($M_w = 7$)	\$10,000	\$500,000	\$30	0.9 0.8	$0, 0.5, 1, 2$	$\chi_1^\psi = 0.5,\ \chi_2^\psi = 1$	5, 2

used to reduce the number of scenarios into a smaller set. The total number of scenarios is reduced to 10 scenarios. Solutions to the MILPs used in the scenario reduction procedure and the stochastic optimization models were computed using CPLEX 12.10 (CPLEX, 2021) and programmed using Python 3.7 (Python, 2021) on a 3.2 GHz Intel Core i5 iMac machine with 24 GB of RAM.

Regarding solution times and optimality gaps, we would like to emphasize that solving ICIs deterministic restoration problems using commercial MILP solvers such as CPLEX is hard, especially for large problem instances involving travel time and vehicle routing considerations (Garay-Sianca & Pinkley, 2021; Moreno *et al.*, 2019; Morshedlou *et al.*, 2018). In such deterministic problems, optimality gaps can go up to 50% or even higher (Garay-Sianca & Pinkley, 2021; Morshedlou *et al.*, 2018). Hence, the stochastic problem instances considered here for both cases cannot be solved for optimality within a prescribed time limit. However, based on our preliminary analysis, a time limit of 6 hours (21600 seconds) is the approximate time after which the optimality gap tends to level off with the implementation of Benders algorithm to solve all instances. Algorithm 1 was implemented using callbacks with Benders cuts added as lazy constraints. Table 4.3 summarizes the dimensions of problem instances.

Table 4.3. Problem size of different study instances

Instance	No. of continuous variables	No. of binary variables	No. of constraints	No. of Scenarios	No. of work crews (power, water)	Number of repair modes (power, water)	Max computational time (s)
Case 1 ($M_w = 6$)	336,971	359,372	503,670	10	2,2	2,2	21,000
Case 2 ($M_w = 7$)	406,511	428,572	608,850	10	2,3	2,2	21,000
Deterministic (Case 1)	33,696	36,182	51,002	1	2,2	2,2	1,800
Deterministic (Case 2)	40,647	43,686	61,043	1	2,3	2,2	3,600

4.4.4 Results

The first part of this section summarizes the results related to the various features of the developed mean-risk model including a comparison of the proposed solution approach to standard MILP solvers, and the second part shows the added benefit of implementing flexible restoration strategies and PFI in total cost reduction and resilience improvement.

Mean-risk model

The developed ICINRP using a mean-risk measure is solved using Algorithm 1. Table 4.4 compares the proposed Benders decomposition algorithm with CPLEX showing the added value of the proposed solution algorithm. The solutions found by the decomposition algorithm outperformed the ones found by CPLEX in all instances. Additionally, the decomposition algorithm was capable of solving all instances with a maximum optimality gap of about 24%. In contrast, CPLEX was not able to find any feasible solution for one of the instances (i.e., $M_w = 6$ ($\zeta = 0.5$)). The maximum optimality gap of solved instances for CPLEX was approximately 57%. It is worth pointing out that the lower bounds found by CPLEX and the decomposition algorithm for the instances were similar, which are higher (tighter) than the WSs lower bounds by about 10% for all instances. For the first case ($M_w = 6$), the highest optimality gap found using Benders decomposition algorithm was

14.637% compared to more than triple that value at 50%.456 for CPLEX. Furthermore, in the second case ($M_w = 7$), the highest optimality gap found using Benders decomposition algorithm was 23.319% compared to 56.88% for the commercial solver. Using the proposed Benders algorithm, the average optimality gaps for cases 1 and 2 were about 13% and 20%, respectively. In contrast, the average optimality gaps using CPLEX solver for cases 1 and 2 were about 32% and 46%, respectively. These average values are about double the average gaps of the decomposition algorithm. Overall, these findings favor the proposed solution approach and show the added benefit of adapting it over commercial solvers.

Table 4.4. Comparison of Benders decomposition and CPLEX solver solutions for the different instances with 10 reduced scenarios

Case	CPLEX standard solver			Benders decomposition		
	Computational time (s)	Gap(%)	Objective value	Computational time (s)	Gap(%)	Objective value
$\boldsymbol{M_w = 6\ (\zeta = 0)}$	21648.783	17.279	18.142	21617.794	12.849	17.514
$\boldsymbol{M_w = 6\ (\zeta = 0.5)}$	21600.000	-	-	21618.569	14.477	30.599
$\boldsymbol{M_w = 6\ (\zeta = 1)}$	21605.193	50.456	58.771	21616.394	14.637	42.986
$\boldsymbol{M_w = 6\ (\zeta = 2)}$	21609.664	29.233	81.635	21661.764	12.791	66.632
$\boldsymbol{M_w = 7\ (\zeta = 0)}$	21612.699	56.880	90.808	21664.057	23.319	47.302
$\boldsymbol{M_w = 7\ (\zeta = 0.5)}$	21606.937	38.043	96.661	21615.361	21.666	75.205
$\boldsymbol{M_w = 7\ (\zeta = 1)}$	21612.841	41.277	143.474	21614.859	20.328	102.743
$\boldsymbol{M_w = 7\ (\zeta = 2)}$	21607.326	50.304	271.706	21620.736	17.480	154.189

Regarding the mean-risk model, the choice of the risk coefficient ζ in the proposed framework can alter the optimal plan; that is, increasing the value of ζ increases the relative importance of the risk term resulting in more conservative (risk-averse) plans. For instance, the CVaR values for case 1 showed a significant decrease with the increase of the risk coefficient value from 0 to 2 as shown in Figure 4.3. This decrease in CVaR values is associated with a gradual increase in the expected total cost across scenarios for the different risk coefficients as illustrated in Figure 4.3. The same findings are true for case 2 with a

steeper trend in CVaR values as shown in Figure 4.4.

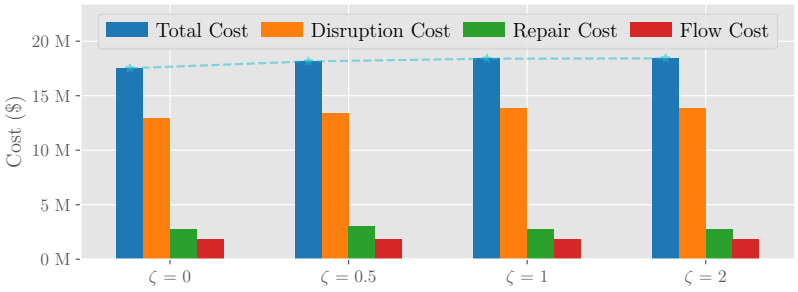

(a) Expected costs as ζ varies in Case 1 ($M_w = 6$)

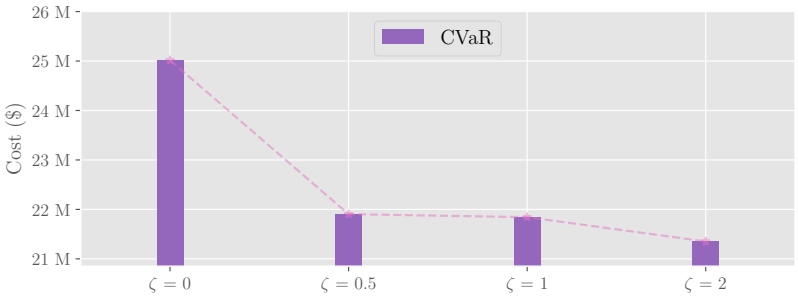

(b) CVaR values as ζ varies in Case 1 ($M_w = 6$)

Figure 4.3. Case 1 ($M_w = 6$): Detailed expected cost values of demand, repair, flow, and the overall expected total cost, as well as the CVaR information for different values of ζ

In ICINs restoration problems, disruption costs are expected to be higher than other costs combined, otherwise optimal solutions can be found by prioritizing a reduction in repair and flow costs over disruption costs (Almoghathawi *et al.*, 2021). Here, the detailed costs are presented for both cases in Figures 4.3 and 4.4 showing that disruption cost constitutes the major portion of the total cost under all risk coefficients. In addition, trends of objective values, total and disruption costs, and CVaR values under both cases across the different risk coefficients are shown in Figures 4.5 and 4.6; this shows that in mean-risk models, the objective value increases linearly with the increase of the risk coefficient. Moreover, both the expected total and disrupted costs exhibit a similar raising trend with the change of the risk coefficient; this similarity can be explained by knowing that the disruption cost represents

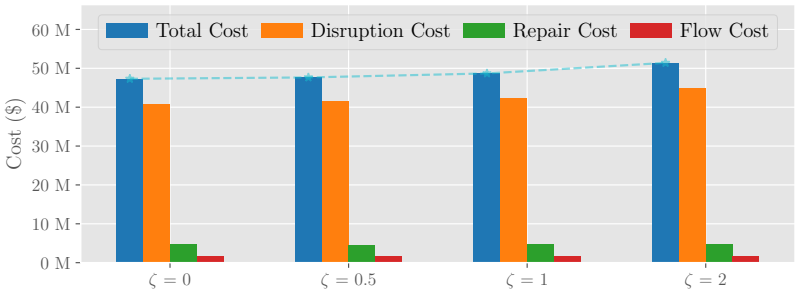

(a) Expected costs as ζ varies in Case 2 ($M_w = 7$)

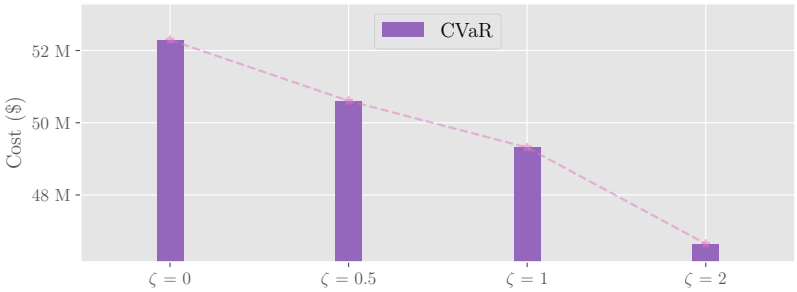

(b) CVaR values as ζ varies in Case 2 ($M_w = 7$)

Figure 4.4. Case 2 ($M_w = 7$): Detailed cost values of demand, repair, flow, and the overall expected total cost, as well as the CVaR information for different values of ζ

the major portion of the total cost as explained earlier.

Tables 4.5 and 4.6 summarize the detailed outputs of the model for both cases—using different choices of the risk coefficient—including cost values, system and individual network resilience values, objective values, and other outputs for both cases. For case 1, the total resilience (or system resilience) and its related total disruption cost both decrease with the risk coefficient increase. The repair cost, however, looks constant across all risk coefficients indicating that the number of chosen disrupted components to be restored and their associated repair modes are almost the same for case 1. For case 2, the repair cost shows a similar behavior across all the values of ζ. Additionally, the flow cost could be described as constant across the values of ζ for both cases. The resilience curves of the power network, water network, and system under the different risk coefficients can be found

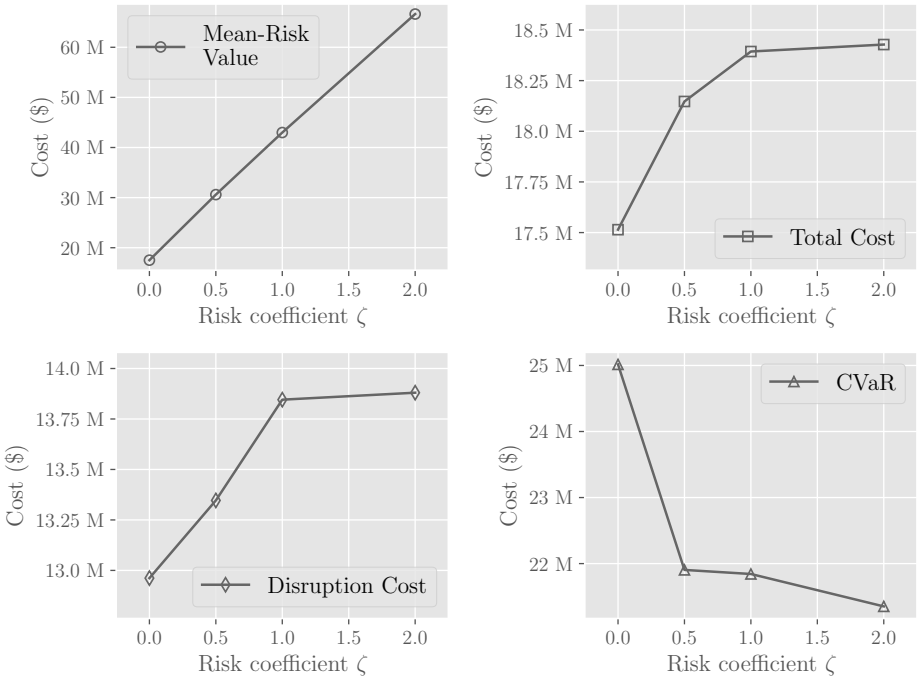

Figure 4.5. Case 1 ($M_w = 6$): Trends of objective value, expected total cost, expected disruption cost, and CVaR with the increase of ζ

in the Appendix.

To assess the added value of stochastic models compared to a deterministic approach, the value of stochastic solution (VSS) is a well-known measure in the literature, which is designed to indicate whether the added benefit of modeling randomness using a risk-neutral stochastic optimization approach (Birge & Louveaux, 2011). However, the VSS cannot be implemented directly on risk-averse problems (Noyan, 2012). Accordingly, we adopt the risk-averse version of the VSS known as the mean-risk value of stochastic solution (MRVSS) (see Noyan (2012) for details), which measures the possible gain from solving stochastic models incorporating a mean-risk function. In particular, this measure represents the difference between the mean-risk expected value (MREV) problem (which results from solving the standard model with fixed first-stage decision variables whose values are obtained

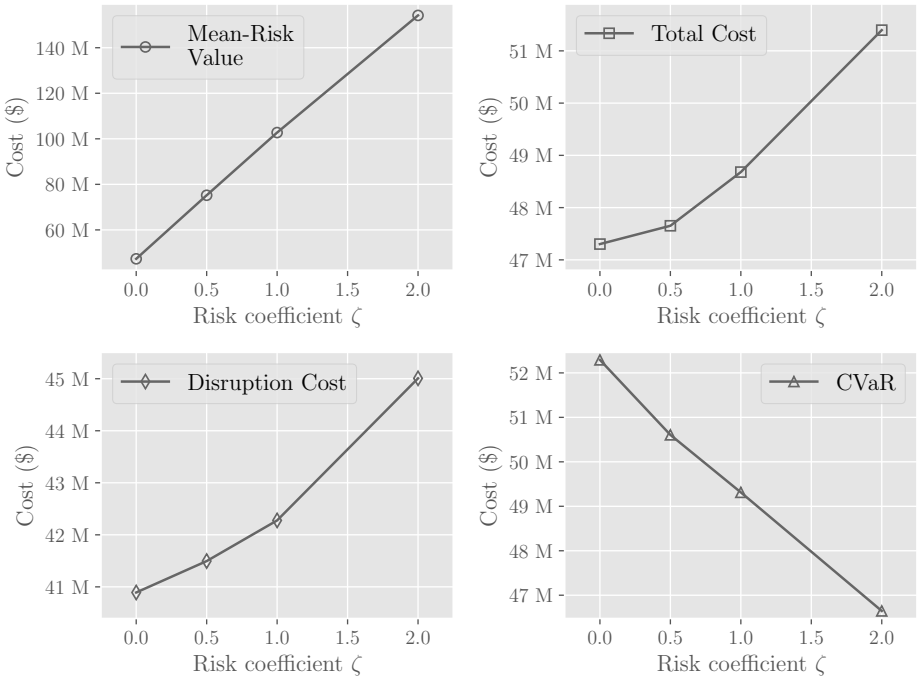

Figure 4.6. Case 2 ($M_w = 7$): Trends of objective value, expected total cost, expected disruption cost, and CVaR with the increase of ζ

by solving a deterministic version of the standard model that replaces all random parameters with their expected values) and the mean-risk standard model solution. Higher values of MRVSS indicate a more added value in adapting a mean-risk approach over an expected value approach. Note that the MRVSS is equivalent to VSS when the risk coefficient $\zeta = 0$.

For case 1 ($M_w = 6$), it can be seen that the MRVSS values are positive numbers ranging between 2.285M and 10.295M and increase with the increase of the risk coefficient ζ; this indicates the significance of solving mean-risk models over the expected value (deterministic) approaches. However, the increase of MRVSS with ζ is not reflected on the ratio between the MRVSS and the associated objective value, which does not show a clear trend with approximate values of 13%, 11%, 12%, and 15% for $\zeta = 0$, 0.5, 1, and 2, respectively. For $\zeta = 0$, the added value of a stochastic solution is \$2.285M (i.e., the

Table 4.5. Case 1 ($M_w = 6$): Detailed expected cost values, MRVSS, expected flow, and expected resilience information under different risk coefficients

	Risk coefficient parameter			
	$\boldsymbol{\zeta = 0}$	$\boldsymbol{\zeta = 0.5}$	$\boldsymbol{\zeta = 1}$	$\boldsymbol{\zeta = 2}$
Objective value (M)	17.514	30.599	42.986	66.632
CVaR ($M)	25.016	21.904	21.843	21.352
MRVSS (M)	2.285	3.417	4.962	10.295
Total disruption cost ($M)	12.962	13.347	13.846	13.880
Total repair cost ($M)	2.750	3.000	2.750	2.750
Total flow cost ($M)	1.803	1.801	1.798	1.798
Total resilience	0.816	0.810	0.805	0.804
Power network disruption cost ($M)	6.707	6.729	7.945	7.879
Power network repair cost ($M)	1.750	2.250	2.000	2.000
Power network flow cost ($M)	0.989	0.989	0.983	0.983
Power network resilience	0.821	0.820	0.788	0.789
Power network aggregated received flow (MWh)	19389.300	19387.118	19265.504	19272.070
Water network disruption cost ($M)	6.255	6.618	5.901	6.001
Water network repair cost ($M)	1.000	0.750	0.750	0.750
Water network flow cost ($M)	0.814	0.812	0.815	0.815
Water network resilience	0.812	0.801	0.822	0.819
Water network aggregated received flow (MG)	159.545	159.182	159.899	159.799

overall cost of the deterministic solution is \$2.285M higher than the stochastic solution). For other values of ζ, the MRVSS varies between a ζ-weighted value of 3M up to 10M. For case 2 ($M_w = 7$), the values of MRVSS are even higher given the larger disruption scenario for this case despite the higher overall optimality gaps in this case compared to case 1. In fact, implementing the deterministic approach for this case can cause a 10-20% increase in the expected economic losses compared to a mean-risk plan with a specific risk level α and risk weighted importance ζ. Hence, this shows that applying deterministic plans for larger disruptions involves high risk and could result in more socioeconomic losses. Overall, these results indicate that it is significant to solve mean-risk models to obtain preferred solutions for a specified set of risk parameters.

Table 4.6. Case 2 ($M_w = 7$): Detailed expected cost values, MRVSS, expected flow, and expected resilience information under different risk coefficients

	Risk coefficient parameter			
	$\zeta = 0$	$\zeta = 0.5$	$\zeta = 1$	$\zeta = 2$
Objective value(M)	47.302	75.205	102.743	154.189
CVaR ($M)	52.293	50.606	49.313	46.646
MRVSS (M)	9.678	10.415	16.287	16.772
Total disruption cost ($M)	40.892	41.495	42.277	45.007
Total repair cost ($M)	4.750	4.500	4.750	4.750
Total flow cost ($M)	1.660	1.657	1.653	1.639
Total resilience	0.757	0.726	0.752	0.725
Power network disruption cost ($M)	16.402	16.474	12.786	14.996
Power network repair cost ($M)	2.500	2.500	2.500	2.500
Power network flow cost ($M)	0.939	0.939	0.958	0.947
Power network resilience	0.686	0.629	0.712	0.662
Power network aggregated received flow (MWh)	18419.820	18412.648	18781.405	18560.355
Water network disruption cost ($M)	24.490	25.022	29.491	30.011
Water network repair cost ($M)	2.250	2.000	2.250	2.250
Water network flow cost ($M)	0.721	0.718	0.695	0.693
Water network resilience	0.828	0.824	0.792	0.789
Water network aggregated received flow (MG)	141.310	140.778	136.309	135.789

Flexible restoration strategies and PFI

As illustrated in Section 4.2, the proposed optimization model for solving the ICINRP considers flexible restoration strategies that are expected to enhance the resulting optimal plans. In addition, the proposed model allows for partial functioning and interdependency, with a slight modification to the standard model formulation, supporting non-binary state ICIs restoration. Here, we compare the applied flexible restoration strategies to restricted ones and study the impact of PFI on restoration plans.

Regarding the restoration strategies, Tables 4.7 and 4.8 summarize the detailed outputs (i.e., cost values, system and individual network resilience values, and CVaR values) of the model with risk coefficient $\zeta = 1$ under flexible (i.e., multicrew and multimode repair settings) and restricted (i.e., single crew and single mode settings) plans for cases 1 and 2, respectively. In Tables 4.7 and 4.8, the first column represents the standard model with

$\zeta = 1$, the second column represents the standard model with $\zeta = 1$ except that each failed component is restored by at most one crew (single crew setting), the third column represents the standard model with $\zeta = 1$ except that each failed component can only be fully restored (single repair mode), and the PFI column represents the standard model with $\zeta = 1$ except that partial functioning and interdependencies are allowed. Overall, both the objective value and CVaR value are lower under flexible restoration strategies for cases 1 and 2. This indicates that flexible restoration planning can significantly reduce the main costs associated with restoration, namely disruption and repair costs, as well as the associated risk measure. Comparing the multicrew setting to the single crew setting, the reduction in the objective value is about 25% and 36% for cases 1 and 2, respectively. For multimode repair vs. single mode repair, the reduction in the objective value is approximately 12% and 20% for cases 1 and 2, respectively. Note that the gain from adapting flexible restoration strategies is more significant for the second case with a higher number of disrupted components. Disruption costs behave similarly to the objective value for both cases and under both restoration strategies (i.e., multicrew and multimode repair). In contrast, repair costs are similar between the multicrew and single crew settings; however, they are higher in the single repair mode setting, significantly higher for case 2, indicating that the imperfect repair mode for multiple components is optimal. Surprisingly, multimode repair did not only reduce the repair costs by %8 and 27% for cases 1 and 2, respectively, but also reduced the disruption costs (improved resilience) for both cases by 10% for case 1 and 20% for case 2.

For a resilience-based benchmarking of the different restoration strategies, a comparison of the resilience of power network, water network, and system under flexible and restricted restoration plans for cases 1 and 2 is shown in Figures 4.7 and 4.8, respectively.

Table 4.7. Case 1 ($M_w = 6$): Detailed cost values, flow, and resilience information under SC, SM, and PFI for $\zeta = 1$

	Standard Model ($\zeta = 1$)	**Single Crew**	**Single Repair Mode**	**PFI**
Objective value (M)	42.986	57.604	48.968	29.463
CVaR ($M)	21.843	29.642	25.773	14.381
Total disruption cost ($M)	13.846	20.699	15.405	7.753
Total repair cost ($M)	2.750	2.750	3.000	2.750
Total flow cost ($M)	1.798	1.763	1.790	1.829
Total resilience	0.805	0.712	0.781	0.893
Power network disruption cost ($M)	7.945	14.127	7.946	5.506
Power network repair cost ($M)	2.000	2.000	2.000	2.250
Power network flow cost ($M)	0.983	0.951	0.983	0.995
Power network resilience	0.788	0.622	0.788	0.853
Power network aggregated received flow (MWh)	19265.504	18647.284	19265.372	19509.405
Water network disruption cost ($M)	5.901	6.571	7.459	2.247
Water network repair cost ($M)	0.750	0.750	1.000	0.500
Water network flow cost ($M)	0.815	0.812	0.808	0.834
Water network resilience	0.822	0.802	0.775	0.932
Water network aggregated received flow (MG)	159.899	159.229	158.341	163.553

From the first glance, one can see that the resilience of both networks and the system is higher with multicrew and multimode restoration strategies. For instance, in case 1, the power network resilience under multicrew setting is significantly higher than under a single crew setting. This indicates the existence of critical components in the power network whose rapid restoration can significantly improve the resilience of the network. In contrast, the effect of multicrew setting on the water network resilience is minor. Conversely, multimode repair improved only the resilience of the water network under the same case. For case 2, with a higher number of disrupted components, the resilience of both power and water networks showed a substantial improvement under multicrew and multimode settings. All these improvements in the resilience of both individual networks are clearly reflected on the system resilience for both case studies and under both flexible restoration strategies.

Regarding PFI, Tables 4.7 and 4.8 summarize the detailed outputs (i.e., cost values, system and individual network resilience values, and CVaR values) of the standard model,

Table 4.8. Case 2 ($M_w = 7$): Detailed cost values, flow, and resilience information under SC, SM, and PFI for $\zeta = 1$

	Standard Model ($\zeta = 1$)	**Single Crew**	**Single Repair Mode**	**PFI**
Objective value (M)	102.743	161.303	128.854	83.569
CVaR ($M)	49.313	83.061	61.543	39.845
Total disruption cost ($M)	42.277	67.719	52.712	32.521
Total repair cost ($M)	4.750	4.500	6.500	4.750
Total flow cost ($M)	1.653	1.523	1.600	1.703
Total resilience	0.752	0.613	0.684	0.788
Power network disruption cost ($M)	12.786	19.160	16.831	12.551
Power network repair cost ($M)	2.500	2.250	3.500	2.500
Power network flow cost ($M)	0.958	0.925	0.937	0.959
Power network resilience	0.712	0.568	0.621	0.717
Power network aggregated received flow (MWh)	18781.405	18144.010	18376.940	18804.894
Water network disruption cost ($M)	29.491	48.559	35.881	19.970
Water network repair cost ($M)	2.250	2.250	3.000	2.250
Water network flow cost ($M)	0.695	0.598	0.663	0.744
Water network resilience	0.792	0.658	0.747	0.859
Water network aggregated received flow (MG)	136.309	117.241	129.919	145.830

under risk coefficient $\zeta = 1$, with and without PFI for both cases. It can be seen that partial functioning and interdependency significantly reduced the disruption costs for both cases. That is, resilience is improved by PFI since allowing a disrupted component to partially function—before full restoration—can help deliver more flow to demand nodes, especially in the first time periods after disruption. This situation is the opposite of a binary status setting of components where disrupted components continue to be disrupted until fully restored. In addition, the reduction in disruption costs decreases the risk gradually compared to a non-PFI setting. The results from applying PFI can link resilience to reliability and maintainability engineering through systems with multiple states or state-dependent systems. It might be of interest to study the relation between resilience, reliability, and maintainability for a network having state-dependent critical components and how a tri-level framework can be developed to improve all three aspects. To sum up, ICINs systems featuring PFI are expected to be more resilient than non-PFI due to the flexibility of their post-disruption

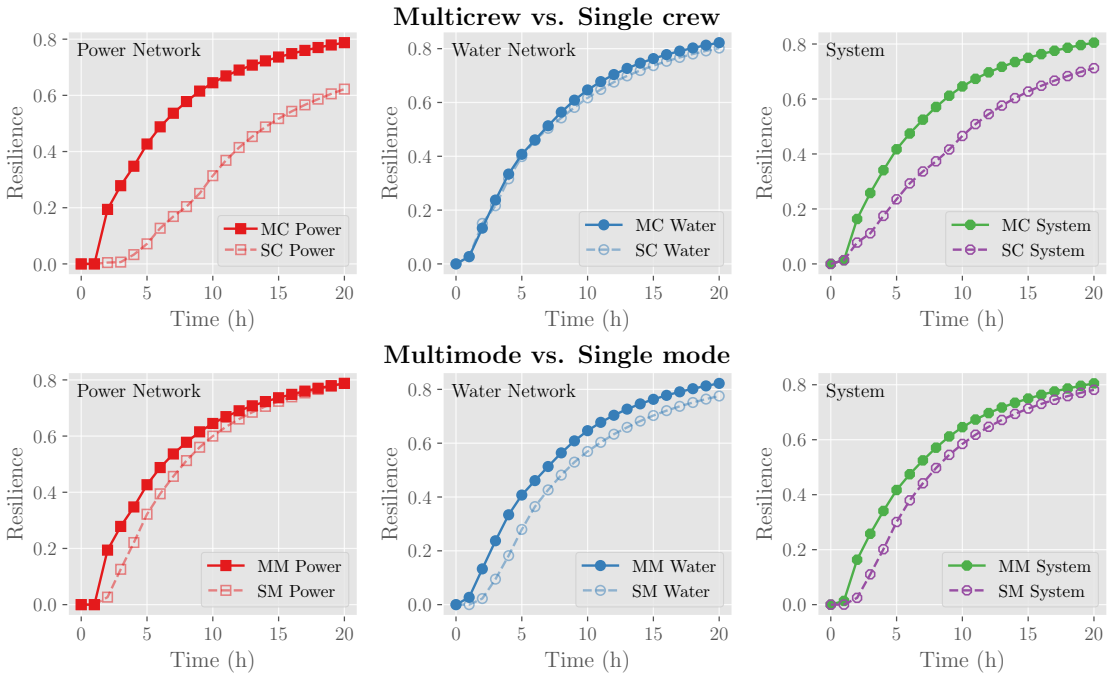

Figure 4.7. Case 1 ($M_w = 6$): Comparison of the resilience of the overall system and individual networks under SC vs. MC, and SM vs. MM settings

restoration plans.

4.5 Conclusion and future work

In this paper, a two-stage stochastic restoration optimization model using mixed-integer linear programming is proposed to solve the ICINRP under a mean-risk cost-based objective function. Moreover, the mean-risk model features flexible restoration planning strategies including multicrew repair of a single component and multimode repair, and also considers partial functioning and interdependencies of components across networks. The proposed model: (i) determines the set of failed components to be restored, (ii) selects the repair mode for each failed component, (iii) assigns each crew the set of failed components to be restored individually or concurrently, (iv) and schedules the baseline restoration sequence across scenarios for each crew such that the associated costs of disruption,

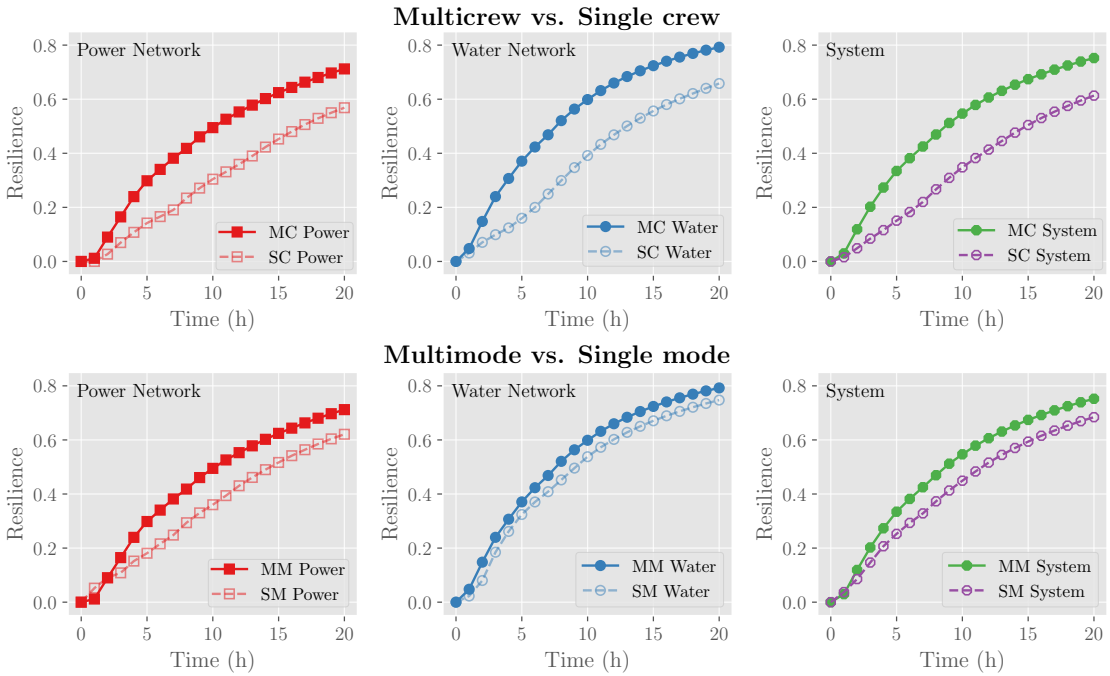

Figure 4.8. Case 2 ($M_w = 7$): Comparison of the resilience of the overall system and individual networks under SC vs. MC, and SM vs. MM settings

repair, and flow of the system of ICIs are minimized. Additionally, as post-disruption restoration tasks occur in a highly dynamic environment, which is subject to a fair amount of uncertainty, the mean-risk model considers two important sources of uncertainty associated with restoration panning: (i) repair task durations, and (ii) travel times of crews between failed components.

The proposed approach was demonstrated using a real-life case study based on the system of power and water networks in Shelby County, TN, U.S. under two hypothetical earthquakes. The mean-risk model was solved using the developed Benders decomposition algorithm, which outperformed the CPLEX standard solver as demonstrated. Our first finding was the significance of adapting mean-risk stochastic models over deterministic counterparts. This was demonstrated through the positive values of MRVSS under all cases. It is also found that the restoration plan can be altered based on the associated risk

weighted importance. In particular, smaller values of the risk weighted importance factor can result in plans with low expected total costs but with high costs under worst-case scenarios. In contrast, higher values of the risk weighted importance factor can result in plans with slightly higher expected total costs but with less costs associated with worst-case scenarios. Regarding the flexible restoration strategies and PFI, both implementations demonstrated the added value in reducing the overall costs and mitigating risks.

As for future work, the proposed model could be extended to consider the transportation network as a direct interdependent network. That is, the current approach assumes that CI networks, other than the underlying transportation network, are the ones being restored. Hence, the problem becomes not only focused on the restoration of CIs, but also on coordinating the process of finding the best routes and schedules for crews to repair damaged components in the transportation network. In addition, it is possible to extend the current model to introduce a facility location problem where work crews are dispatched to disrupted component locations rather than a direct travel between components. In such problems, the goal is to find the optimal location of these facilities from a set of candidate sites considering the fixed cost of establishing such facilities as well as other crew-related variable costs. Moreover, considering economic measures of the resilience of communities interacting with these ICINs, as well as the associated risks can be one of the future directions of this work. This future direction can also be associated with studying other types of interdependencies that affect both CIs and communities such as geographic interdependency to mitigate the related socioeconomic risks.

Appendix A

A.1 Resilience of the system and individual infrastructure networks under different risk coefficient solution plans

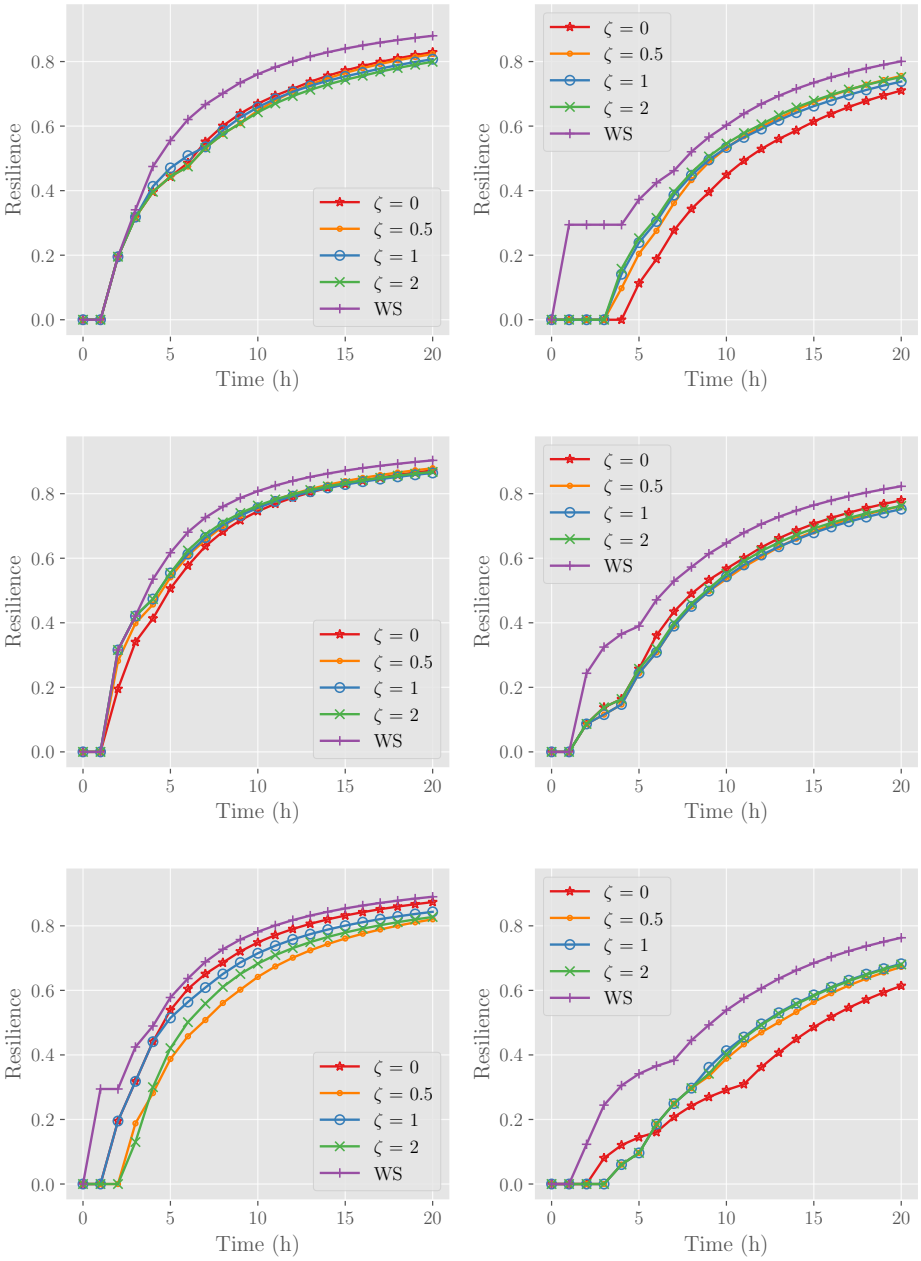

Figure 4.9. Case 1 ($M_w = 6$): Comparison of system resilience curves under different risk coefficient solution plans for a sample of reduced scenarios

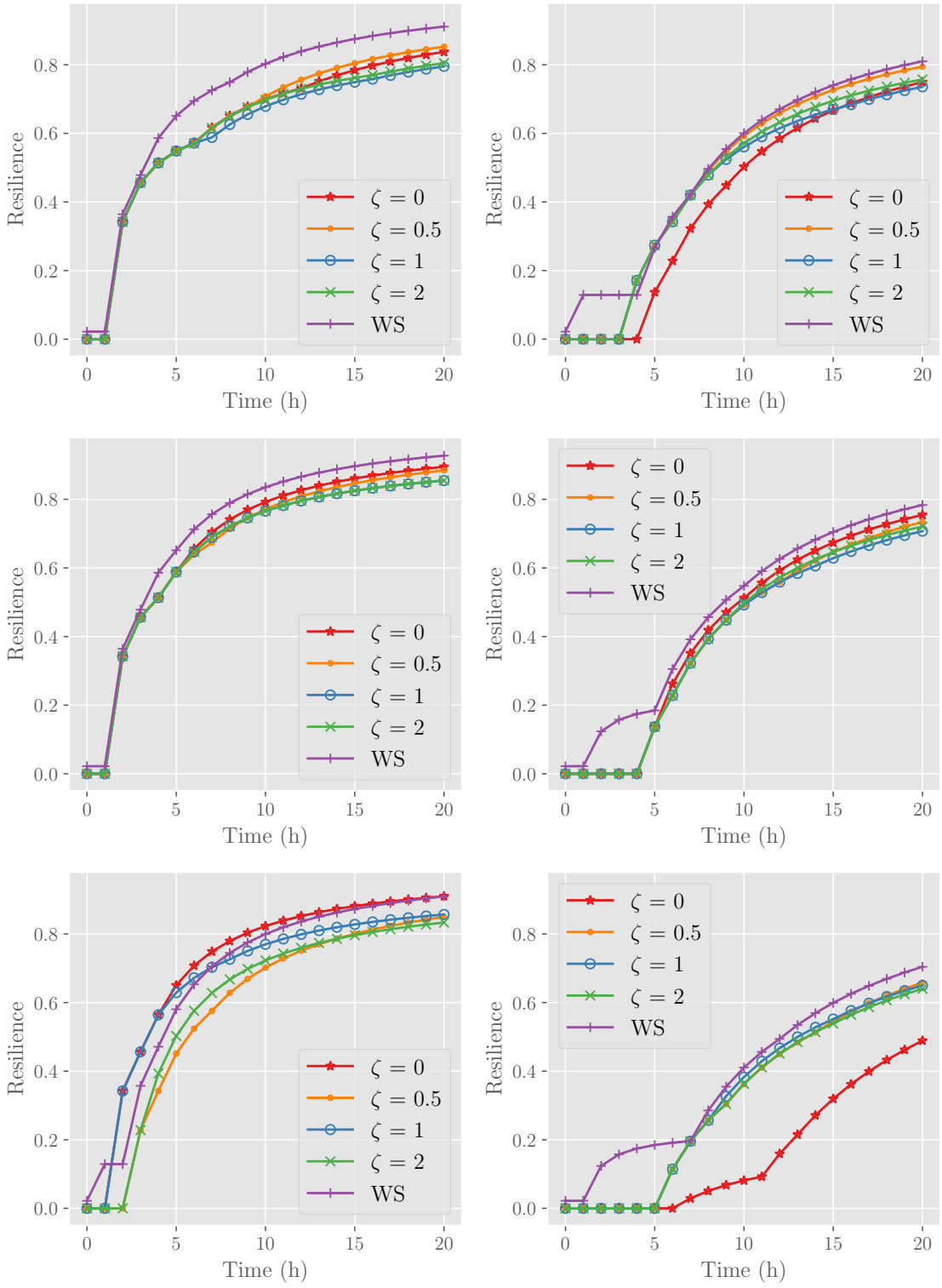

Figure 4.10. Case 1 ($M_w = 6$): Comparison of power network resilience curves under different risk coefficient solution plans for a sample of reduced scenarios

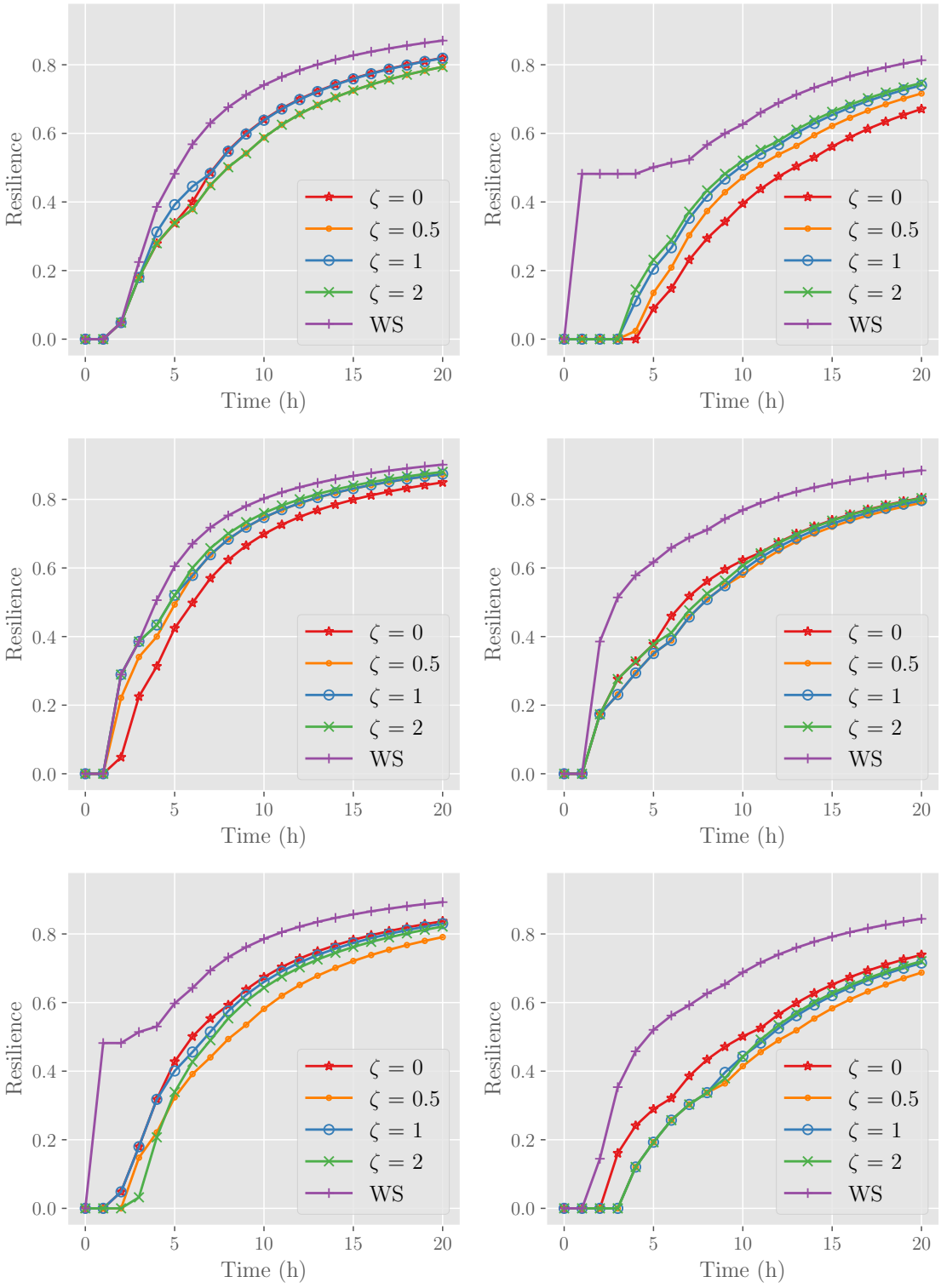

Figure 4.11. Case 1 ($M_w = 6$): Comparison of water network resilience curves under different risk coefficient solution plans for a sample of reduced scenarios

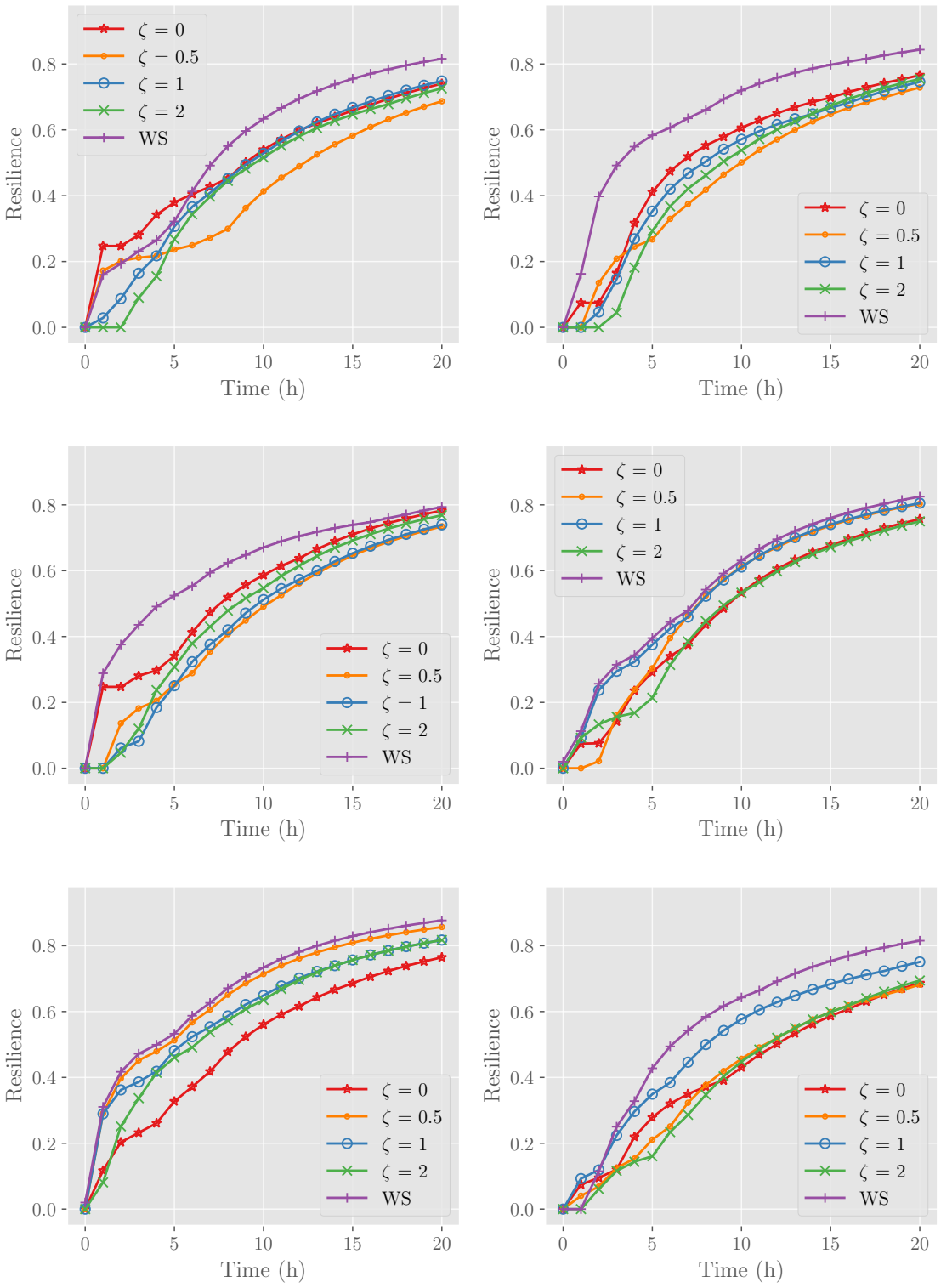

Figure 4.12. Case 2 ($M_w = 7$): Comparison of system resilience curves under different risk coefficient solution plans for a sample of reduced scenarios

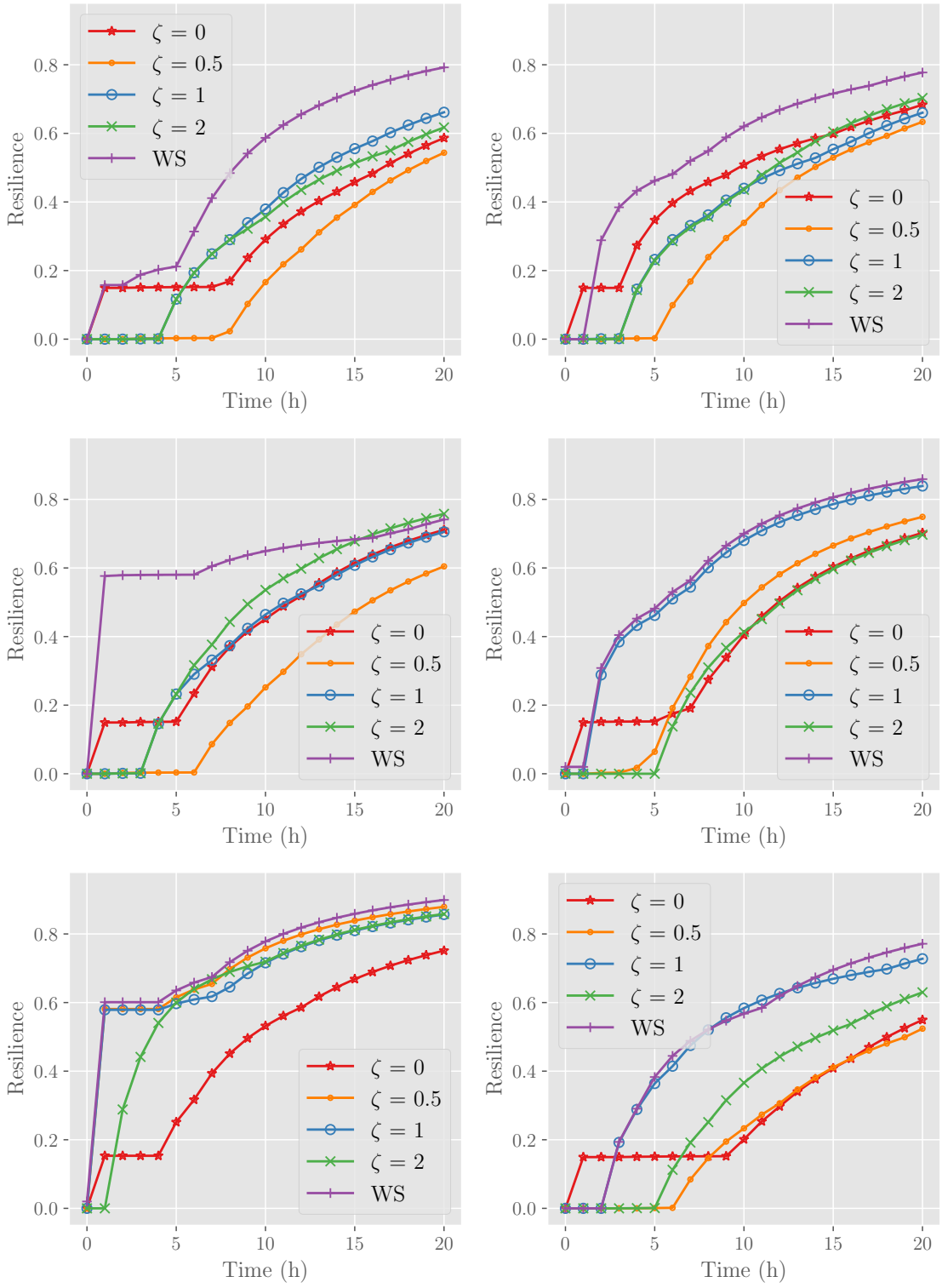

Figure 4.13. Case 2 ($M_w = 7$): Comparison of power network resilience curves under different risk coefficient solution plans for a sample of reduced scenarios

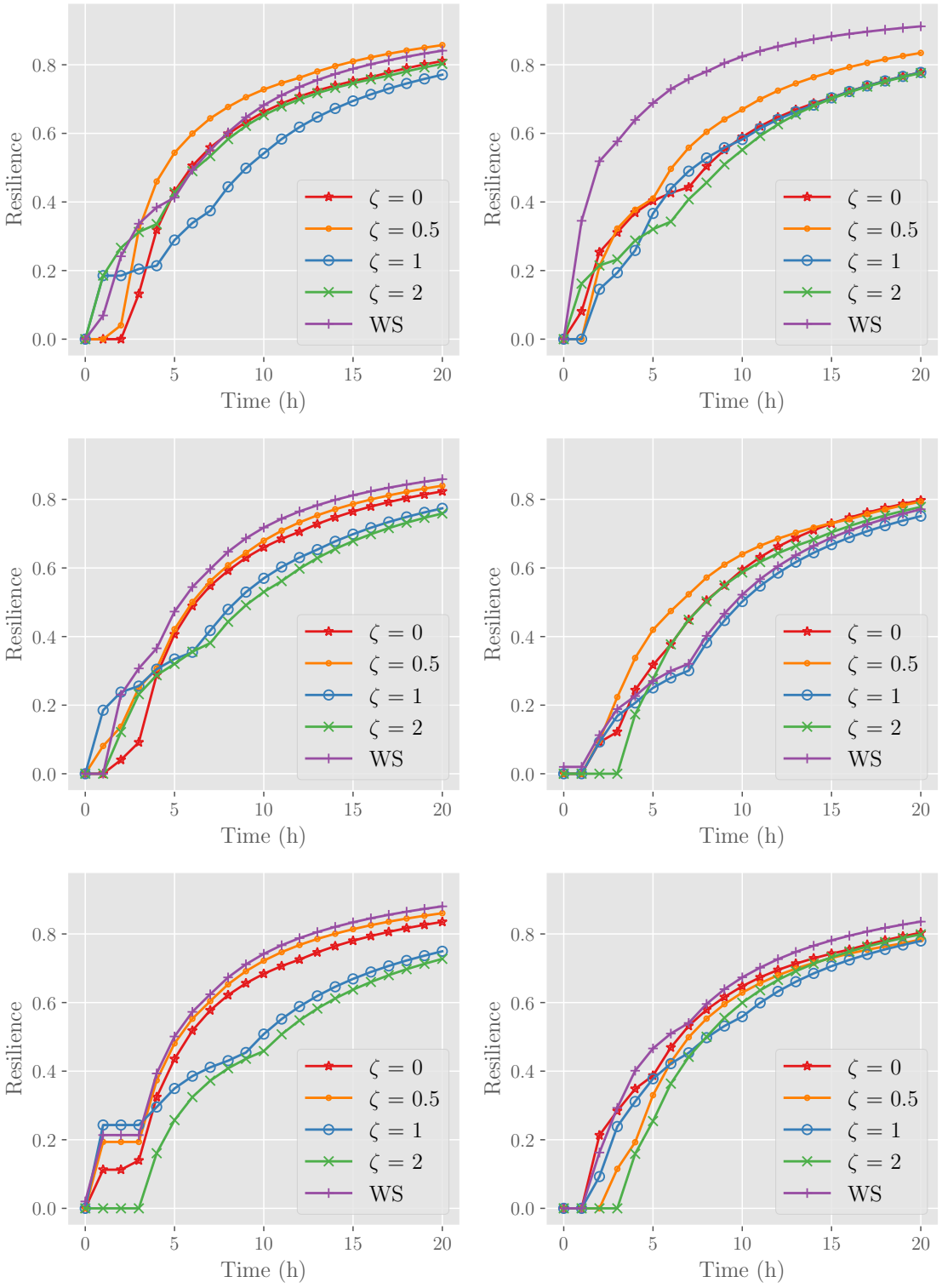

Figure 4.14. Case 2 ($M_w = 7$): Comparison of water network resilience curves under different risk coefficient solution plans for a sample of reduced scenarios

References

Abdelkader, Y. H. (2004). Evaluating project completion times when activity times are Weibull distributed. *European Journal of Operational Research*, *157*(3), 704–715. doi: 10.1016/S0377-2217(03)00269-8

Ahuja, R. K., Magnanti, T. L., & Orlin, J. B. (1993). *Network flows: theory, algorithms, and applications*. Upper Saddle River, NJ, USA: Prentice-Hall, Inc.

Alkhaleel, B. A., Liao, H., & Sullivan, K. M. (2021). Risk and resilience-based optimal post-disruption restoration for critical infrastructures under uncertainty. *European Journal of Operational Research*. doi: 10.1016/j.ejor.2021.04.025

Almoghathawi, Y., Barker, K., & Albert, L. A. (2019). Resilience-driven restoration model for interdependent infrastructure networks. *Reliability Engineering and System Safety*, *185*, 12–23. doi: 10.1016/j.ress.2018.12.006

Almoghathawi, Y., González, A. D., & Barker, K. (2021). Exploring recovery strategies for optimal interdependent infrastructure network resilience. *Networks and Spatial Economics*, *21*(1), 229–260. doi: 10.1007/s11067-020-09515-4

Amin, M. (2002). Toward secure and resilient interdependent infrastructures. *Journal of Infrastructure Systems*, *8*(3), 67–75. doi: 10.1061/(ASCE)1076-0342(2002)8:3(67)

Assad, A., Moselhi, O., & Zayed, T. (2020). Resilience-driven multiobjective restoration planning for water distribution networks. *Journal of Performance of Constructed Facilities*, *34*(4), 04020072. doi: 10.1061/(asce)cf.1943-5509.0001478

Azucena, J., Alkhaleel, B., Liao, H., & Nachtmann, H. (2021). Hybrid simulation to support interdependence modeling of a multimodal transportation network. *Simulation Modelling Practice and Theory*, *107*, 102237. doi: 10.1016/j.simpat.2020.102237

Baidya, P. M., & Sun, W. (2017). Effective restoration strategies of interdependent power system and communication network. *The Journal of Engineering*, *2017*(13), 1760–1764. doi: 10.1049/joe.2017.0634

Barker, K., Lambert, J. H., Zobel, C. W., Tapia, A. H., Ramirez-Marquez, J. E., Albert, L., ... Caragea, C. (2017). Defining resilience analytics for interdependent cyber-physical-social networks. *Sustainable and Resilient Infrastructure*, *2*(2), 59–67. doi: 10.1080/23789689.2017.1294859

Benders, J. F. (1962). Partitioning procedures for solving mixed-variables programming problems. *Numerische Mathematik*, *4*, 238–252.

Birge, J. R., & Louveaux, F. (2011). *Introduction to stochastic programming*. New York,

NY: Springer. doi: 10.1007/978-1-4614-0237-4

Bruneau, M., Chang, S. E., Eguchi, R. T., Lee, G. C., O'Rourke, T. D., Reinhorn, A. M., ... von Winterfeldt, D. (2003). A framework to quantitatively assess and enhance the seismic resilience of communities. *Earthquake Spectra*, *19*, 733–752. doi: 10.1193/1.1623497

Bruninx, K. (2014). A practical approach on scenario generation and & reduction algorithms for wind power forecast error scenarios..

Buldyrev, S. V., Parshani, R., Paul, G., Stanley, H. E., & Havlin, S. (2010). Catastrophic cascade of failures in interdependent networks. *Nature*, *464*(7291), 1025–1028. doi: 10.1038/nature08932

Buldyrev, S. V., Shere, N. W., & Cwilich, G. A. (2011). Interdependent networks with identical degrees of mutually dependent nodes. *Physical Review E*, *83*(1), 016112. doi: 10.1103/physreve.83.016112

Campbell, R. J., & Lowry, S. (2012). Weather-related power outages and electric system resiliency. Washington, DC: Library of Congress.

Casalicchio, E., Galli, E., & Ottaviani, V. (2009). MobileOnRealEnvironment-GIS: A federated mobile network simulator of mobile nodes on real geographic data. In *2009 13th IEEE/ACM international symposium on distributed simulation and real time applications.* IEEE. doi: 10.1109/ds-rt.2009.25

Cavdaroglu, B., Hammel, E., Mitchell, J. E., Sharkey, T. C., & Wallace, W. A. (2011). Integrating restoration and scheduling decisions for disrupted interdependent infrastructure systems. *Annals of Operations Research*, *203*(1), 279–294. doi: 10.1007/s10479-011-0959-3

Çelik, M. (2016). Network restoration and recovery in humanitarian operations: Framework, literature review, and research directions. *Surveys in Operations Research and Management Science*, *21*(2), 47–61. doi: 10.1016/j.sorms.2016.12.001

Center for Research on the Epidemiology of Disasters (CRED). (2021). *EM-DAT: The emergency events database. number of natural disaster.* (Available at: https://public .emdat.be/)

Chen, J., Lim, C. H., Qian, P. Z., Linderoth, J., & Wright, S. J. (2014). Validating sample average approximation solutions with negatively dependent batches.

Coffrin, C., Van Hentenryck, P., & Bent, R. (2012). Last-mile restoration for multiple interdependent infrastructures. *Proceedings of the National Conference on Artificial Intelligence*, *26(1)*, 455–463.

CPLEX, IBM. (2021). *CPLEX Optimizer — IBM.* https://www.ibm.com/analytics/cplex-optimizer.

Danziger, M. M., Shekhtman, L. M., Bashan, A., Berezin, Y., & Havlin, S. (2016). Vulnerability of interdependent networks and networks of networks. In *Understanding complex systems* (pp. 79–99). Switzerland: Springer International Publishing. doi: 10.1007/978-3-319-23947-7_5

de la Torre, L. E., Dolinskaya, I. S., & Smilowitz, K. R. (2012). Disaster relief routing: Integrating research and practice. *Socio-Economic Planning Sciences*, *46*(1), 88–97. (Special Issue: Disaster Planning and Logistics: Part 1) doi: 10.1016/j.seps.2011.06.001

Di Muro, M. A., La Rocca, C. E., Stanley, H. E., Havlin, S., & Braunstein, L. A. (2016). Recovery of interdependent networks. *Scientific Reports*, *6*(22834), 1–11. doi: 10.1038/srep22834

Dupačová, J., Gröwe-Kuska, N., & Römisch, W. (2003). Scenario reduction in stochastic programming. *Mathematical Programming*, *95*(3), 493–511. doi: 10.1007/s10107-002-0331-0

Enayaty Ahangar, N., Sullivan, K. M., & Nurre, S. G. (2020). Modeling interdependencies in infrastructure systems using multi-layered network flows. *Computers and Operations Research*, *117*, 104883. doi: 10.1016/j.cor.2019.104883

Escudero, L. F., Garín, M. A., & Unzueta, A. (2017). Scenario cluster Lagrangean decomposition for risk averse in multistage stochastic optimization. *Computers and Operations Research*, *85*, 154–171. doi: 10.1016/j.cor.2017.04.007

Eusgeld, I., Nan, C., & Dietz, S. (2011). "system-of-system" approach for interdependent critical infrastructures. *Reliability Engineering and System Safety*, *96*(6), 679–686. doi: 10.1016/j.ress.2010.12.010

Executive Office of the President, Council of Economic Advisers. (2013). *Economic benefits of increasing electric grid resilience to weather outages.* Washington, D.C.: The Council.

Fang, Y., Pedroni, N., & Zio, E. (2016). Resilience-based component importance measures for critical infrastructure network systems. *IEEE Transactions on Reliability*, *65*(2), 502–512. doi: 10.1109/tr.2016.2521761

Fang, Y., & Sansavini, G. (2017). Emergence of antifragility by optimum postdisruption restoration planning of infrastructure networks. *Journal of Infrastructure Systems*, *23*(4), 04017024. doi: 10.1061/(ASCE)IS.1943-555X.0000380

Fang, Y., & Sansavini, G. (2019). Optimum post-disruption restoration under uncertainty for

enhancing critical infrastructure resilience. *Reliability Engineering and System Safety*, *185*(January 2019), 1–11. doi: 10.1016/j.ress.2018.12.002

Fares, R. L., & King, C. W. (2017). Trends in transmission, distribution, and administration costs for u.s. investor-owned electric utilities. *Energy Policy*, *105*, 354–362. doi: 10.1016/j.enpol.2017.02.036

Force, Hurricane Sandy Rebuilding Task Force. (2013). *Hurricane Sandy rebuilding strategy* (US). Washington, DC.

Franchin, P., & Cavalieri, F. (2015). Probabilistic assessment of civil infrastructure resilience to earthquakes. *Computer-Aided Civil and Infrastructure Engineering*, *30*(7), 583–600. doi: 10.1111/mice.12092

Garay-Sianca, A., & Pinkley, S. G. N. (2021, February). Interdependent integrated network design and scheduling problems with movement of machines. *European Journal of Operational Research*, *289*(1), 297–327. doi: 10.1016/j.ejor.2020.07.013

Ghorbani-Renani, N., González, A. D., Barker, K., & Morshedlou, N. (2020). Protection-interdiction-restoration: Tri-level optimization for enhancing interdependent network resilience. *Reliability Engineering and System Safety*, *199*, 106907. doi: 10.1016/j.ress.2020.106907

Gong, J., Lee, E. E., Mitchell, J. E., & Wallace, W. A. (2009). Logic-based MultiObjective optimization for restoration planning. In E. W. Chaovalitwongse (Ed.), *Springer optimization and its applications* (Vol. 30, pp. 305–324). Boston, MA: Springer US. doi: 10.1007/978-0-387-88617-6_11

González, A. D., Dueñas-Osorio, L., Sánchez-Silva, M., & Medaglia, A. L. (2016). The interdependent network design problem for optimal infrastructure system restoration. *Computer-Aided Civil and Infrastructure Engineering*, *31*(5), 334–350. doi: 10.1111/mice.12171

Guidotti, R., Chmielewski, H., Unnikrishnan, V., Gardoni, P., McAllister, T., & van de Lindt, J. (2016). Modeling the resilience of critical infrastructure: the role of network dependencies. *Sustainable and Resilient Infrastructure*, *1*(3-4), 153–168. doi: 10.1080/23789689.2016.1254999

Haimes, Y. Y., & Jiang, P. (2001). Leontief-based model of risk in complex interconnected infrastructures. *Journal of Infrastructure Systems*, *7*(1), 1–12. doi: 10.1061/(asce)1076-0342(2001)7:1(1)

HDR. (2012). *City of Raymore - Water storage and water supply study.* Available at: https://www.raymore.com/home/showpublisheddocument?id=1176.

Heitsch, H., & Römisch, W. (2003). Scenario reduction algorithms in stochastic programming. *Computational Optimization and Applications*, *24*(2/3), 187–206. doi: 10.1023/a:1021805924152

Helbing, D. (2013). Globally networked risks and how to respond. *Nature*, *497*(7447), 51–59. doi: 10.1038/nature12047

Henry, D., & Ramirez-Marquez, J. E. (2012). Generic metrics and quantitative approaches for system resilience as a function of time. *Reliability Engineering and System Safety*, *99*, 114–122. doi: 10.1016/j.ress.2011.09.002

Holden, R., Val, D. V., Burkhard, R., & Nodwell, S. (2013). A network flow model for interdependent infrastructures at the local scale. *Safety Science*, *53*, 51–60. doi: 10.1016/j.ssci.2012.08.013

Horejšová, M., Vitali, S., Kopa, M., & Moriggia, V. (2020, June). Evaluation of scenario reduction algorithms with nested distance. *Computational Management Science*, *17*(2), 241–275. doi: 10.1007/s10287-020-00375-4

Hosseini, S., Barker, K., & Ramirez-Marquez, J. E. (2016). A review of definitions and measures of system resilience. *Reliability Engineering and System Safety*, *145*, 47–61. doi: 10.1016/j.ress.2015.08.006

Humphreys, B. E. (2019). *Critical infrastructure: Emerging trends and policy considerations for congress* (No. CRS Report No. R45809.) Washington, DC: Congressional Research Service.

Karagiannis, G. M., Chondrogiannis, S., Krausmann, E., & Turksezer, Z. I. (2017). *Power grid recovery after natural hazard impact* (Tech. Rep. No. EUR 28844 EN). Luxembourg. doi: 10.2760/87402

Karakoc, D. B., Almoghathawi, Y., Barker, K., González, A. D., & Mohebbi, S. (2019). Community resilience-driven restoration model for interdependent infrastructure networks. *International Journal of Disaster Risk Reduction*, *38*, 101228. doi: 10.1016/j.ijdrr.2019.101228

Kim, Y., Spencer, B. F. J., Song, J., Elnashai, A. S., & Stokes, T. (2007). Seismic performance assessment of interdependent lifeline systems. *MAE Center Report*, *CD Release 07-16*.

Kleywegt, A. J., Shapiro, A., & Homem-de-Mello, T. (2002, January). The sample average approximation method for stochastic discrete optimization. *SIAM Journal on Optimization*, *12*(2), 479–502. doi: 10.1137/s1052623499363220

Krokhmal, P., Palmquist, J., & Uryasev, S. (2002). Portfolio optimization with conditional

value-at-risk objective and constraints. *Journal of risk*, *4*, 43–68.

Lawrence Berkeley National Laboratory and Nexant, Inc. (2021). *The interruption cost estimate (ice) calculator - lawrence berkeley national laboratory and nexant, inc.* (Available at: https://icecalculator.com/home)

Lee II, E. E., Mitchell, J. E., & Wallace, W. A. (2007). Restoration of services in interdependent infrastructure systems: A network flows approach. *IEEE Transactions on Systems, Man, and Cybernetics, Part C (Applications and Reviews)*, *37*(6), 1303–1317. doi: 10.1109/TSMCC.2007.905859

Little, R. G. (2002). Controlling cascading failure: Understanding the vulnerabilities of interconnected infrastructures. *Journal of Urban Technology*, *9*(1), 109–123. doi: 10.1080/106307302317379855

Manuel, J. (2013). *The long road to recovery: Environmental health impacts of hurricane sandy* (Vol. 121) (No. 5). Environmental Health Perspectives. doi: 10.1289/ehp.121-a152

Meltzer, A., Beck, S., Ruiz, M., Hoskins, M., Soto-Cordero, L., Stachnik, J. C., ... Mercerat, E. D. (2019, March). The 2016 mw 7.8 pedernales, ecuador, earthquake: Rapid response deployment. *Seismological Research Letters*, *90*(3), 1346–1354. doi: 10.1785/0220180364

Memphis Light, Gas and Water Division (MLGW). (2021). *Facts & figures - 2017.* Available at: http://www.mlgw.com/images/content/files/pdf/FactsFigures2018.pdf.

Mendonca, D., Lee, E., & Wallace, W. (2004). Impact of the 2001 world trade center attack on critical interdependent infrastructures. In *2004 IEEE international conference on systems, man and cybernetics (IEEE cat. no.04ch37583)* (Vol. 5). IEEE. doi: 10.1109/icsmc.2004.1401165

Mete, H. O., & Zabinsky, Z. B. (2010). Stochastic optimization of medical supply location and distribution in disaster management. *International Journal of Production Economics*, *126*(1), 76–84. (Improving Disaster Supply Chain Management – Key supply chain factors for humanitarian relief) doi: 10.1016/j.ijpe.2009.10.004

Min, H.-S. J., Beyeler, W., Brown, T., Son, Y. J., & Jones, A. T. (2007). Toward modeling and simulation of critical national infrastructure interdependencies. *IIE Transactions*, *39*(1), 57–71. doi: 10.1080/07408170600940005

Mooney, E. L., Almoghathawi, Y., & Barker, K. (2019). Facility location for recovering systems of interdependent networks. *IEEE Systems Journal*, *13*(1), 489–499. doi: 10.1109/jsyst.2018.2869391

Morales, J. M., Pineda, S., Conejo, A. J., & Carrión, M. (2009). Scenario reduction for futures market trading in electricity markets. *IEEE Transactions on Power Systems*, *24*(2), 878–888. doi: 10.1109/TPWRS.2009.2016072

Moreno, A., Munari, P., & Alem, D. (2019). A branch-and-benders-cut algorithm for the crew scheduling and routing problem in road restoration. *European Journal of Operational Research*, *275*(1), 16–34. doi: 10.1016/j.ejor.2018.11.004

Morshedlou, N., González, A. D., & Barker, K. (2018). Work crew routing problem for infrastructure network restoration. *Transportation Research Part B: Methodological*, *118*, 66–89. doi: 10.1016/j.trb.2018.10.001

Noyan, N. (2012). Risk-averse two-stage stochastic programming with an application to disaster management. *Computers and Operations Research*, *39*(3), 541–559. doi: 10.1016/j.cor.2011.03.017

Nurre, S. G., Cavdaroglu, B., Mitchell, J. E., Sharkey, T. C., & Wallace, W. A. (2012). Restoring infrastructure systems: An integrated network design and scheduling (INDS) problem. *European Journal of Operational Research*, *223*(3), 794–806. doi: 10.1016/j.ejor.2012.07.010

Nurre, S. G., & Sharkey, T. C. (2014). Integrated network design and scheduling problems with parallel identical machines: Complexity results and dispatching rules. *Networks*, *63*(4), 306–326. doi: 10.1002/net.21547

Ouyang, M. (2014). Review on modeling and simulation of interdependent critical infrastructure systems. *Reliability Engineering and System Safety*, *121*, 43–60. doi: 10.1016/j.ress.2013.06.040

Ouyang, M., & Wang, Z. (2015). Resilience assessment of interdependent infrastructure systems: With a focus on joint restoration modeling and analysis. *Reliability Engineering and System Safety*, *141*, 74–82. doi: 10.1016/j.ress.2015.03.011

Peerenboom, J., Fisher, R., Rinaldi, S., & Kelly, T. (2002). Studying the chain reaction. *Electric Perspectives*, *27*(1), 22–35.

Python. (2021). *Python.org.* https://www.python.org/.

Rachev, S. T. (1991). *Probability metrics and the stability of stochastic models, scenario.* Chichester New York: Wiley.

Rahmaniani, R., Crainic, T. G., Gendreau, M., & Rei, W. (2017). The benders decomposition algorithm: A literature review. *European Journal of Operational Research*, *259*(3), 801–817. doi: 10.1016/j.ejor.2016.12.005

Rinaldi, S. (2004). Modeling and simulating critical infrastructures and their interdependencies. In *37th annual hawaii international conference on system sciences, 2004. proceedings of the* (pp. 5–8). IEEE. doi: 10.1109/hicss.2004.1265180

Rinaldi, S. M., Peerenboom, J. P., & Kelly, T. K. (2001). Identifying, understanding, and analyzing critical infrastructure interdependencies. *IEEE Control Systems*, *21*(6), 11–25. doi: 10.1109/37.969131

Rockafellar, R. T., & Uryasev, S. (2000). Optimization of conditional value-at-risk. *The Journal of Risk*, *2*(3), 21–41. doi: 10.21314/jor.2000.038

Saidi, S., Kattan, L., Jayasinghe, P., Hettiaratchi, P., & Taron, J. (2018). Integrated infrastructure systems—a review. *Sustainable Cities and Society*, *36*, 1–11. doi: 10.1016/j.scs.2017.09.022

Sharkey, T. C., Cavdaroglu, B., Nguyen, H., Holman, J., Mitchell, J. E., & Wallace, W. A. (2015, July). Interdependent network restoration: On the value of information-sharing. *European Journal of Operational Research*, *244*(1), 309–321. doi: 10.1016/j.ejor.2014.12.051

Sharma, N., Tabandeh, A., & Gardoni, P. (2017). Resilience analysis: a mathematical formulation to model resilience of engineering systems. *Sustainable and Resilient Infrastructure*, *3*(2), 49–67. doi: 10.1080/23789689.2017.1345257

Tootaghaj, D. Z., Bartolini, N., Khamfroush, H., & Porta, T. L. (2017, September). Controlling cascading failures in interdependent networks under incomplete knowledge. In *2017 IEEE 36th symposium on reliable distributed systems (SRDS).* Hong Kong: IEEE. doi: 10.1109/srds.2017.14

Unsihuay, C., Lima, J. W. M., & de Souza, A. Z. (2007, June). Modeling the integrated natural gas and electricity optimal power flow. In *2007 IEEE power engineering society general meeting* (pp. 24–28). Tampa, FL: IEEE. doi: 10.1109/pes.2007.386124

Vugrin, E. D., Turnquist, M. A., & Brown, N. J. (2014). Optimal recovery sequencing for enhanced resilience and service restoration in transportation networks. *International Journal of Critical Infrastructures*, *10*(3/4), 218–246. doi: 10.1504/IJCIS.2014.066356

Wallace, W., Mendonca, D., Lee, E., Mitchell, J., Wallace, J., & Monday, J. (2003). Managing disruptions to critical interdependent infrastructures in the context of the 2001 world trade center attack. in beyond september 11th: An account of. *Post-Disaster Research, special publication*, *39*, 165–198.

White House. (2013). *Presidential Policy Directive/PPD-21 : Critical Infrastructure Security and Resilience. Office of the Press Secretary: Washington, DC.* [Administration of Barack Obama]. Washington, DC..

Wolfram, C. (2021). *Measuring the economic costs of the PG&E outages.* (Available at: https://energyathaas.wordpress.com/2019/10/14/measuring-the-economic-costs-of-the-pge-outages/)

Wyss, G. D., & Jorgensen, K. H. (1998). A User ' s Guide to LHS : Sandia's Latin Hypercube Sampling Software Acknowledgments. *Distribution*(February), 88. doi: 98-0210

Zhang, C., Kong, J.-j., & Simonovic, S. P. (2018). Restoration resource allocation model for enhancing resilience of interdependent infrastructure systems. *Safety Science*, *102*, 169–177. doi: 10.1016/j.ssci.2017.10.014

Zhang, P., & Peeta, S. (2011). A generalized modeling framework to analyze interdependencies among infrastructure systems. *Transportation Research Part B: Methodological*, *45*(3), 553–579. doi: 10.1016/j.trb.2010.10.001

Zhang, Y., Yang, N., & Lall, U. (2016). Modeling and simulation of the vulnerability of interdependent power-water infrastructure networks to cascading failures. *Journal of Systems Science and Systems Engineering*, *25*(1), 102–118. doi: 10.1007/s11518-016-5295-3

Zimmerman, R. (2001). Social implications of infrastructure network interactions. *Journal of Urban Technology*, *8*(3), 97–119. doi: 10.1080/106307301753430764

Chapter 5

Summary and Future Work

5.1 Risk and resilience-based optimal post-disruption restoration for critical infrastructures under uncertainty

Chapter 3 proposes risk-neutral and risk-averse two-stage stochastic optimization models for CI restoration planning, where post-disruption restoration tasks occur in a highly dynamic environment and thus subject to a considerable amount of uncertainty. The models address two important challenges facing restoration planning, which are the accessibility of failed components and uncertainty associated with restoration task durations and possible starting times. The proposed approach was demonstrated using a real-life case study based on the RTE 400 kV French electric power transmission network. Additionally, the proposed models in Chapter 3 present a practical framework for risk-neutral and risk-averse resilience-based applications and possibly other applications with task scheduling procedures involving a fair amount of uncertainty. However, the models in the present study assume that the restoration plan is determined initially and cannot be altered afterwards. Indeed, relaxing this assumption by enabling sequential change of the plan as time goes on will add more flexibility to the models. However, migrating the models from the two-stage setting into a more dynamic multi-stage stochastic optimization framework will significantly increase the computational time. Such computational differences can be tested using time-consistent risk-averse measures such as Expected CVaR (Homem-de-Mello & Pagnoncelli, 2016) and Expected Conditional Stochastic Dominance (Escudero *et al.*, 2017). In addition, the

presented study considers the transportation network as a factor affecting the restoration plan without being restored when damaged. Therefore, coordinating the restoration of the transportation network with another critical infrastructure network could be considered for future work. In fact, the literature on resilience of transportation networks is generally studied separately from other critical infrastructures due to the different nature of such networks and their restoration planning strategies (Zhou *et al.*, 2019). Thus, an effort to merge both the resilience of transportation networks and other critical infrastructure networks could be a valuable extension to the current model and to the related literature. Additionally, the current approach only focuses on one phase of resilience planning (i.e., restoration). Hence, considering multi-phase planning for resilience, with an understanding of the tradeoffs between the available vulnerability reduction resources and the resilience achieved through restoration enhancement could be among the future research directions. For instance, integrating interdiction approaches with recovery plans seems to be a good starting point for resilience planning (Ghorbani-Renani *et al.*, 2020). Finally, resilience planning could be investigated by studying the network criticality analysis of its components, which affects the network failure as well as the recovery process.

5.2 Model and solution method for mean-risk cost-based post-disruption restoration of interdependent critical infrastructure networks

In Chapter 4, we propose a two-stage stochastic restoration optimization model using mixed-integer linear programming to solve the interdependent critical infrastructure networks restoration problem (ICINRP) under a mean-risk cost-based objective function. Moreover, the mean-risk model features flexible restoration planning strategies including

multicrew repair of a single component and multimode repair, and also considers partial functioning and interdependencies of components across networks. The proposed model: (i) determines the set of failed components to be restored, (ii) selects the repair mode for each failed component, (iii) assigns each crew the set of failed components to be restored individually or concurrently, (iv) and schedules the baseline restoration sequence across scenarios for each crew such that the associated costs of disruption, repair, and flow of the system of interdependent critical infrastructures (ICIs) are minimized. Additionally, as post-disruption restoration tasks occur in a highly dynamic environment, which is subject to a fair amount of uncertainty, the mean-risk model considers two important sources of uncertainty associated with restoration panning: (i) repair task durations, and (ii) travel times of crews between failed components. The proposed approach was demonstrated using a real-life case study based on the system of power and water networks in Shelby County, TN, U.S. under two hypothetical earthquakes.

As for future work, the proposed model could be extended to consider the transportation network as a direct interdependent network. That is, the current approach assumes that critical infrastructure (CI) networks, other than the underlying transportation network, are the ones being restored. Hence, the problem becomes not only focused on the restoration of CIs, but also on coordinating the process of finding the best routes and schedules for crews to repair damaged components in the transportation network. In addition, it is possible to extend the current model to introduce a facility location problem where work crews are dispatched to disrupted component locations rather than a direct travel between components. In such problems, the goal is to find the optimal location of these facilities from a set of candidate sites considering the fixed cost of establishing such facilities

as well as other crew-related variable costs. Moreover, considering economic measures of the resilience of communities interacting with these interdependent critical infrastructure networks (ICINs), as well as the associated risks can be one of the future directions of this work. This future direction can also be associated with studying other types of interdependencies that affect both CIs and communities such as geographic interdependency to mitigate the related socioeconomic risks. Additionally, considering different sources of uncertainty is a possible extension to the current approach (Reilly *et al.*, 2021). Finally, integrating the current restoration framework with immediate post-disruption machine learning damage detection approaches (Xu *et al.*, 2019) could be a useful addition to the literature on disaster management.

References

Escudero, L. F., Garín, M. A., & Unzueta, A. (2017). Scenario cluster Lagrangean decomposition for risk averse in multistage stochastic optimization. *Computers and Operations Research*, *85*, 154–171. doi: 10.1016/j.cor.2017.04.007

Ghorbani-Renani, N., González, A. D., Barker, K., & Morshedlou, N. (2020). Protection-interdiction-restoration: Tri-level optimization for enhancing interdependent network resilience. *Reliability Engineering and System Safety*, *199*, 106907. doi: 10.1016/j.ress.2020.106907

Homem-de-Mello, T., & Pagnoncelli, B. K. (2016, feb). Risk aversion in multistage stochastic programming: A modeling and algorithmic perspective. *European Journal of Operational Research*, *249*(1), 188–199. doi: 10.1016/j.ejor.2015.05.048

Reilly, A. C., Baroud, H., Flage, R., & Gerst, M. D. (2021). Sources of uncertainty in interdependent infrastructure and their implications. *Reliability Engineering & System Safety*, *213*, 107756. doi: 10.1016/j.ress.2021.107756

Xu, J. Z., Lu, W., Li, Z., Khaitan, P., & Zaytseva, V. (2019). *Building damage detection in satellite imagery using convolutional neural networks.*

Zhou, Y., Wang, J., & Yang, H. (2019). Resilience of transportation systems: Concepts and comprehensive review. *IEEE Transactions on Intelligent Transportation Systems*, *20*(12), 4262–4276. doi: 10.1109/tits.2018.2883766